

**SYNTHESIS, CHARACTERIZATION AND CATALYTIC  
APPLICATION OF CARBONYL COMPLEXES OF  
MOLYBDENUM AND TUNGSTEN IN EPOXIDATION  
OF SOME ALKENES**

**Aloice O. Ogweno**

**A dissertation in partial fulfilment of the requirements for the  
degree of Master of Science in the Department of Chemistry,  
University of the Western Cape, South Africa**



**Supervisor: Dr. Martin O. Onani**

## DECLARATION

I, **Aloice Omondi Ogwen**, declare that “SYNTHESIS AND CHARACTERIZATION OF CARBONYL COMPLEXES OF MOLYBDENUM AND TUNGSTEN AND THEIR CATALYTIC APPLICATION IN EPOXIDATION OF SOME ALKENES” is my own work and that all sources I have used or quoted have been acknowledged by means of complete referencing at the end of each chapter.



.....

Aloice Omondi Ogwen

.....

Date

## ABSTRACT

In this thesis we describe the synthesis of several carbonyl complexes of molybdenum and tungsten, compounds (C1-C10). The compounds C1- C4 are zero valent carbonyl complexes containing N-base ligands prepared by following a common synthetic procedure. Compounds C1 and C2 were metal pentacarbonyl of 3-(1-methylpyrrolidin-2-yl) pyridine while C3 and C4 are metal tetracarbonyl complexes of 3, 5-dimethylpyrazole, (M=Mo, W).

The compounds C5-C10 are divalent metal carbonyl complexes. Compounds C5 and C6 were 3,5-dimethylpyrazole dibromotricarbonyl metal complexes prepared from the dibromotetracarbonyl metal dimers at room temperature while the compounds C7 and C8 were cyclopentadienyl halogenoaryltricarbonyl complexes prepared from the cyclopentadienyl metal dimers.

Compounds C9 and C10 were prepared from cyclopentadienyl metal dimers by reacting the  $[\text{CpM}(\text{CO})_3]^-$  anion with  $\text{CCl}_4$  to obtain  $[\text{CpM}(\text{CO})_3\text{Cl}]$  and further reacted with 3-(1-methylpyrrolidin-2-yl) pyridine. All the compounds, C1-C10, were characterized by the standard analytical techniques such as FTIR,  $^1\text{H}$ ,  $^{13}\text{C}$  NMR; and UV-Vis spectroscopy. Compound C4 was characterized by X-ray crystallography. The structure is depicted as having a distorted octahedral geometry around the metal centre.

The compounds C1-C10 were then tested towards the epoxidation of selected cyclic and straight chain alkenes. The substrates used were *cis*-cyclooctene (Cy<sub>8</sub>), 1-octene (C<sub>8</sub>) cyclohexene (Cy<sub>6</sub>), 1-hexene (C<sub>6</sub>) and styrene (Sty). The epoxidation reactions were carried out at a temperature of 55 °C using tertbutylhydroperoxide (TBHP) as the oxidant and dichloroethane (DCE) as the solvent. The metal carbonyl complexes were pre-activated by

first reacting them with the oxidant TBHP to obtain the metal-oxo complexes which are the active compounds for epoxidation reactions. The products were analyzed using GC techniques. The compounds, **C1-C10** showed a promising activity towards epoxidation reactions owing to the high conversions obtained by these compounds. For example, conversions of 81% (1-octene), 90% (*cis*-cyclooctene) were obtained by compound **C5**, 87% (*cis*-cyclooctene-compound **C3**, 95% (*cis*-cyclooctene-compound **C7**) and 69% (*cis*-cyclooctene-compound **C4**) for an average period of 24 h. The divalent metal carbonyl complexes showed a higher activity but with poor selectivity towards the expected epoxides compared to the zero valent metal carbonyl complexes.



## ACKNOWLEDGEMENTS

I would like to thank the Almighty God for making this possible for me, his glory, love and grace has been with me always.

Secondly, I would like to express my sincere thanks to Dr Martin O. Onani for his sincere support, guidance, worthy advices and patience, because of him this research project was successful.

Thirdly I acknowledge the sincere and worthy support from my cousin Dalin Ngcobo for her loving and hearty support, Professor Emmanuel Iwouha for his financial support and Mr Ochieng for his great support.

I would also like to thank the staff in the Department of Chemistry, University of the Western Cape especially Timothy Lesch, B. De Wet and Andile Manty for lending a helping hand whenever I needed help with various analytical techniques and chemicals.

I would also like to thank my colleagues from the Organometallic Research Group, Paul Mushonga, William Motswainyana, Mududuzi Radebe, Asanda busa and Miss Manana Molestsane for their moral and emotional support and co-operation as I was carrying out my project work. Together with them I would like to thank Henry Mwangi and Njomo Njagi.

Financial support received from NRF is also greatly acknowledged.

Lastly but not least I would like to thank my family and friends, Mr & Mrs Ogwen, Jim, Jael, Nifry, Mr & Mrs Onyango and Mr. Mboya for the encouragement and inestimable support throughout my previous and current studies.

## CONFERENCE CONTRIBUTIONS

This work has been peer reviewed in the following conference presentation:

**Oral presentation:** *Synthesis, characterization and catalytic application of nitrogen-base carbonyl complexes of molybdenum and tungsten in olefin epoxidation.* A. Ogweno, M.

Onani. Catalytic society of South Africa (CATSA) held at Misty Hills Conference Centre, Muldersdrift, Gauteng, South Africa, 13<sup>th</sup>-16<sup>th</sup> November, 2011

**Oral presentation:** *Novel 3, 5-dimethylpyrazole group 6 metal carbonyl complexes,*

A. Ogweno, M. Onani. 4<sup>th</sup> Walter Sisulu University International Research Conference held at International Convention Centre, East London, Eastern Cape, South Africa, 16<sup>th</sup> -19<sup>th</sup> August 2011



## PAPERS

1. **Aloice O. Ogweno**, Martin O. Onani, 1-Chlorotricarbonyl [eta] 5-cyclopentdienyl Molybdenum (II)-*Manuscript accepted for publication.*
2. Onani M. O., **Ogweno, A. O**, Muriithi, N. T., Nyawade, E. A. Synthesis and characterization of Nitrogen base-substituted metal carbonyl complexes of molybdenum and tungsten-*Manuscript in preparation*
3. **O. Ogweno**, M. O. Onani, Review paper on Molybdenum and Tungsten for Olefin Epoxidation- *Manuscript in preparation*

## CONTENTS

DECLARATION .....	ii
ABSTRACT.....	iii
ACKNOWLEDGEMENTS .....	v
CONFERENCE CONTRIBUTIONS .....	vi
CONTENTS.....	vii
LIST OF FIGURES .....	xi
LIST OF SHEMES .....	xiv
LIST OF TABLES.....	xv
ABBREVIATIONS .....	xvii
CHAPTER 1 .....	1
1.0 Introduction.....	1
1.1 Zero valent molybdenum and tungsten carbonyl complexes.....	3
1.1.1 Carbonyl ligands.....	4
1.1.2 Lewis base ligands.....	5
1.1.3 Unsaturated straight chain organic molecules.....	5
1.1.4 Unsaturated cyclic organic molecules.....	6
1.2 Divalent molybdenum and tungsten carbonyl complexes.....	7
1.2.1 Dihalotetracarbonyl Mo and W dimer complexes.....	8
1.2.2 <i>bis</i> -coordinated dihalotricarbonyl Mo and W complexes.....	9
1.2.3 Cyclic alkenes tricarbonyl metal (II) complexes.....	10
1.3 Substitution reactions of metal hexacarbonyls.....	11
1.4 Nitrogen-base carbonyl complexes of molybdenum and tungsten .....	16
1.5 Electronic spectral studies.....	18
1.6 Catalytic epoxidation by molybdenum and tungsten complexes.....	18
1.7 Mechanism of epoxidation reaction.....	21
1.8 Aims and objectives .....	23
1.9 References .....	25

CHAPTER 2 .....	32
2.0 Experimental Section .....	32
2.1 General remarks .....	32
2.2 Instrumentation.....	33
2.3 Olefin epoxidation reactions .....	34
2.4 Synthesis of 3-(1-methylpyrrolidin-2-yl) pyridine complexes.....	37
2.4.1 3-(1-methylpyrrolidin-2-yl) pyridine pentacarbonyl molybdenum (0), $[Mo(CO)_5(C_{10}H_{14}N_2)]-$ (C1) .....	37
2.4.2 3-(1-methylpyrrolidin-2-yl) pyridine pentacarbonyl tungsten (0), $[W(CO)_5-$ $(C_{10}H_{14}N_2)]-$ (C2).....	38
2.5 Synthesis of 3, 5-dimethylpyrazole complexes.....	38
2.5.1 bis(substituted-di-3,5-dimethylpyrazole)tetracarbonyl molybdenum (0), $[Mo(CO)_4(C_5H_8N_2)_2]-$ (C3).....	38
2.5.2 bis(substituted-3,5-dimethylpyrazole)tetracarbonyl tungsten (0), $[W(CO)_4(C_5-$ $H_8N_2)_2]-$ (C4) .....	39
2.5.3 dibromo-bis(substituted-3,5-dimethylpyrazole)tetracarbonyl molybdenum (II) $[Mo(CO)_4Br_2(C_5H_8N_2)_2]-$ (C5) .....	40
2.5.4 dibromo-bis(substituted-3,5-dimethylpyrazole)tetracarbonyl tungsten(II), $[W(CO)_4Br_2(C_5H_8N_2)_2]-$ (C6).....	40
2.6 Synthesis of 1-(bromomethyl)-4-methylenebenzyl cyclopentadienylcarbonyl complexes.....	41
2.6.1 1-(bromomethyl)-4-methylenebenzyl cyclopentadienyl tricarbonyl molybdenum (II), $[CpMo(CO)_3-CH_2-C_6H_4-CH_2Br]-$ (C7) .....	41
2.6.2 1-(bromomethyl)-4-methylenebenzyl cyclopentadienyl tricarbonyl tungsten (II), $[CpW(CO)_3-CH_2-C_6H_4-CH_2Br]-$ (C8).....	42
2.7 Synthesis of 3-(1-methylpyrrolidin-2-yl) pyridine cyclopentadienyl chlorotricarbonyl complexes.....	43
2.7.1 3-(1-methylpyrrolidin-2-yl) pyridine cyclopentadienyl chlorotricarbonyl molybdenum (II), $[CpMo(CO)_3Cl(C_{10}H_{14}N_2)]-$ (C9) .....	43



2.7.2 3-(1-methylpyrrolidin-2-yl) pyridine cyclopentadienyl tricarbonyl tungsten (II), [CpW(CO) <sub>2</sub> Cl (C <sub>10</sub> H <sub>14</sub> N <sub>2</sub> )]- (C10).....	44
2.8 References .....	45
CHAPTER 3 .....	46
3.0 Results and Discussion.....	46
3.1 3-(1-methylpyrrolidin-2-yl) pyridine pentacarbonyl complexes (C1=Mo, C2= W).....	46
3.1.1 IR spectroscopic analysis of C1 and C2 .....	47
3.1.2. <sup>1</sup> H NMR spectroscopic analysis of C1 and C2.....	50
3.1.3 <sup>13</sup> C NMR spectroscopic analysis of C1 and C2.....	52
3.2 bis-3, 5-dimethylpyrazole tetracarbonyl complexes .....	53
3.2.1 IR spectroscopic analysis of C3 and C4 .....	54
3.2.2 <sup>1</sup> H NMR spectroscopic analysis of C3 and C4.....	56
3.2.3 <sup>13</sup> C NMR spectroscopic analysis of C3 and C4.....	58
3.2.4 X-ray crystallographic analysis .....	59
3.3 dibromo-bis-3, 5-dimethylpyrazole complexes tetracarbonyl complexes, (C5=Mo, C6=W).....	63
3.3.1 IR spectroscopic analysis.....	63
3.3.2 <sup>1</sup> H NMR spectroscopic analysis.....	66
3.3.3 <sup>13</sup> C NMR spectroscopic analysis .....	68
3.4 1-(bromomethyl)-4-methylenebenzylcyclopentadienyltricarbonyl complexes,8(C7=Mo, C8=W).....	69
3.4.1 IR spectroscopic analysis of compounds C7 and C8 .....	70
3.4.2 <sup>1</sup> H NMR spectroscopic analysis of compounds C7 and C8 .....	72
3.4.3 <sup>13</sup> C NMR spectroscopic analysis of compounds C7 and C8 .....	73
3.5 3-(1-methylpyrrolidin-2-yl) pyridine cyclopentadienyl tricarbonyl complexes (C9=Mo, C10=W).....	76
3.5.1 IR spectroscopic analysis.....	76
3.5.2 <sup>1</sup> H NMR spectroscopic analysis.....	78
3.5.3 <sup>13</sup> C NMR spectroscopic analysis .....	79
3.6 Electronic transition measurements .....	81

3.7 Evaluation of compounds, C1-C10 as catalysts for epoxidation .....	83
3.8 References .....	92
CHAPTER 4 .....	96
4.1 Conclusions .....	96
4.2 Recommendations .....	97
APPENDIX.....	99



UNIVERSITY *of the*  
WESTERN CAPE

## LIST OF FIGURES

<b>Figure 1.1:</b> Types of M-CO bond interaction (a-c).....	4
<b>Figure 1.2:</b> Metal- carbonyl bonding modes (a-c).....	4
<b>Figure 1.3:</b> Lewis base coordination to the transition metal (a-c).....	5
<b>Figure 1.4:</b> Coordination of straight chain alkenes.....	6
<b>Figure 1.5:</b> Coordination modes of cyclopentadienyl ligand (a-c).....	7
<b>Figure 1.6:</b> Structure of dihalotetracarbonyl metal dimer.....	8
<b>Figure 1.7:</b> Lewis base ligand $\sigma$ -bonding and transition metal $\pi$ -back-donation to the $\pi^*$ -orbital of the <i>trans</i> carbonyl ligand.....	13
<b>Figure 1.8:</b> Effect of $\sigma$ -donation on the IR stretching frequency of the <i>trans</i> carbonyl.....	14
<b>Figure 1.9:</b> (a) <i>cis</i> -bis-substituted tetracarbonyl.....	15
<b>Figure 1.9:</b> (b) <i>fac</i> -trisubstituted tricarbonyl.....	15
<b>Figure 1.10:</b> Catalytic application of molybdenum compounds. US patents, according to type of compound.....	20
<b>Figure 3.1:</b> IR spectrum of 3-(1-methylpyrrolidin-2-yl) pyridine pentacarbonyl molybdenum (0)-(C1).....	47
<b>Figure 3.2:</b> $^1\text{H}$ NMR spectrum of 3-(1-methylpyrrolidin-2-yl) pyridine pentacarbonyl molybdenum (0)-(C1).....	50

<b>Figure 3.3:</b> $^{13}\text{C}$ NMR spectrum of 3-(1-methylpyrrolidin-2-yl) pyridine	
pentacarbonyl molybdenum (0)-(C1).....	52
<b>Figure 3.4:</b> IR spectrum of 3, 5-dimethylpyrazole tetracarbonyl	
tungsten (0)- (C4).....	54
<b>Figure 3.5:</b> $^1\text{H}$ NMR spectrum of 3, 5-dimethylpyrazole tetracarbonyl	
molybdenum (0)-(C3).....	56
<b>Figure 3.6:</b> Crystal structure of 3, 5-dimethylpyrazole tetracarbonyl	
tungsten (0)-C4.....	59
<b>Figure 3.7:</b> IR spectrum of dibromo-bis-3, 5-dimethylpyrazole tricarbonyl	
tungsten (II)- (C6).....	64
<b>Figure 3.8:</b> $^1\text{H}$ NMR spectrum of dibromo-bis-3, 5-dimethylpyrazole tricarbonyl	
molybdenum (II)-(C5).....	66
<b>Figure 3.9:</b> $^{13}\text{C}$ NMR spectrum of dibromo-bis-3, 5-dimethylpyrazole tricarbonyl	
tungsten (II)-(C5).....	68
<b>Figure 3.10:</b> IR spectrum of 1-(bromomethyl)-4-methylenebenzyl	
cyclopentadienyl tricarbonyl molybdenum (II) - (C7).....	70
<b>Figure 3.11:</b> $^1\text{H}$ NMR spectrum of 1-(bromomethyl)-4-methylenebenzyl	
cyclopentadienyl tricarbonyl tungsten (II)-(C8).....	71
<b>Figure 3.12:</b> $^{13}\text{C}$ NMR spectrum of 1-(bromomethyl)-4-methylenebenzyl	
cyclopentadienyl tricarbonyl molybdenum (II)-(C7).....	74
<b>Figure 3.13:</b> IR spectrum 3-(1-methylpyrrolidin-2-yl) pyridine cyclopentadienyl	
tricarbonyl molybdenum (II) - (C9).....	76

**Figure 3.14:**  $^1\text{H}$  NMR spectrum of 3-(1-methylpyrrolidin-2-yl) pyridine  
cyclopentadienyl tricarbonyl tungsten (II)-(C10).....78

**Figure 3.15:**  $^{13}\text{C}$  NMR spectrum of 3-(1-methylpyrrolidin-2-yl) pyridine  
cyclopentadienyl tricarbonyl tungsten (II)-(C10).....79

**Figure 3.16:** Conversions of  $\text{C}_8$  and  $\text{C}_8$  using TBHP as oxidant.....84



## LIST OF SHEMES

<b>Scheme 1.1:</b> Ring opening reactions of epoxides.....	2
<b>Scheme 1.2:</b> Synthesis of seven coordinated metal carbonyl complex.....	9
<b>Scheme 1.3:</b> Synthesis of heptacoordinated cyclopentadienyl tricarbonyl (II).....	10
<b>Scheme 1.4:</b> General epoxidation reaction.....	21
<b>Scheme 1.5:</b> Oxidation of metal carbonyl precursor to metal-oxo derivatives.....	20
<b>Scheme 1.6:</b> Mechanism of Epoxidation of olefin.....	21
<b>Scheme 2.1:</b> Catalyzed Epoxidation reaction.....	34
<b>Scheme 3.1:</b> Synthesis of pentacarbonyl complexes-C1 and C2.....	46
<b>Scheme 3.2:</b> Synthesis of 3, 5-dimethylpyrazole tetracarbonyl metal complexes C3 and C4.....	53
<b>Scheme 3.3:</b> Synthesis of dibromo-bis-3, 5-dimethylpyrazole tricarbonyl metal complexes C5 and C6.....	63
<b>Scheme 3.4:</b> Synthesis of 1-(bromomethyl)-4-methylenebenzyl cyclopentadienyl tricarbonyl metal complexes, C7 and C8.....	69
<b>Scheme 3.5:</b> Synthesis of 3-(1-methylpyrrolidin-2-yl) pyridine cyclopentadienyl tricarbonyl metal complexes C9 and C10.....	76
<b>Scheme 3.6:</b> Ring opening reaction of 2-phenyloxirane to form benzaldehyde and other by-products.....	88

## LIST OF TABLES

<b>Table 3.1:</b> A summary of IR data for 3-(1-methylpyrrolidin-2-yl) pyridine, C1 and C2.....	49
<b>Table 3.2:</b> A summary of $^1\text{H}$ NMR data for 3-(1-methylpyrrolidin-2-yl) pyridine, C1 and C2.....	51
<b>Table 3.3:</b> A summary of $^{13}\text{C}$ NMR for 3-(1-methylpyrrolidin-2-yl) pyridine, C1 and C2.....	53
<b>Table 3.4:</b> A summary of IR data for 3, 5-dimethylpyrazole, C3 and C4.....	56
<b>Table 3.5:</b> A summary of $^1\text{H}$ NMR for 3, 5-dimethylpyrazole, C3 and C4.....	58
<b>Table 3.6:</b> A summary of $^{13}\text{C}$ NMR for compounds C3 and C4.....	58
<b>Table 3.7:</b> Selected bond angles ( $^\circ$ ) and bond lengths ( $\text{\AA}$ ) for compound C4.....	60
<b>Table 3.8:</b> Crystallographic data and structure refinement for compound C4.....	62
<b>Table 3.9:</b> A summary of IR data for 3, 5-dimethylpyrazole, C5 and C6.....	65
<b>Table 3.10:</b> A summary of $^1\text{H}$ NMR for 3, 5-dimethylpyrazole, C5 and C6.....	67
<b>Table 3.11:</b> A summary of $^{13}\text{C}$ NMR for compounds C5 and C6.....	69
<b>Table 3.12:</b> A summary of IR data for compounds C7 and C8.....	71
<b>Table 3.13:</b> A summary of $^1\text{H}$ NMR for complexes, C7 and C8.....	73
<b>Table 3.14:</b> A summary of $^{13}\text{C}$ NMR for compounds C7 and C8.....	74
<b>Table 3.15:</b> A summary of IR data for 3-(1-methylpyrrolidin-2-yl) pyridine, C9 and C10.....	77
<b>Table 3.16:</b> A summary of $^1\text{H}$ NMR for 3-(1-methylpyrrolidin-2-yl) pyridine, C9 and C10.....	79
<b>Table 3.17:</b> A summary of $^{13}\text{C}$ NMR for 3-(1-methylpyrrolidin-2-yl) pyridine, C9 and C10.....	80

<b>Table 3.18:</b> Electronic Spectral data for compounds <b>C1- C10</b> in DCM and MeOH.....	82
<b>Table 3.19:</b> A summary of the retention times for the standard samples (Cy <sub>8</sub> , Cy <sub>8</sub> epoxide, Sty, Sty epoxide and Isooctane).....	83
<b>Table 3.20:</b> Epoxidation results for the compound <b>C4</b> .....	86
<b>Table 3.21:</b> A summary of conversion, yield and selectivity of the substrate by <b>C1</b> and <b>C5</b> after 24 h reactions.....	89
<b>Table 3.22:</b> A summary of conversion, yield and selectivity of the substrates by of <b>C4</b> after 24 h and 48 h reactions.....	90
<b>Table 3.23:</b> A summary of conversion, yield and selectivity of the substrate by <b>C7</b> and <b>C8</b> after 48 h reactions.....	91





## ABBREVIATIONS

Å	angstrom
br	broad
CDCl <sub>3</sub>	deuterated chloroform
CO	carbonyl
Cr	Chromium
DCE	dichloroethane
DCM	Dichloromethane
FT-IR	Fourier Transform Infrared spectroscopy
g	gram(s)
GC	gas chromatography
h	hours
Hz	hertz
IR	Infrared
<i>J</i>	coupling constant
m	multiplet
m	medium
M-CO	metal-carbonyl bond
MeCN	acetonitrile
MeOH	methanol
MHz	megahertz
min	minutes

mL	millilitres
mmol	millimoles
Mo	Molybdenum
NMR	Nuclear Magnetic Resonance
Nu	nuclear
ppm	parts per million
r.t.	room temperature
ROMP	ring opening metathesis polymerization
s	singlet
sh	shoulder
t	triplet
TBHP	tertbutylhydroperoxide
THF	tetrahydrofuran
TOF	turn over frequency
UV-Vis	ultraviolet visible light
vs	very strong
W	Tungsten
w	weak
$\alpha$	alpha
$\beta$	beta
$\delta$	chemical shift



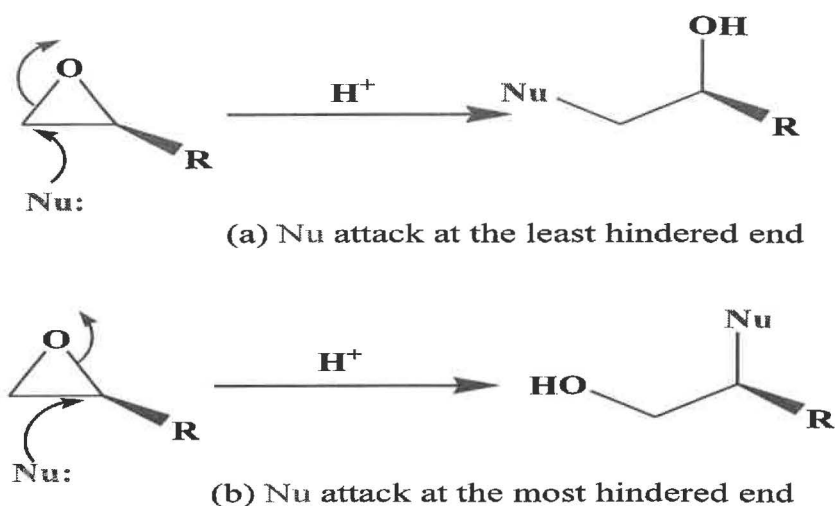
# CHAPTER 1

## 1.0 Introduction

Transition metal complexes have received great attention over the years because of their vast application as catalysts in several chemical transformations and biological reactions. The chemical transformation of organic compounds into different useful intermediates and finished compounds make use of the transition metal properties such as variable oxidation states. Some of the catalytic reactions to which they have been applied include oligomerization, polymerization, C-C coupling, epoxidation and oxidation reactions among other applications [1].

The suitability of any transition metal complex as a catalyst depends on its performance and economic efficiency. Highly selective, thermally stable and highly active catalysts are generally preferred particularly for industrial applications. The various chemical properties associated with these transition metals explain their preferential use as catalysts. Moreover, different ligands systems can be easily coordinated onto them to modify their chemical properties and catalytic performance. Moreover, they can be easily designed for a particular reaction and also to suit a particular reaction condition.

The transformation of alkenes into the corresponding oxiranes/epoxides and involving the addition of oxygen atom onto the double bond of the unsaturated organic compounds is one of the catalytic processes that heavily utilize the transition metal compounds [2,3]. The resulting epoxides are important intermediates which can further undergo ring-opening reactions with various reagents to give mono- or bi-functional organic products as illustrated by scheme 1.1 These products are important both in the chemical and pharmaceutical industries [2,4].



**Scheme 1.1:** Ring opening reactions of epoxides

Epoxides are produced in large scale for application in the manufacture of other chemical compounds such as surface active agents, fumigants, synthetic resins, cements, adhesives, fine chemicals and anti-freezing additives. However, small scale production of epoxides is aimed at synthesizing chemicals and reagents for laboratory and pharmaceutical use, for example, synthesizing therapeutic drugs, agrochemicals and food additives [5]. Some of the transition metals which have been applied in catalytic epoxidation include those from group 5, 6 and 7 such as V, Mo, W, Cr, Mg and Re [6-8]. Of these, Mo and W metal complexes have shown high efficiency in the laboratory and industrial catalytic epoxidation [9,10]. Out of the various Mo and W catalysts investigated towards epoxidation, nitrogen base complexes are numerous because of their favourable thermal and electronic properties. This thesis therefore focuses on the synthesis and characterization of metal carbonyl complexes of molybdenum and tungsten and their application as epoxidation catalysts on some selected alkenes. The complexes prepared in this work include the nitrogen-base zero valent and divalent metal complexes. The catalytic evaluation carried out is aimed at establishing the electronic and steric effects of the substrates on the catalytic activities of these new complexes. The following section discusses the chemistry of the zero valent molybdenum and

tungsten complexes. The section elaborates the chemical properties of different  $\sigma$  and  $\pi$ -donor ligands such as carbon donor (carbonyl), non-carbon donor (N-, P-, Cl, Br, Alkyl), straight chain and cyclic unsaturated organic molecules.

### 1.1 Zero valent molybdenum and tungsten carbonyl complexes

Organometallic chemistry of molybdenum and its chemical analogue, tungsten dates back to the mid 20<sup>th</sup> century. These transition elements of group 6 exhibit a range of oxidation states *i.e.* from -2 to +6. This wide variation of oxidation state enhances their diverse chemistry and influences the nature of the complexes they form. Typically, their halides and oxides commonly exist in high oxidation states, +4 to +6 while the carbonyls complexes have low oxidation states ranging between -1 to +1. The halides and oxides of these metals are prone to hydrolysis while their carbonyls compounds are relatively stable. The oxidation states between +2 and +4 are characterized by a mixture of halide, oxide and carbonyl complexes and display diverse and interesting types of reactions [11].

The transition metal carbonyls are one of the most important types of metal complexes known for a long time, for instance Mo and W hexacarbonyls are the known most stable zero valent carbonyl complexes of these two transition metals. They are white, air stable octahedral structured crystals characterized by IR stretching frequencies of 1998  $\text{cm}^{-1}$  and 2004  $\text{cm}^{-1}$  assigned to the carbonyl bond. Other zero valent complexes which can be derived from the metal hexacarbonyls include a mixture of  $\text{C}\equiv\text{O}$  and other electron donor ligands such as N-, P-, As- and O- donor coordinated complexes.

In general, Mo and W complexes display close similarity in terms of their chemical properties and when compared to Cr, which is the first element in the group, they show significant differences [12,13]. In all these complexes, the carbonyls act as Lewis bases. Since different Lewis bases have different electron donor and acceptor abilities, they

influence both the properties of the metal centre and the existing neighbouring ligands and depending on these properties, the Lewis base ligands can be classified as carbon-donor ligands, non-carbon donor ligands, unsaturated straight chain and cyclic organic molecules.

### 1.1.1 Carbonyl Ligands

Carbonyl ligands are good  $\pi$ -acceptor compared to other electron donor ligands. They can therefore stabilize electron-rich low-valent metal centres [14]. The bond between the metal and the  $C\equiv O$ , ( $M-C\equiv O$ ) exhibit three types of interactions, as shown in Figure 1.1 below.

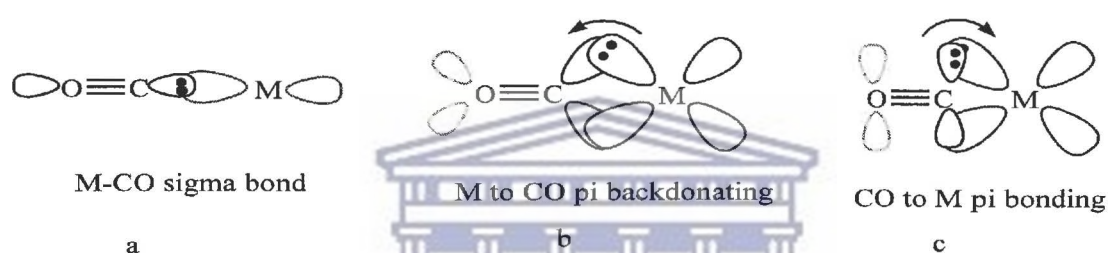


**Fig 1.1:** Types of M-CO bond interaction (A-C)

The carbonyl ligand can also exhibit three bonding modes;  $\mu_1$ -terminal,  $\mu_2$ -bridging and  $\mu_3$ -bridging modes as shown in Figure 1.2.

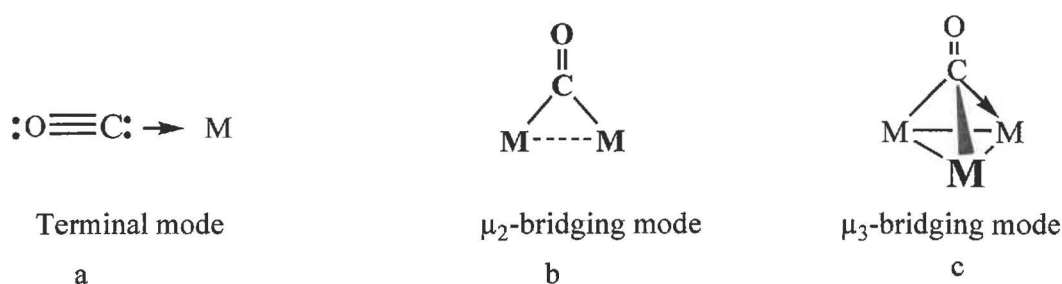


**Fig. 1.2:** Metal- carbonyl bonding modes (a-c)

The stretching frequencies of the carbonyl ligand decreases as the bonding mode moves from terminal ( $1850-2120\text{ cm}^{-1}$ ) to  $\mu_2$ -bridging ( $1720-1850\text{ cm}^{-1}$ ) and to  $\mu_3$ -bridging mode ( $1500-1730\text{ cm}^{-1}$ ). These carbonyl complexes and their derivatives are the most studied type of transition metal complexes due to their relative thermal stabilities.

### 1.1.2 Lewis base Ligands

Lewis base ligands are non-carbon  $\sigma$  donor ligands with the ability to form complexes by donating one or more lone pair of electron to the empty  $d$ -orbitals of the transition metal as shown in Figure 1.3.

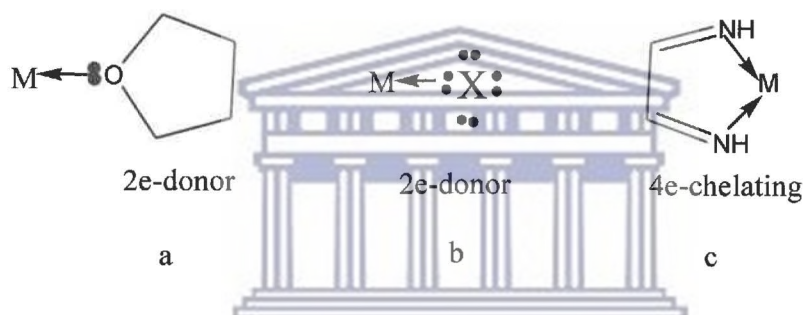


**Fig 1.3:** Lewis base coordination to the transition metal (A-C)

These include group 15 (N-, P- and As-), group 16 (O-, S-, Se-) and group 17 (F<sup>-</sup>, Cl<sup>-</sup>, Br<sup>-</sup>, and I<sup>-</sup>) donor ligands. The stabilities of their complexes are defined with the ability to donate the electrons to the metals empty  $d$ -orbitals.

### 1.1.3 Unsaturated straight chain organic molecules

Unsaturated organic molecules such as alkenes and alkynes can also act as Lewis base sigma donor ligands. The alkene ligands also accept back-donation of electrons into their empty  $\pi^*$ -orbitals as shown in Figure 1.4. Through the  $\sigma$  and  $\pi^*$ -orbitals back-donation, they are able to coordinate to the transition metal.

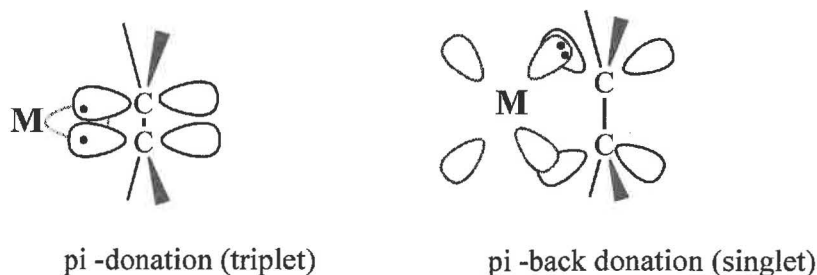
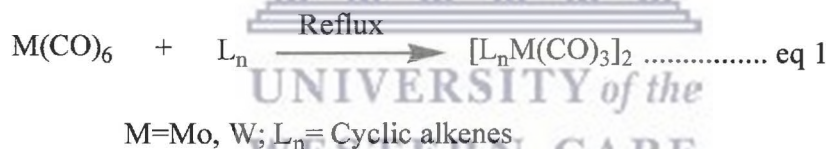


**Fig 1.4:** Coordination of straight chain alkenes

#### 1.1.4 Unsaturated cyclic organic molecules

Cyclic unsaturated hydrocarbons such as benzene, cyclopentadienyl, indene, mesitylene and phenanthrene are also Lewis base ligands because they have  $\pi$ - electrons. They coordinate onto the transition metals by donating their resonating  $\pi$ -electrons into the empty  $d$ -orbitals of the metals [15,16]. The reaction of these unsaturated cyclic hydrocarbons and the metal hexacarbonyls proceed according to equation 1 below [17,18].



These cyclic unsaturated hydrocarbons exhibit different coordination modes which are defined by the number of electrons donated to the empty  $d$ -orbitals of the transition metals. When these cyclic unsaturated hydrocarbons are thermally or photochemically reacted with the metal carbonyls, the type of coordination mode they exhibit determines the number of terminal carbonyl ligands substituted. The three diagrams in Figure 1.5 illustrate three different coordination modes of cyclopentadienyl ligand:  $\eta^5$  (A),  $\eta^3$  (B), or  $\eta^1$  (C) coordination modes.



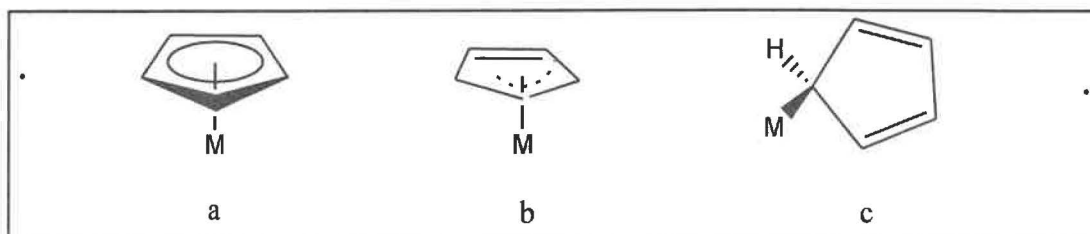
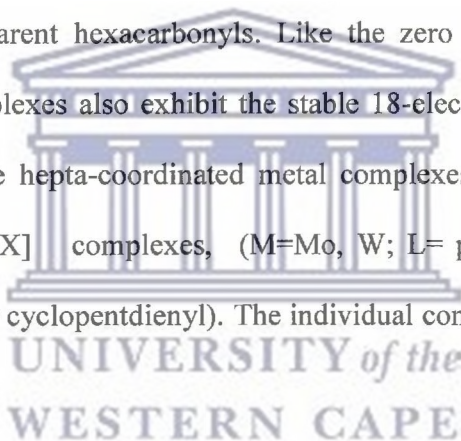


**Fig 1.5:** Coordination modes of cyclopentadienyl ligand (a-c)

## 1.2 Divalent molybdenum and tungsten carbonyl complexes

The Mo and W are also able to form hepta-coordinated complexes and bind weakly coordinating ligands which improve or impose novelty in their catalytic activities and photochemical properties. These hepta-coordinated complexes in most cases exist as divalent complexes derived from the parent hexacarbonyls. Like the zero valent transition metal complexes, these divalent complexes also exhibit the stable 18-electron configuration [19]. Some of the examples of these hepta-coordinated metal complexes include  $[M(CO)_4X_2]_2$ ,  $[MX_2L_2(CO)_3]$  and  $[CpM(CO)_3X]$  complexes, (M=Mo, W; L= phosphines, arsines and nitrogen bases; X=halides; Cp = cyclopentadienyl). The individual complexes are discussed in the following sections.



### 1.2.1 Dihalotetracarbonyl Mo and W dimer complexes

The dihalotetracarbonyl metal dimers,  $[M(CO)_4X_2]_2$  ( $M=Mo, W$ ;  $X=Br, Cl$ ) are prepared by photochemical oxidation of the metal hexacarbonyls in cyclohexane in the presence of the halogens or directly in  $CCl_4$  [20-22]. Alternatively, they can be prepared by halogen oxidation of the metal hexacarbonyl in dichloromethane at  $-78\text{ }^\circ\text{C}$  [23]. They exist as dimers because their mononuclear species, 16 electrons configuration, are very unstable and decompose rapidly in air. They are reported to be good starting materials for several reactions including the preparation of hepta-coordinated tricarbonyl complexes. These *halo*-bridged complexes,  $[M(CO)_4X_2]_2$  ( $M=Mo, W$ ;  $X=Br, Cl$ ) Fig. 1.6, readily dissolve in coordinating solvent such as acetonitrile to give corresponding mononuclear complexes [22,24].

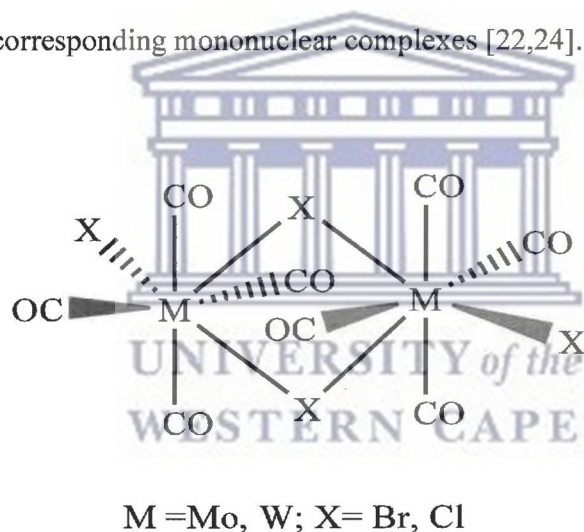
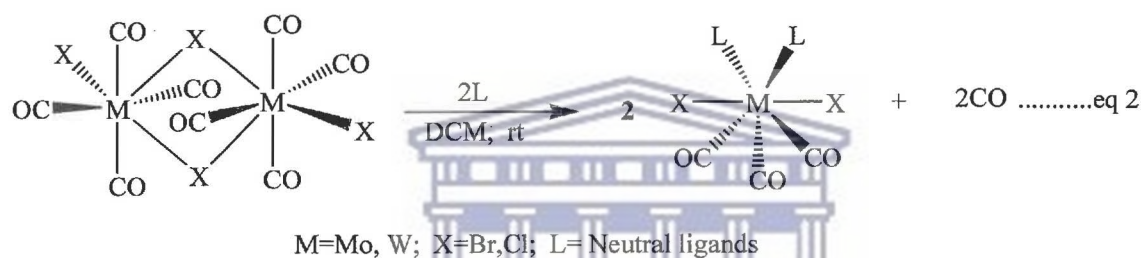


**Fig 1.6:** Structure of dihalotetracarbonyl metal dimer

The  $[M(CO)_4Br_2]_2$  ( $M= Mo, W$ ) dimers are orange powders and can be handled in air when dry. They have been tested towards metathesis of alkene and are found to be able to retain their catalytic properties for more than six months if stored under inert atmosphere at 253K [25].

### 1.2.2 bis-coordinated dihalotricarbonyl Mo and W complexes

The hepta-coordinated complexes,  $[MX_2L_2(CO)_3]$ , (M= Mo, W; X= Cl, Br, I) are successfully prepared from dihalotetracarbonyl metal dimers,  $[M(CO)_4X_2]_2$  by stirring the neutral ligands together with the metal dimer, equation 2, in non-coordinating solvents or by displacement process of the weakly coordinating solvent molecules such as acetonitrile and tetrahydrofuran [26, 27, 28]. The ease and the faster rate with which the carbonyl ligands are displaced in these types of dimer complexes predicts their possible use as catalysts precursors [25].



**Scheme 1.2:** Synthesis of seven coordinated metal carbonyl complex

Similarly, the above compounds may be prepared by oxidation of the zero-valent tricarbonyl complexes with the halogens at 195 K, equation 3 [19, 29]



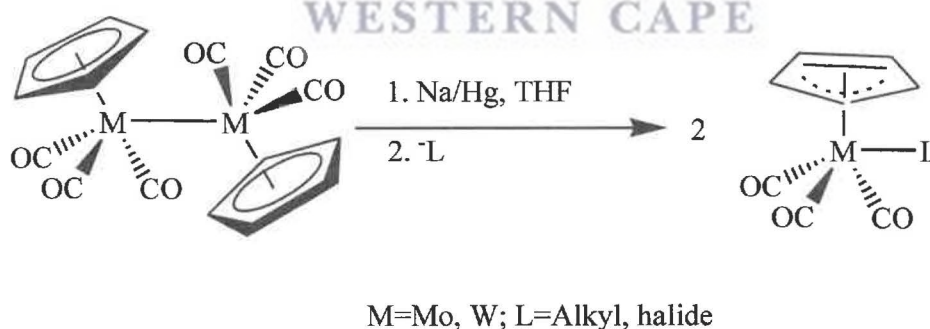
M=Mo, W, L= neutral ligand, X=Br, Cl

Interestingly, Westland and Muriithi observed that the dihalotetracarbonyl metal dimers,  $[M(CO)_4X_2]_2$  (M=Mo, W; X=Br, Cl) react with weaker field ligands with low stabilizing ability such as nitriles, pyridine and tetrahydrofuran via disproportionation of the M(II) to give both the zero  $M(CO)_6$  and the trivalent,  $[MX_3L_3]$  compounds while strong stabilizing ligands such as As- and N- donor ligands preserve the oxidation state of the metals. They also observed that the tungsten analogue,  $[W(CO)_4Cl_2]_2$  reacted with pyridine via a

disproportionation to  $W(0)$  and  $WCl_4(Py)_2$  and that the  $WCl_4(Py)_2$  further transform to  $WCl_3(Py)_3$  upon raising the temperature to  $140\text{ }^\circ\text{C}$  [30]. The bromo- and chloro- derivatives of these hepta-coordinated complexes have been reported to have one geometric conformation in solid state which is depicted with the three carbonyl stretching frequencies observed in their IR spectra. In most cases they exhibit distorted capped octahedron geometry about the metal centre. Their structures as studied by Drew *et al.* have one carbonyl ligand in the unique capping position and one of the halide atom in the capped face [31]. The halide atoms are depicted to be in mutual *trans* position with each other [31-33].

### 1.2.3 Cyclic alkenes tricarbonyl metal (II) complexes

The other type of divalent transition metal complexes involve  $[L_nM(CO)_3X]$ , ( $M=Mo, W$ ;  $L_n=C_5H_5, C_5Me_5, indene, mesitylene$ ;  $X=alkyl, Cl, Br, I$ ). These complexes are easily synthesized from the  $[L_nM(CO)_3]_2$  metal dimers. Scheme 1.2 illustrates the general synthetic procedure for mononuclear cyclopentadienyl metal (II) complex [34].



**Scheme 1.3:** Synthesis of hepta-coordinated cyclopentadienyl tricarbonyl (II) [35]

The reaction proceeds through the initial formation of intermediate,  $[CpM(CO)_3]^-$  anion as shown in equation 4, which further react with the L moiety to produce  $[CpM(CO)_3L]$ . The  $[CpM(CO)_3]^-$  ion can also be obtained by photolytic homolysis of the metal dimers [36,37].

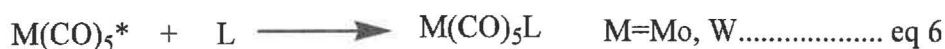


Dessy *et al.* observed that the chemical reduction process, equation 4, which leads to the formation of  $[\text{CpM}(\text{CO})_3]^-$  ion is an irreversible process [38]. However, starting with molybdenum hexacarbonyl, Abrantes *et al.* synthesized chloro derivative,  $[\text{Cp}^*\text{Mo}(\text{CO})_3\text{Cl}]$ , ( $\text{Cp}^* = \text{C}_5\text{Me}_5$ ) [35]. The metal hexacarbonyl was refluxed in propanitrile. The  $[\text{Mo}(\text{CO})_3(\text{EtCN})_3]$  was isolated and  $\text{Cp}^*$  dissolved in toluene was added and the mixture stirred at room temperature. The  $\text{CCl}_4$  was then added to obtain  $[\text{Cp}^*\text{Mo}(\text{CO})_3\text{Cl}]$ , ( $\text{Cp}^* = \text{C}_5\text{Me}_5$ ). The complexes could be easily handled in the air for a long period without decomposition [35].

### 1.3 Substitution reactions of metal hexacarbonyls

The pioneering work on the organomolybdenum chemistry was done by the Nobel laureates Fischer and Wilkinson. They successfully synthesized molybdenum carbonyl derivatives by substituting terminal carbonyls with molecules such as arenes, azulenes,  $\pi$ -cyclopentadienyl, cycloheptatriene, and benzene. Later, the application studies on the roles played by molybdenum in bio-enzymes, high solubility of its salts, abundance and its ability to catalyze olefin disproportionation revolutionized the study of the chemistry of molybdenum [39-41]. Most of these properties are similarly exhibited by W within the same group as Mo. The modern synthetic chemistry aims at stabilizing the known short-lived organometallic intermediates in reactions to utilize their unique properties in the syntheses of other prime compounds [42]. The processes such as carbonyl ligand substitution from the Mo and W hexacarbonyls and subsequently their derivatives are essential in understanding the chemistry of these transition metal complexes either as chemo- or biocatalysts [43]. The terminal

carbonyl ligands of the Mo and W hexacarbonyls are normally strongly bonded and the complexes are very stable such that most Lewis base ligands cannot easily displace them. However, their derivatives with ethers, nitriles and amines provides an easy starting compounds for the syntheses of other Lewis base derivatives because they are weakly coordinating ligands [44,45]. The process of ligand substitution in these transition metal complexes depends on: the overall electron count of the metal complex, the existing ligands on the metal and the steric and electronic properties of the coordinated and the incoming ligands. More specifically, it largely depends on the level of coordinative saturation of the parent metal complexes. These properties put together may lead to either ligand substitution or addition in the complex. Coordinatively saturated complexes exclusively prefer the dissociative substitution pathway while the coordinatively unsaturated complexes usually incorporate the incoming ligands, except for few cases when they have to undergo ligand dissociation [46]. The substitution of the carbonyl ligands in Mo and W hexacarbonyls by Lewis base occurs through a dissociative substitution pathway because the metal hexacarbonyl themselves are coordinatively saturated and the Lewis bases are better electron donors [47]. The process takes place in steps and up to three carbonyl ligands can be displaced by Lewis base donor ligands from groups 15 and 16 (N-, As-, P-, O-, S-) as well as unsaturated hydrocarbons [13,48]. The process go through a complete meta-carbonyl ligand, M-C, bond rapture resulting into dissociative loss of a CO ligand followed by the displacement by a Lewis base ligand, equation 5 and 6 [49].



L- Lewis base ligand

\* coordinatively unsaturated metal carbonyl (16-electrons system)

The dissociation of the C≡O from the metal hexacarbonyl, equation 5 results into a pentacarbonyl intermediate,  $M(CO)_5^*$ , ( $M= Mo, W$ ). The central metal environment in the intermediated is similar to that in coordinative unsaturated state (16-electrons). These coordinative unsaturations make the intermediates very reactive hence it shows non-selectivity towards reaction with any two different and competitive incoming Lewis base ligands [50]. Strong lone pair electron donors immediately coordinate onto the metal centre forming a  $\sigma$ -bond. The resulting derivatives are then stabilized by the removal of the negative charge supplied by the incoming Lewis base ligand through the ligand–metal interaction. As it is well known, the metal back-donates the electrons from filled metallic  $d$ -orbitals into vacant antibonding  $\pi^*$ -orbitals of the ligands as shown in Figure 1.7 [47].



**Figure 1.7:** Lewis base ligand  $\sigma$ -bonding and transition metal  $\pi$ -back-donation to the  $\pi^*$ -orbital of the *trans* carbonyl ligand

The effect of back-donation process is observed when the IR stretching frequencies of the terminal carbonyl ligand/s *trans*- to the Lewis base ligand/s are relatively higher than the *cis*-carbonyl ligands. This IR stretching frequencies can be used to distinguish the carbonyl ligands on the *trans* position from those in the *cis* position. The IR stretching frequencies of the carbonyl bond of *trans*-carbonyls appear higher compared to the *cis*-carbonyls [51]. The extent to which the  $\pi$ - back-donation takes place is influenced by the number and nature of

the Lewis base ligand [46]. Figure 1.8 shows the effect the nature of the Lewis base ligand on the stretching frequencies of the *trans* carbonyl ligands.

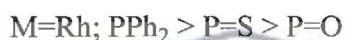
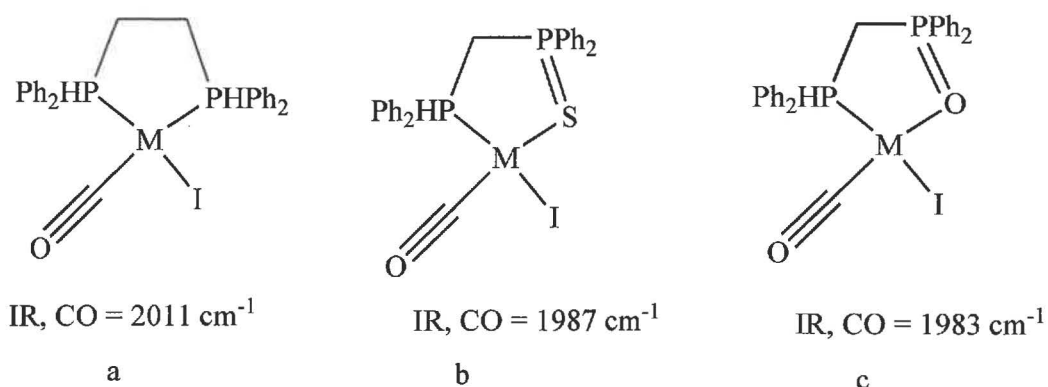


**Fig 1.8:** Effect of  $\sigma$ -donation on the IR stretching frequency of the *trans* carbonyl (a-c) [46]

Good  $\sigma$ -donating ligands do not compete with the carbonyl for the  $\pi$ -back-donation and therefore increases the M-C $\equiv$ O bond strength. They do not compete for the *meta*- to  $\pi$ -back bonding. The illustration in Fig 1.8 shows that PPh<sub>2</sub> is a better  $\sigma$ -donor than P=S and P=O. The electron-back-donation to the terminal ligands, particularly to the *trans* carbonyl ligand is also influenced by the nature of the metal centre; it is observed to be greater for Mo compared to W because W is electron rich than Mo [52].

On the other hand, the poor charge acceptance property exhibited by the Lewis base ligands explains why only up to three terminal carbonyl ligands of the metal hexacarbonyl can be substituted for a mononuclear complex. This is because the extra charge on the metal centre donated by the coordinated Lewis base ligands are transferred to the  $\pi^*$ -orbitals of the carbonyl carbon. This back-donation process makes the M-C $\equiv$ O bond stronger but weakens the *trans* C $\equiv$ O stretching frequency [53].



This also explains why consequent substitution of the  $C\equiv O$  ligands on a metal carbonyl derivative involves the displacement of the *cis*-carbonyl ligands rather than their *trans*-counterparts [54]. However, halides and ligands with electron donor and acceptor properties similar to carbonyl ligands such as acetylene can displace all the  $C\equiv O$  ligands [47]. Ligands with poor electron donors and  $\pi$ - acceptor ability compared to  $C\equiv O$  such as pyridine and amines do not compete with the *trans*- $C\equiv O$  ligands for  $\pi$ -back-donation and thus are regularly used to synthesize other Lewis base donor complexes [43]. Their complexes show higher IR stretching frequencies for the *trans* carbonyls compared to other N-, donor ligands as well as P- and As- ligands.

The back-donation is also believed to create a mesomeric form,  $M=C=O^-$  on the *trans*-carbonyl, where the negatively charge oxygen atom,  $O^-$ , repels any incoming Lewis base ligand. These two observations strongly suggest the preference of formation of *cis*-isomers for *bis*-coordinated metal tetracarbonyl (Fig 1.9a) and *fac*- isomers of the *tri*-coordinated metal tricarbonyl complexes (Fig. 1.9b). However, *bis*-tetracarbonyl complexes of the *trans*-isomers have been isolated in good yields when the refluxing time is lengthened [55].

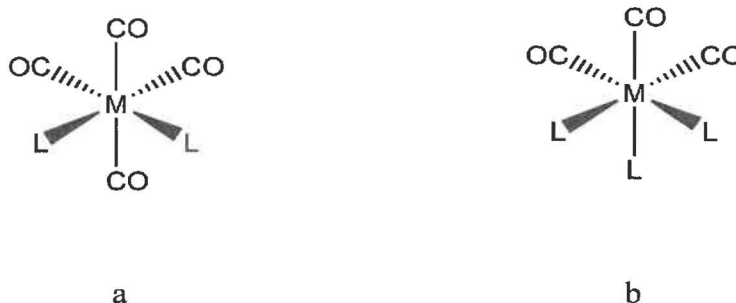


**Fig 1.9:** (a) *cis*-bis-substituted tetracarbonyl (b) *fac*-trisubstituted tricarbonyl

The polarity of the zero valent transition metal carbonyl complex derivatives increases from 0 to 3-coordinated complexes. This is because as the number of the poor electron acceptor ligands increases the charge also build up on the metal centre [47]. This explains why the solubility of the neutral ligand metal carbonyl complexes in polar solvents increases with increase in the number of coordinated ligands. However, the  $\pi$ -bonded complexes such as [(diglyme)M(CO)<sub>3</sub>], [(indene)M(CO)<sub>3</sub>], (M=Mo, W) have similar properties as the parent carbonyls. They are non-polar, volatile and soluble in most organic solvents.

#### 1.4 Nitrogen-base carbonyl complexes of molybdenum and tungsten

Transition metal carbonyl derivatives of nitrogen donor ligands have attracted a lot of interests owing to their thermal stability and better electronic properties for catalytic applications [56]. Specifically, the molybdenum and tungsten metal derivatives have been widely investigated for application in various catalytic reactions such as oxidation and polymerization [57,58]. They may be prepared through photo irradiation of the respective metal hexacarbonyl and the nitrogen bases in weakly coordinating solvents or by substituting the hemilabile ligands of the transition metal carbonyl derivatives with the strong nitrogen donor ligands [55, 59, 60].

The structural stereochemistry of these carbonyl derivatives can be easily deduced by their IR spectra. This is because the carbonyl region ( $1800\text{ cm}^{-1}$  and  $2100\text{ cm}^{-1}$ ) in the IR spectrum is very unique for each complex [55]. The patterns of the carbonyl stretching frequencies successfully distinguish one coordination type from another and are therefore finger printing. Generally, the *mono*-substituted Mo and W pentacarbonyls show IR stretching frequencies in the region between  $1800\text{ cm}^{-1}$ -  $2080\text{ cm}^{-1}$ . The IR band of the highest stretching frequency which is characteristically weak is always assigned to the *trans*-carbonyl ( $2065\text{-}2080\text{ cm}^{-1}$ )

for group 6 metals. In most cases, these pentacarbonyl complexes have square pyramidal molecular structure and  $C_{4v}$  symmetry [47,61]. They are known to be unstable complexes with W forming relatively stable  $M(CO)_5L$  compounds compared to Mo. They are slightly air-sensitive in solution and therefore are preferably handled in inert atmosphere [62]. Bis-substituted tetracarbonyls show four carbonyl stretching frequencies between  $1800\text{ cm}^{-1}$  and  $2020\text{ cm}^{-1}$  in an octahedral molecular structure with  $C_{2v}$  symmetry [60- 64]. The zero-valent tri-substituted tricarbonyl metal complexes are usually characterized by three IR stretching frequencies in the region between  $1800\text{ cm}^{-1}$  and  $2000\text{ cm}^{-1}$  which is unique for the *fac*-isomers and are relative stable in solid state at low temperatures [65]

The molybdenum and tungsten carbonyl derivatives have similar preparation procedures, however, the tungsten complexes take relatively longer to prepare compared to those of molybdenum because of low reactivity and stronger metal-carbonyl, M-C bond. King and Fronzaglia observed that tungsten hexacarbonyl is not a suitable starting material for the synthesis of olefin substituted metal carbonyl complexes. However, they were able to synthesis both molybdenum and chromium carbonyl derivative starting from the corresponding metal hexacarbonyls. This observation is based on the fact that tungsten hexacarbonyl is inert as a result of strong  $W-C\equiv O$  bond created by both  $\sigma$  and  $d\pi-p\pi$  back-donations interaction [52,59,66]. The same property of tungsten hexacarbonyl explains why Beall and Houk were not able to obtain any tungsten carbonyl derivative after refluxing benzocycloheptatriene with  $W(CO)_6$  and  $[W(CO)_3(MeCN)_3]$  but were able to get traces of similar products from Mo and Cr hexacarbonyl [67]

## 1.5 Electronic Spectra studies

The electronic studies are conducted on the compounds to establish the formation of the complexes and to identify if charge transfer reactions were taking place. This spectroscopic study combined with the IR and NMR is very important for proposing the structures of the transition metal complexes [68]. In general, chemical compounds have the ability to absorb both the ultraviolet and visible light a feature which is distinct among different compounds. The UV and visible light absorbed causes excitations of electrons in the  $\sigma$  and  $\pi$ -orbitals and non-bonding orbitals within the molecules. It is therefore important to understand the transitions resulting from the excitations in order to deduce the structures of these compounds and to predict their reactivity. When a molecule absorbs energy from the UV or visible light, the energy is used to promote an electron from Highest Occupied Molecular Orbital (HOMO) to the Lowest Unoccupied Molecular Orbital (LUMO). Out of the HOMOs,  $\sigma$ -orbitals have the lowest energy followed by the  $\pi$ -orbitals and the non-bonding orbitals (containing lone pair electrons) consecutively. There are two unoccupied molecular orbitals;  $\sigma^*$  and  $\pi^*$  [68]. Between the  $\sigma^*$  and  $\pi^*$ , the former has a higher energy compared to the latter. In UV-Vis spectroscopic study of the transition metal complexes, only the possible transitions are expected to be visible and any extra band/s indicates a charge transfer state [69].

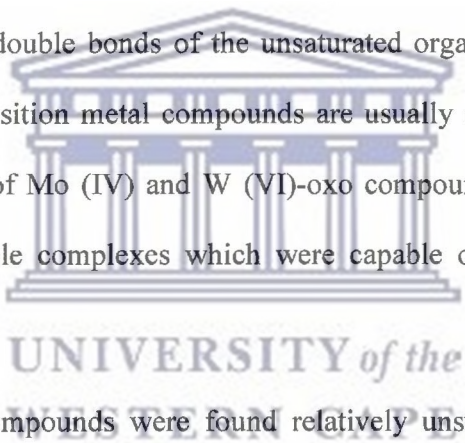
## 1.6 Catalytic epoxidation by molybdenum and tungsten complexes

Most of the compounds produced from chemical and pharmaceutical industries pass through at least a catalytic step [70]. Catalysis is divided into three main sub-groups: homogeneous, heterogeneous and biocatalysis. The divisions are based on the mode of interaction between the catalyst and the substrate during the reaction [71]. Homogeneous catalysts exist in the same phase as the substrates while heterogeneous catalysts exist in different phase. Heterogeneous catalytic systems may exist as either a solid-liquid, immiscible liquid-liquid

and solid-gas systems where the former is the catalyst while the latter is the substrate. Enzymatic or biocatalysis on the other hand is based on the mode of substrate-catalyst active site interaction [72].

Out of the many existing catalytic reactions, oxidation reaction is one of the main areas common in academic and industrial research [71]. Olefins are some of the most important substrates oxidized to other organic products such as epoxides, alcohols, aldehyde and ketone in catalytic oxidation processes. They are not only applied in catalytic oxidation but also susceptible to other significant synthetic and industrial catalytic reactions such as ring opening, metathesis, oligomerization, polymerization and hydrogenation [70,73,74].

Due to relative stability of the double bonds of the unsaturated organic molecules towards different types of reactions, transition metal compounds are usually used to easily catalyze them [22,75]. The prominence of Mo (IV) and W (VI)-oxo compounds came after Mioum and co-workers discovered stable complexes which were capable of being employed for catalytic epoxidation [76].



The M(IV)-oxo (M=Mo,W) compounds were found relatively unstable and decomposed during their synthetic processes. However, they were later found to be easily derived from the corresponding metal carbonyl precursors. The corresponding metal carbonyl complexes could be easily transformed to the high oxidation state oxides and peroxides analogues, by oxidative decarbonylation using various oxygen sources [77]. Figure 1.10 is a graph showing the data obtained in a research conducted to establish the catalytic application of molybdenum compounds between the year 1981- 2001 as depicted by the US patents. The results show that molybdenum oxide compounds is highly used as catalyst compared to the sulphide, carbide, and nitride compounds.

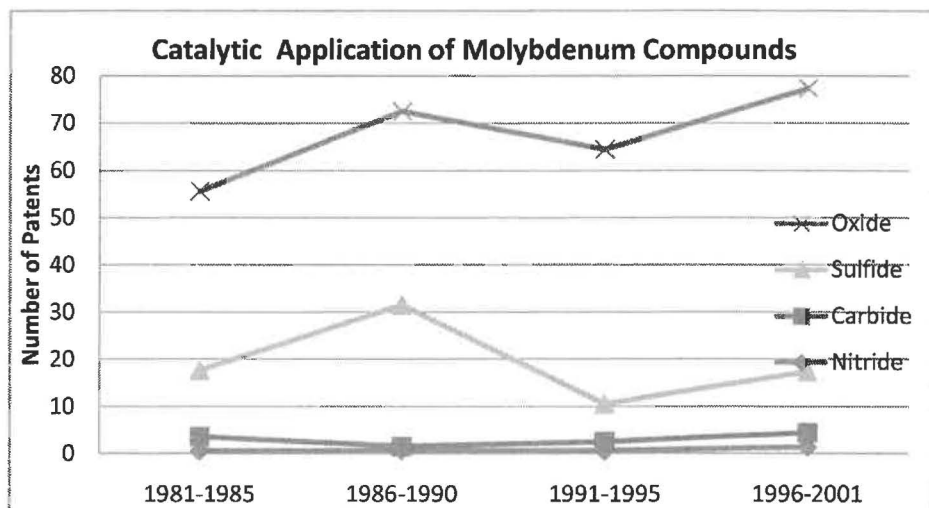
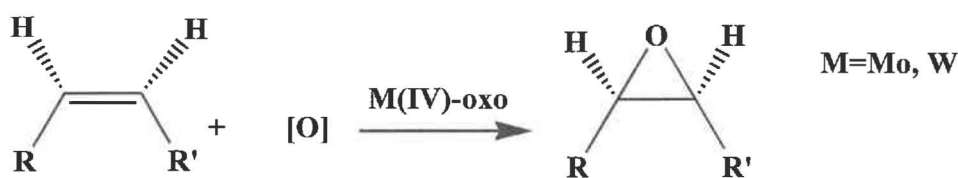
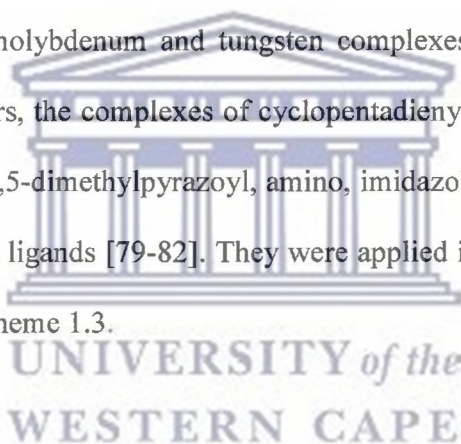


**Fig 1.10:** Catalytic application of molybdenum compounds. US patents according to type of compound [78]

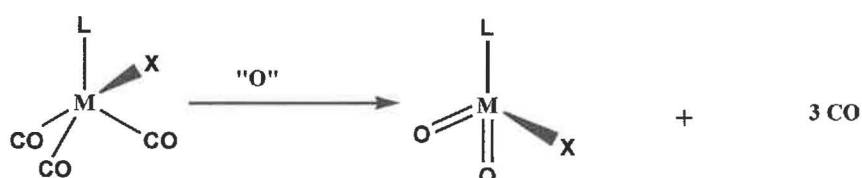
Most of the high valent oxo-molybdenum and tungsten complexes studied for the olefin epoxidation include among others, the complexes of cyclopentadienyl ligands and N-donor base ligands such as bipyridyl, 3,5-dimethylpyrazoyl, amino, imidazole, porphyrin, oxazoline phenanthroline and phosphorous ligands [79-82]. They were applied in epoxidation reactions as illustrated in the following Scheme 1.3.



**Scheme 1.4:** General epoxidation reaction

These cyclopentadienyl and the N-donor complexes are most preferred because of their ability to form thermally stable complexes and are resistant to oxidation as opposed to P-donor complexes [83]. However, the metal-oxo derivatives are notably less air stable and decompose rapidly in solution hence their corresponding metal carbonyl precursors which are

easily transformed to metal-oxo by *in situ* oxidation are preferred for catalytic applications [84]. The *in situ* oxidation of the carbonyl precursors takes place as depicted by Scheme 1.4 below [85,86]. Hydrogen peroxide and alkyl peroxides are preferably used as the oxygen sources for both oxidative decarbonylation of the metal carbonyl precursors and epoxidation [87,88].



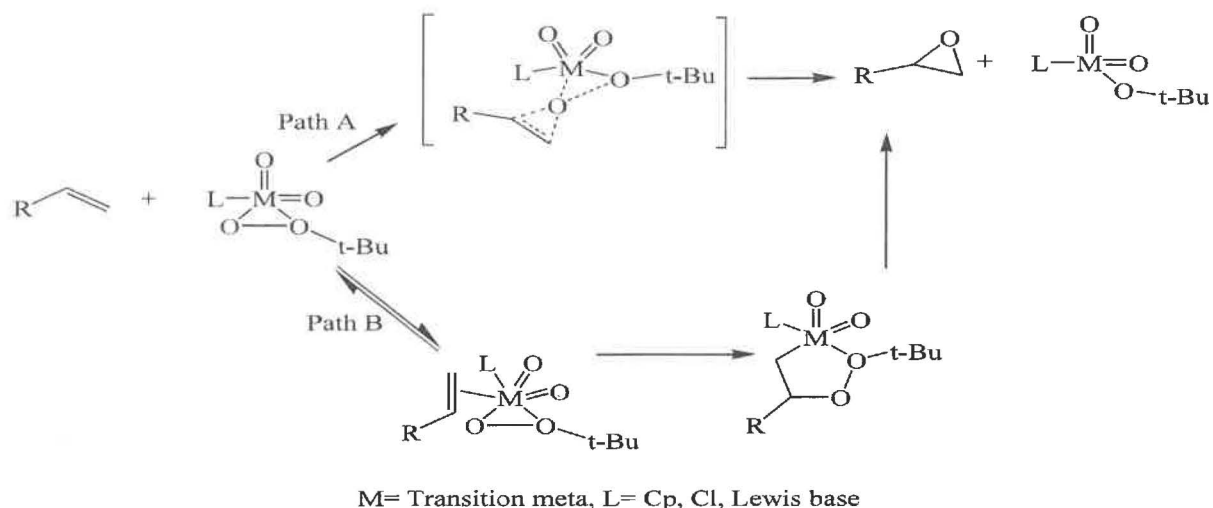
M= Mo, W, L = Cp, Cp\* ligand, X= Alkyl, halide

"O"= Oxygen atom from oxidants

**Scheme 1.5:** Oxidation of metal carbonyl precursor to metal-oxo derivatives

### 1.7 Mechanism of Epoxidation reaction

Various transition metal catalysts have been applied for both laboratory and industrial epoxidation of olefins. For example, the methyltrioxorhenium, MTO and MoO<sub>3</sub> have been applied in industrial epoxidation of alkenes using the oxidants hydrogen peroxides, and tertbutylhydroperoxide, TBHP respectively [89,90]. The mechanism of the epoxidation process by these transition metal catalysts is proposed to occur through either of the two pathways as shown in Scheme 1.5 [91, 92].



**Scheme 1.6:** Mechanism of epoxidation of olefin [92]

Path A depicts that the reaction is initiated by the binding of the terminal oxygen atoms of the oxidant to the metal centre. The oxidant is then activated by the catalyst in readiness for the expected oxygen transfer. The alkene/substrate then binds to the activated oxygen atom; Scheme 1.5-Path A. Path B illustrates an intermolecular nucleophilic attack of coordinated alkene/substrate by the oxidant. The substrate together with the oxidant forms a five-member metallacycle, producing an epoxide and a dioxo-peroxo complex, Scheme 1.5-Path B. In either of the cases, the presence of the transition metal centre is a prerequisite for the transfer of the oxygen atom from the oxidant to the alkene/substrate [93,94].

In the previously studied transition metal catalyzed epoxidation reactions, several oxygen sources were used to produce the epoxide products. The oxidants used include molecular oxygen, hydrogen peroxide, alkyl peroxides, urea-hydrogen peroxide, trimethylsilyl peroxide, sodium hypochlorate among others [95].

From the discussion in this chapter, the properties of Lewis base ligands and their corresponding molybdenum and tungsten complexes are highlighted. The findings of this review are very important in predicting the chemical and physical properties of these



complexes towards their reactivity and molecular structures. The importance of the epoxides as intermediates in the synthesis of other organic compounds has also been highlighted and the process of catalytic epoxidation of alkenes/olefins into their corresponding epoxides is discussed. Using these findings, we synthesized new metal carbonyl complexes, determine their physical properties and to evaluate their catalytic activity towards epoxidation.

### 1.8 Aims and objectives

The review on the chemistry of the synthesis and properties of the zero- and di-valent molybdenum and tungsten carbonyl complexes gives an insight of the unique characteristics of these complexes that make them suitable for the application as catalysts in various chemical reactions. Their recorded performance as oxidation catalysts and ease of preparation are some of the motivating reasons for the vast research work done, a fact that is supported by the richly available literature material.

In this study new nitrogen base and cyclopentadienyl carbonyl complexes of molybdenum and tungsten were prepared, characterized and tested for epoxidation of some selected alkenes. The rationale behind the study was to test new types of both zero and divalent carbonyl complexes of molybdenum and tungsten and to compare their catalytic performance on epoxidation of both straight chain and cyclic alkenes substrate molecules. This was motivated by the recorded performance of the two transition metals particularly toward catalytic oxidation reactions.

The objectives of this study are therefore to:

- i. Synthesize and characterize nitrogen-base carbonyl complexes of Mo (0) and W (0)
- ii. Synthesize and characterize dibromo nitrogen-base carbonyl complexes of Mo(II) and W(II)

- iii. Synthesize and characterize cyclopentadienyl carbonyl complexes of Mo(II) and W(II)
- iv. Evaluate these compounds olefin epoxidation of some selected alkenes
- v. Compare the catalytic activities of these compounds on epoxidation.

The next chapters discuss the synthesis and characterization and the results obtained from characterization and catalytic evaluation of these metal carbonyl complexes towards catalytic epoxidation.



## 1.8 References

---

1. L. Bencze, G. Szalai, J. G. Hamilton, J. J. Rooney, *J. Mol. Catal. A: Chem.*, 1997, **115**, 193-197
2. M. Bagherzadeh, S. E. Ghazali, *Chem. Eng.*, 2010, 131-138
3. K. Kamata, K. Yonehara, Y. Sumida, K. Yamaguchi, I. S. Hikichi, N. Mizuno, *Science*, 2003, **300**, 964-966
4. M. Selvaraj, S. W. Song, S. Kawi, *Microporous and Mesoporous Materials*, 2008, **110**, 427-479
5. D. Hoegaerts, B. F. Sels, D. E. de Vos, F. Verpoort, P. A. Jacobs. *Catal. Today*, 2000, **60**, 209-218
6. G. Grivani, S. Tangestaninejad, M. H. Habibi, V. Mirkhani, M. Moghadam, *Appl. Catal. A: Gen.*, 2006, **299**, 131-136
7. A.C. Cope, R.W. Siekman, *J. Am. Chem. Soc.*, 1965, **87**, 3272-3273
8. G. Natta, P. Pino, G. Mazzanti, *J. Am. Chem. Soc.*, 1957, **79**, 2975-2976
9. M. H. Dickman, M. T. Pope. *Chem. Rev.*, 1994, **94**, 569-584
10. L. Cao, M. Yang, G. Wang, Y. Wei, D. Sun, *J. Polym Sci Pol Chem: Part A: Polymer Chemistry*, 2010, **48**, 558-562.
11. V. A. S. Falconer, S. S. Lemos, J. R. S. Politi, G. A. Casagrande, E. S. Lang, R. A. Barrow, *Inorg. Chem. Commun.* 2009, **12**, 580-582
12. Q. Zhang, K. Sterke, C. Scholzke, A. Hofmeister, J. Magull, *Inorg. Chim. Acta.*, 2007, **360**, 3400-3407

- 
13. L. Hirsivaara, *Coordination Chemistry of arylphosphanes*, Academic dissertation, University of Oulu, Finland, 2001
14. A. Visek, Jr. *Coord. Chem. Rev.*, 2002, **230**, 225-242
15. D. Michael, P. Mingos, *J. Organomet. Chem.*, 2001, **635**, 1-8
16. R. J. Angelici, *J. Chem. Educ.*, 1968, **45**, 119-120
17. M. L. H. Green, *Some Organic Chemistry of Molybdenum and Related Topics*, *Inorg. Chem. Lab*, South parks Rd, Oxford, England, 373-388
18. C. Lopez, M. A. Munoz-Hernandez, D. Morales-morales, F. del Rio, S. Hernandez-Ortega, R. A. Toscano, J. J. Garcia, *J. Organomet. Chem.*, 2003, **672**, 58-65
19. A. M. Bond, R. Colton, K. McGregor, *Organometallics*, 1990, **9**, 1227-1230
20. T. Szymanska-buzar, T. Glowiak, *J. Organomet. Chem.*, 1995, **498**, 207-214
21. T. Szymanska-buzar, *J. Organomet. Chem.*, 1989, **375**, 85-89
22. T. Szymanska-buzar, *J. Mol. Catal. A: Chemical*, 1997, **123**, 113-122
23. M. W. Anker, R. Colton, I. B. Tomkins, *Aust. J. Chem.*, 1967, **21**, 1143-1163
24. F. A. Cotton, L. R. Falvello, J. H. Meadows, *Inorg. Chem.*, 1985, **24**, 514-517
25. A.D. Malkov, I. R. Baxendale, D. Dvorack, D. J. Mansfield, P. Kocovsky, *J. Organomet. Chem.*, 1999, **64**, 2737-2750
26. A.D. Westlands, N. Muriithi, *Inorg. Chem.*, 1972, **11**, 2971-2975

- 
27. M. Al-Jahdali, P. K. Baker, A. J. Lavery, M. M. Meehan, D. J. Muldoon, *J. Mol. Catal. A: Chem.*, 2000, **159**, 51–62
28. A. V. Malkov, I. R. Baxendale, D. Dvorack, D. J. Mansfield, P. Kocovsky, *J. Organomet. Chem.*, 1999, **64**, 2737-2750
29. A. M. Bond, R. Colton, J. J. Jackowski, *Inorg. Chem.*, 1975, **14**, 274-278
30. A. D. Westlands, N. Muriithi, *Inorg. Chem.*, 1973, **12**, 2356-2361
31. P. K. Baker, A. I. Clark, M. G. Drew, M. C. Durrant, R. L. Richards, *Polyhedron*, 1998, **17**, 1407-1413
32. M. G. B. Drew, P. K. Baker, E. M. Armstrong, S. G. Fraser, D. J. Muldoon, A. J. Lavery, A. Shawcross, *Polyhedron*, 1995, **14**, 617-620
33. P. K. Baker, *Chem. Soc. Rev.*, 1998, **27**, 125-132
34. F. Amor, P. Royo, T. P. Spaniol, J. Okuda, *J. Organomet. Chem.*, 2000, **604**, 126–131
35. M. Abrantes, A. M. Santos, J. Mink, F. E. Khun, J. Rocha, *Organometallics*, 2003, **22**, 2112-2118
36. M. Tiletz, *Inorg. Chem.*, 1994, **33**, 3121-3126
37. J. F. Cahoon, M. F. Kling, K. R. Sawyer, H. Frei, C. B. Harris, *J. Am. Chem. Soc.* 2006, **128**, 3152-3153
38. R. E. Dessy, F. E. Stary, R. B. King, M. Waldrop, *J. Am. Chem. Soc.* 1966, **88**, 471-476
39. E. A. Zuech, W. B. Hughes, D. H. Kubicek, E. T. Kittleman, *J. Am. Chem. Soc.* 1970, **92**, 528-531

- 
40. J. T. Spence, H. H. Chancy, *Inorg. Chem.*, 1963, **2**, 319-323
41. R. Hille, *Chem. Rev.* 1996, **96**, 2757-2816
42. Y. G. Budnikova, T. V. Gryaznova, O. G. Sinyashin, S. A. Katsyuba, T. P. Gryaznova, M. P. Egorov, *J. Organomet. Chem.*, 2007, **692**, 4067-4072
43. T. Leysens, D. Peters, A. G. Orpen, J. N. Harvey, *Organometallics*, 2007, **26**, 2637-2645
44. C. M. L Kerr, F. Williams, *J. Am. Chem. Soc.*, 1971, **93**, 2807-2808
45. A. P. Abbott, A. V. Malkov, N. Zimmermann, J. B. Raynor, G. Ahmed, J. Steele, P. Kocovsky, *Organometallics*, 1997, **16**, 3690-3695
46. [chem-faculty.lsu.edu/stanley/webpub/.../chap11-substitution-rxns.doc](http://chem-faculty.lsu.edu/stanley/webpub/.../chap11-substitution-rxns.doc), accessed on 26/10/201
47. I. W. Stolz, G. R. Dobson, R. K. Sheline, *Inorg. Chem.*, 1963, **2**, 323-352
48. R. B King, *Inorg. Chem.*, 1970, **7**, 1936-1937
49. N. N. Litchin, L. A. Roseberg, M. Imamura, *Inorg. Commun.* 1962, 3589
50. E. Bayram, S. Ozkar, *J. Organomet. Chem.*, 2006, **691**, 3267-3273
51. I. W. Stolz, H. H. Hass, R. K. Sheline, *J. Am. Chem. Soc.* 1965, **87**, 716-718
52. R. B. King, A. Fronzaglia, *Inorg. Chem.* 1966, **5**, 1837

- 
53. D. W. Smith, *Inorganic substances: a prelude to the study of descriptive inorganic chemistry*, Press syndicate of the University of Cambridge, Trumpington Street, Cambridge CB2, 1990, 46-47
54. J. D. Atwood, T. L. Brown, *J. Am. Chem. Soc.* 1975, **97**, 3380–3385
55. D. J. Darensbourg, R. L. Kump, *Inorg. Chem.* 1978, **17**, 2680-2682
56. S. O. Ojwach, J. Darkwa, *Inorg. Chim. Acta.*, 2010, **363**, 1947-1964
57. M. S. Saraiva, C. D. Nunes, T. G. Nunes, M. J. Calhorda, *J. Mol. Catal. A: Chem.*, 2010, **321**, 92–100
58. S. M. Bruno, B. Monterio, M. S. Balula, F. M. Pedro, M. Abrantes, A. A. Valante, M. Pillinger, P. Ribeiro-Claro, F. E. Khun, I. S. Goncalves, *J. Mol. Catal. A: Chem.*, 2006, **260**, 11-18
59. M. Ardon, G. Hogarth, D. T. W. O'scroft, *J. Organomet. Chem.*, 2004, **689**, 2429-2435
60. A. Mentos, *Trans. Met. Chem.*, 1999, **24**, 77-80
61. L. E. Orgel, *Inorg. Chem.* 1961, **1**, 25-29
62. W. Jia, L. Tang, Z. Wang, J. Fang, J. Wang, *Trans. Met. Chem.*, 2001, **26**, 400-402
63. R. Garcia-Rodriguez, D. Miguel, *Dalton Trans*, 2006, 1218-1225
64. L. Tang, P. Yang, *Trans. Met. Chem.*, 2004, **29**, 31-34
65. P. K. Baker, M. G. B. Drew, M. M. Meehan, E. E. Parker, *J. Chem. Crystall.* 2003, **33**, 669-672

- 
66. K. Nakamoto, *Infrared and Raman Spectra of Inorganic and Coordination Compounds*, John Wiley and Sons, Inc., Hoboken, New Jersey, 6<sup>th</sup> Ed. 2009
67. T. W. Beall, I. W. Houk, *Inorg. Chem.*, 1974, **13**, 2280-2282
68. D. L. Paiva, G. M. Lampan, G. S. Kritiz, *Introduction to spectroscopy, A guide for students of Organic Chemistry*, 2<sup>nd</sup> ed., 267-293
69. C.N. R. Rao, *Ultraviolet and visible spectroscopy*, 2<sup>nd</sup> ed., Butterworths, London, 1967, Chapter 11
70. A. C. Miralles, Dissertation on Rhenium, molybdenum and Tungsten organometallic homogeneous catalysts, synthesis, characterization and application in olefin epoxidation, Technische Universität München, 2009
71. B. Cornils, W. A. Herrmann, *J. Catal.* 2002, **216**, 23-31
72. R. A. Sheldon, *Adv. Synth. Catal.*, 2001, **343**, 377-378
73. A. de Klerk, *Ind. Eng. Chem. Res.*, 2005, **44**, 3887-3893
74. <http://www.ias.ac.in/resonance/Sept1999/pdf/Sept1999p63-81.pdf> accessed on 7/11/2011
75. K. B. Sharpless, R. C. Michaelson, *J. Am. Chem. Soc.*, 1973, **95**, 6136-6137
76. G. R. Hass, J. W. Kolis, *Organometallics*, 1998, **17**, 4454-4460
77. J. Zhao, A. M. Santos, E. Herdtweck, F. E. Kuhn *J. Mol. Catal. A: Chem.*, 2004, **222**, 265-271
78. [http://www.imoa.info/moly\\_uses/moly\\_compounds/catalysts.html](http://www.imoa.info/moly_uses/moly_compounds/catalysts.html), accessed on 6/7/2011
79. S. Gil, R. Gonzalez, R. Mestres, V. Sanz, A. Zapater, *React. Funct. Polymers*, 1999, **42**, 65-72
80. G. Grivani, S. Tangestaninejad, M. H. Habibi, V. Mirkhani, *Catal. Commun.*, 2005, **6**, 375-378



- 
81. Y. Wong, D. K. P. Ng, H. K. Lee, *Inorg. Chem.*, 2002, **41**, 5276-5285
82. Z. Petrovski, M. Pillinger, A.A. Valente, I. S. Gonclaves, A. Hazell, C. C. Romao, *J. Mol. Catal. A: Chem.*, 2005, **227**, 67-73
83. M. R. Buchmeiser, T. Schareina, R. Kempe, K. Wurst, *J. Organomet. Chem.*, 2001, **634**, 39-46
84. C. Freund, M. Abrantes, F. E. Khun, *J. Organomet. Chem.*, 2006, **691**, 3718-3729
85. M. Abrantes, A. M. Santos, J. Mink, F. E. Kuhn, C. C. Romao, *Organometallics*, 2003, **22**, 2112-2118
86. M. K. Trost, R. G. Bergman, *Organometallics*, 1991, **10**, 1172-1178
87. E. Carreiro, A. J. Burke, *J. Mol. Catal. A: Chem.*, 2006, **249**, 123-128
88. M. Bagherzadeh, L. Tahsini, R. Lafiti, L. K. Woo, *Inorg. Chim. Acta.*, 2009, **362**, 3698-3702
89. W. A. Herrmann, R. W. Fischer, D. W. Marz, *Angew. Chem. Int. Ed. Engl.*, 1991, **30**, 1638-1641
90. G. Grivani, S. Tangestaninejad, M. H. Habibi, V. Mirkhani, M. Moghadam, *Appl. Catal. A: Gen.*, 2006, **299**, 131-136
91. M. D. Bryant, PhD Thesis, Marquette University, U.S.A, 2010
92. J. M. Mitchell, N. S. Finney, *J. Am. Chem. Soc.*, 2001, **123**, 862-869
93. A. O. Bouh, A. Hassan, S. L. Scott, *Catalysis Of Organic reactions, Ed., Chemical Industries (Marcel Dekker)*, 2003, 537-543
94. R. Neumann, *A process for epoxidation of alkenes*, International patent WO,98/54165



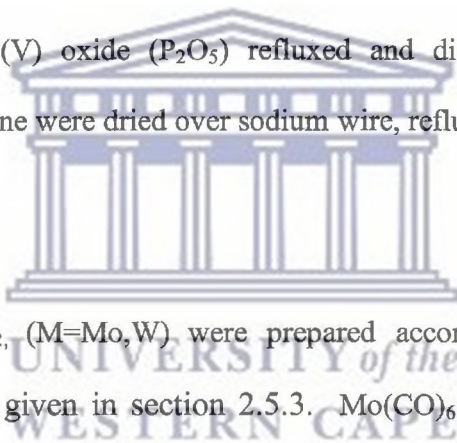
UNIVERSITY *of the*  
WESTERN CAPE

## CHAPTER 2

### 2.0 Experimental Section

#### 2.1 General remarks

All reactions were carried out under dry and oxygen-free nitrogen atmosphere using analar grade reagents and chemicals, nitrogen/vacuum line and following the conventional Schlenk techniques. The solvents used were purified according to standard procedures and purged with dry, oxygen-free nitrogen before being stored in tightly sealed solvent storage bottles [1]. The solvents, Acetonitrile (MeCN) dichloroethane (DCE) and dichloromethane (DCM) were dried over phosphorous (V) oxide ( $P_2O_5$ ) refluxed and distilled under nitrogen. Tetrahydrofuran (THF) and hexane were dried over sodium wire, refluxed and distilled under nitrogen too.



Metal precursors  $[M(CO)_4Br_2]_2$ , (M=Mo,W) were prepared according to the literature procedures [2] and details are given in section 2.5.3.  $Mo(CO)_6$ , (Technical),  $W(CO)_6$ , (97%), cyclopentadienyl molybdenum (II) tricarbonyl dimer, cyclopentadienyl tungsten (II) tricarbonyl dimer, manganese dioxide (>99%), magnesium sulphate ( $\geq 98\%$  (KT)), bromine liquid ( $\geq 99\%$ ), sodium lumps (99%), 3-(1-methylpyrrolidin-2-yl)pyridine ( $\geq 99\%$  GC),  $\alpha$ ,  $\alpha'$ -dibromo-p-xylene ( $\geq 98\%$  GC), and 3,5-dimethylpyrazole ( $\geq 99.0\%$  GC), cis-cyclooctene (95%), cyclooctene oxide (99%) 1-octene (98%), 1,2-epoxyoctane (Aldrich; 96%) styrene (99%), styrene oxide (97%), cyclohexene (99%), cyclohexene oxide (98%), 1-hexene (97%), 1,2-epoxyhexane (97%), isooctane (99.8%) and Tertbutylhydroperoxide, TBHP (80%) were purchased from Aldrich and used without further purification. Each reaction progress was monitored by Infrared (IR) spectrometry and Gas chromatography (GC) as appropriate.

Samples were submitted for elemental analysis at university of Cape Town but have not been analysed because the machine is broken down.

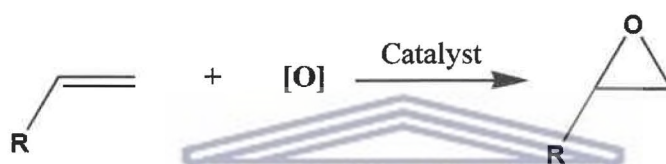
## 2.2 Instrumentation

Infrared spectroscopic measurements in the range between 4000 and 450  $\text{cm}^{-1}$  were recorded on Perkin-Elmer spectrum-100 Series FT-IR spectrophotometer. The  $^1\text{H}$  and  $^{13}\text{C}$  NMR measurements were recorded on a Varian XR200 MHz spectrometer. The  $^1\text{H}$  and  $^{13}\text{C}$  chemical shifts were referenced internally using the residual  $\text{CDCl}_3$  (99.9%) and reported relative to the internal standard tetramethylsilane (TMS). Electronic transitions were recorded on a GBC UV/VIS 920 model spectrophotometer, in the spectral range of 190 nm to 500 nm using a matched quartz cuvettes and path length 1 cm. The electronic transition measurements were taken both in DCM and MeOH to evaluate the effect of polarity in the electronic transitions of the compounds.

Single crystals of compound **C4** suitable for X-ray analysis were grown by slow diffusion of hexane into DCM at  $-4^\circ\text{C}$ . Single X-ray diffraction data were collected on a Bruker KAPPA APEX II DUO diffractometer using graphite-monochromated  $\text{Mo-K}\alpha$  radiation ( $\lambda = 0.71073 \text{ \AA}$ ) at the University of Cape Town. The structures were solved by direct methods using SHELXS-97 and refined by full-matrix least-squares methods based on  $F^2$  using SHELXL-97 and using the graphics interface program X-Seed [3]. The programs X-Seed and POV-Ray were both used to prepare molecular graphic images. All non-hydrogen atoms were refined anisotropically [4]. The structure was successfully refined to R factor of  $\sim 0.01$ . The GC analyses were done on Agilent 7890, GC Column: Agilent 19091J-413;  $325^\circ\text{C}$ : 30 m X 320  $\mu\text{m}$  X 0.25  $\mu\text{m}$ , 5% phenyl methyl Siloxan HP5-column.

### 2.3 Olefin epoxidation reactions

Standard experiments for the liquid-phase epoxidation of *cis*-cyclooctene (Cy<sub>8</sub>), 1-octene (C<sub>8</sub>), Cyclohexene (Cy<sub>6</sub>), 1-hexene (C<sub>6</sub>) and styrene (Sty) were carried out. Tertbutylhydroperoxide, TBHP, was used as oxidant, Isooctane as internal standard (1 mL) and DCE (10 mL), as the solvent for all the reactions. Scheme 2.1 is a general Scheme showing the process of catalytic epoxidation reaction.



**Scheme 2.1: Catalyzed epoxidation reaction**

The catalyst: substrate: oxidant molar ratios of 1:100: 200 were used in all the experiments conducted at 55 °C because most of the similar epoxidation reactions have been carried out successfully in this ratio and at this temperature. TBHP, was used as oxidant because of its relative thermal stability compared to other organic peroxides and the ease of separation of the by-product, tertbutanol from the reaction mixture by simple distillation [5]. DCE was used as solvent of choice for all the reactions because the chlorinated solvents are known to facilitate epoxidation reactions because they easily dissolve both the organic peroxides and the transition metal complexes and they are non-coordinating. DCE was also preferred for these reactions because it has high boiling point (81 °C), suitable for the reactions conducted at 55 °C [6-9].

The catalysts were first stirred with TBHP until the colour change to pale yellow indicating the oxidation of the metal carbonyl compounds to their corresponding high valent dioxo-

metal (IV) compounds as previously observed by Zhao *et al.* They reported that the change of colour of the transition metal carbonyl complexes upon the addition of TBHP is an indication of the formation of high valent dioxo-metal complexes which facilitates oxygen transfer during the catalytic epoxidation [10,11]. The substrates' conversions and epoxides' yields were monitored by sampling at regular intervals. About 1 mL of the reaction mixture was withdrawn each time, diluted with DCM (1 mL) and catalytic amounts of manganese dioxide and magnesium sulphate added to destroy hydrogen peroxide and to remove water respectively. The resulting slurry mixtures were filtered through propylene membrane filters, 30 mm, 0.45  $\mu\text{m}$  pore size. 10  $\mu\text{L}$  of the filtrate from each sample was pipetted and further diluted to 1.4 mL with DCM in a 2 mL GC sample vial. The period for most of the reaction was 24 h but was extended to 48 h for other reactions to establish the thermal stability and efficiency of the catalyst.

The chromatograms obtained for the products were compared with those of the corresponding standard samples commercially obtained from Sigma Aldrich. The Solutions of the standard samples (substrates, internal standard and the corresponding epoxides) were prepared by pipetting 10  $\mu\text{L}$  of each liquid compound and weighing 5% equivalent of each solid catalyst precursor. The mixture was then dissolved in DCM and the solution topped up to 1.4 mL before analysis on the GC. The data obtained; retention times were used to calculate the response factors, R, for each of the substrate and the corresponding peroxide. The following section will highlight the process of calculation of the response factor.

The data used were obtained from the GC analysis of the standard samples, Table 3.9. The retention times were identified by the percentage peak areas, the highest being for the solvent, the second for the dissolved cis-Cyclooctene, Isooctane (internal Standard) and 1,2 epoxyoctane.

The response factor, R, for each of the sample was calculated by using the following equation.

$$R = \frac{[S]}{P. As} * \frac{P. AIS}{[I. S]}$$

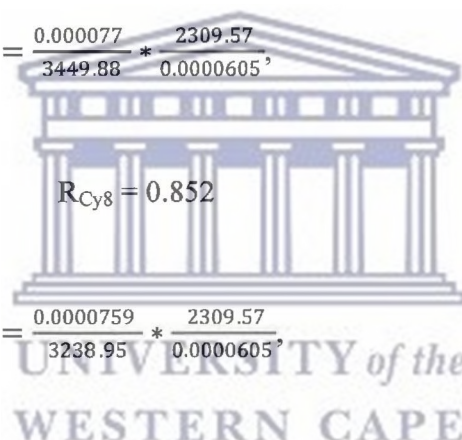
Where,

[I.S]= concentration of the internal standard, Isooctane;

P.As=Peak area of the internal standard; C<sub>y8</sub>= 3449.88, C<sub>y8</sub>O = 3238.95

[S]=concentration of the sample

P.AIS= Peak area of the internal standard; Isooctane = 2309.57


$$R = \frac{0.000077}{3449.88} * \frac{2309.57}{0.0000605}$$
$$R_{C_{y8}} = 0.852$$
$$R = \frac{0.0000759}{3238.95} * \frac{2309.57}{0.0000605}$$
$$R_{C_{y8}O} = 0.894$$

## 2.4 Synthesis of 3-(1-methylpyrrolidin-2-yl) pyridine complexes

### 2.4.1 3-(1-methylpyrrolidin-2-yl) pyridine pentacarbonyl molybdenum (0),

#### *[Mo(CO)<sub>5</sub>(C<sub>10</sub>H<sub>14</sub>N<sub>2</sub>)]-* (C1)

The compound **C1** was prepared following a modified literature procedure [12]. Mo(CO)<sub>6</sub> (0.5 g, 1.89 mmol) was accurately weighed in a clean and dry schlenk tube equipped with a stirrer bar. Freshly distilled MeCN (10 mL) was added and the tube evacuated and filled with dry nitrogen gas. While nitrogen gas was still flowing, a solution of 3-(1-methylpyrrolidin-2-yl) pyridine, (0.30 mL, 1.89 mmol) in acetonitrile (5 mL) was added and the mixture refluxed. The reaction was monitored with regular IR monitoring until no noticeable changes were observed in the IR spectra.

After 8 h the resulting brown solution was filtered under nitrogen and the solvent removed under reduced pressure. The residue was washed with 10 mL of MeCN, recrystallized in DCM/hexane (1:2) and dried under vacuum to give a yellow compound. Yield: 0.58 g (77%). IR (CH<sub>2</sub>Cl<sub>2</sub>), cm<sup>-1</sup>,  $\nu$ (C=O); 2072 m, 1983 sh, 1922 s, 1832 sh,  $\nu$ (C=N); 1602 w,  $\nu$ (C=C); 1578 w,  $\nu$ (C-N); 1314 w. <sup>1</sup>H NMR (CDCl<sub>3</sub>, 200 MHz, rt):  $\delta$  8.49, 8.46 (s, 1H, N=CH, d, 1H, N-CH), 7.75 (d, 1H, CH  $\alpha$ -pyrrolidine), 7.23 (t, 1H, CH- $\beta$ -pyrrolidine), 3.18 (d, 1H, CH- $\alpha$ -Pyrrolidine), 2.38-1.61 (m, 6H, Pyrrolidine ring), 2.15 (s, 3H, CH<sub>3</sub>-pyrrolidine). <sup>13</sup>C NMR  $\delta$  (CDCl<sub>3</sub>, 200 MHz, rt):  $\delta$  214.00, 204.37 (C=O), 154.11, 153.38 (N=CH, N-CH), 141.20 (C-pyridine), 136.36 (CH  $\alpha$ -pyrrolidine), 124.72 (CH- $\beta$ -pyrrolidine), 68.03 (CH-Pyrrolidine), 56.80 (N-CH<sub>2</sub>, pyrrolidine), 40.24 CH<sub>3</sub>-pyrrolidine), 35.51 (CH<sub>2</sub>  $\alpha$ -Pyridine), 22.68 (CH<sub>2</sub>  $\beta$ -pyridine).



#### 2.4.2 3-(1-methylpyrrolidin-2-yl) pyridine pentacarbonyl tungsten (0),



The procedure used to prepare compound **C1** was followed.  $W(CO)_6$ , (0.5g, 1.42mmol) and 3-(1-methylpyrrolidin-2-yl) pyridine, (0.22 mL, 1.42 mmol) was refluxed for 10 hrs in MeCN giving a yellow compound. Yield: 0.43 g (62%). IR ( $CH_2Cl_2$ ),  $cm^{-1}$ ,  $\nu(C=O)$ ; 2075 w, 1997 m, 1928 sh, 1904 s, 1826 sh,  $\nu(C=N)$ ; 1604 w,  $\nu(C=C)$ ; 1581 w,  $\nu(C-N)$ ; 1315 w.  $^1H$  NMR ( $CDCl_3$ , 200 MHz, rt):  $\delta$  8.68, 8.50 (s, 1H,  $J_{HH} = 14$  Hz, N=CH, s, 1H,  $J_{HH} = 10$  Hz N-CH), 7.71 (d, 1H,  $J_{HH} = 8$  Hz CH  $\alpha$ -pyrrolidine), 7.29 (t, 1H,  $J_{HH} = 12$  Hz CH- $\beta$ -pyrrolidine), 3.11 (m, 1H,  $J_{HH} = 32$  Hz, CH- $\alpha$ -Pyrrolidine), 2.39-1.61(m, 6H, Pyrrolidine ring), 2.18 (s, 3H,  $CH_3$ -pyrrolidine).  $^{13}C$  NMR  $\delta$  ( $CDCl_3$ , 200 MHz, rt):  $\delta$  198.75(C=O) 155.35, 149.99 (N=CH, N-CH), 133.08 (CH  $\alpha$ -pyrrolidine), 124.62 (CH- $\beta$ -pyrrolidine), 136.25 (C-pyridine), 68.33 (CH-Pyrrolidine), 55.85 (N- $CH_2$ , pyrrolidine), 38.23  $CH_3$ -pyrrolidine), 32.43 ( $CH_2$   $\alpha$ -Pyridine), 21.37 ( $CH_2$   $\beta$ -pyridine).

#### 2.5 Synthesis of 3, 5-dimethylpyrazole complexes

##### 2.5.1 bis(substituted-di-3,5-dimethylpyrazole)tetracarbonyl molybdenum (0),



Compound **C3** was prepared by suspending  $Mo(CO)_6$ , (0.5 g, 1.89 mmol) in freshly distilled MeCN (15 mL) and 3,5-dimethylpyrazole, (0.181 g, 1.89 mmol) was added and the mixture refluxed for 6 hrs under continuous flow of dry and oxygen-free nitrogen. The reaction was monitored by IR for any changes on the terminal carbonyl stretching frequency region. A dark brown solution formed which was filtered under nitrogen to remove unreacted molybdenum hexacarbonyl. Dry hexane was slowly added to the filtrate and light yellow precipitate formed. The mother liquor was decanted and the precipitate dried under vacuum.

The light yellow solid was again re-crystallized from a dichloromethane/hexane mixture and dried under vacuum. The compound is stable in air but slowly decompose in solution when left in air for a longer time. Yield: 0.56 g (75%). IR (CH<sub>2</sub>Cl<sub>2</sub>), cm<sup>-1</sup>,  $\nu$ (N-H); 3382 br,  $\nu$ (C=O); 2011 w, 1886 s, 1860 sh, 1799 s,  $\nu$ (C=N); 1650 w  $\nu$ (C=C); 1575 s. <sup>1</sup>H NMR (CDCl<sub>3</sub>, 200 MHz, rt):  $\delta$  9.47 (br s, 2H, N-H, pyrazole), 5.88 (d, 2H, CH- pyrazole), 2.25 (s, 6H, CH<sub>3</sub>-C<sup>5</sup>, methyl), 1.95 (s, 6H, CH<sub>3</sub>-C<sup>3</sup>, methyl). <sup>13</sup>C NMR  $\delta$  (CDCl<sub>3</sub>, 200 MHz, rt):  $\delta$  211.88, 204.03 (C=O), 145.30 (C-5, pyrazole), 140.15 (C-3, pyrazole), 106.49 (C-4, pyrazole), 15.46 (CH<sub>3</sub>-C-5, methyl), 10.85 (CH<sub>3</sub>-C-3, methyl).

### 2.5.2 *bis(substituted-3,5-dimethylpyrazole)tetracarbonyl tungsten (0)*,

#### *[W(CO)<sub>4</sub>(C<sub>5</sub>H<sub>8</sub>N<sub>2</sub>)<sub>2</sub>]- (C4)*

The procedure used to prepare compound C3 above was followed. W(CO)<sub>6</sub> (0.5 g, 1.42 mmol) was suspended in freshly distilled acetonitrile (15 mL) and 3,5-dimethylpyrazole (0.136 g, 1.42 mmol) was added. The mixture was refluxed for 8 hrs under continuous flow of dry and oxygen-free nitrogen. A yellow precipitate was obtained after the removal of the mother liquor. The precipitate was dried under reduced pressure, recrystallized from a DCM/hexane mixture and dried under vacuum again. Yield: 0.35 g (51%). IR (CH<sub>2</sub>Cl<sub>2</sub>), cm<sup>-1</sup>,  $\nu$ (N-H); 3420 br,  $\nu$ (C=O); 2001 w, 1926 s, 1872 s, 1815 m,  $\nu$ (C=N); 1656 s  $\nu$ (C=C); 1577 s. <sup>1</sup>H NMR (CDCl<sub>3</sub>, 200 MHz, rt):  $\delta$  9.49 (br s, 2H, N-H, pyrazole) 6.08 (s, 2H, CH- pyrazole), 2.47(s, 6H, CH<sub>3</sub>-C<sup>5</sup>, methyl), 2.01(s, 6H, CH<sub>3</sub>-C<sup>3</sup>, methyl). <sup>13</sup>C NMR  $\delta$  (CDCl<sub>3</sub>, 200 MHz, rt):  $\delta$  219.28, 190.71 (C=O), 144.45 (C-5, pyrazole), 137.59 (C-3, pyrazole) 104.72 (C-4, pyrazole), 14.72(CH<sub>3</sub>-C-5, methyl), 11.92 (CH<sub>3</sub>-C-3, methyl).

### 2.5.3 *dibromo-bis(substituted-3,5-dimethylpyrazole)tetracarbonyl molybdenum (II)*



Compound **C5** was prepared by stirring a mixture of dibromotetracarbonyl molybdenum (II) dimer,  $[\text{Mo}(\text{CO})_4\text{Br}_2]_2$  and excess 3,5-dimethylpyrazole in DCM. The dimer was first prepared by following the literature procedure [2].  $\text{Mo}(\text{CO})_6$  (0.5 g, 1.89 mmol) was suspended in freshly distilled DCM (10 mL). The resulting suspension was reacted with a solution of bromine liquid in DCM (5 mL) at  $-78^\circ\text{C}$  for over 30 min to obtain a yellow solution. The solvent was removed under reduced pressure at  $-78^\circ\text{C}$ . The  $[\text{Mo}(\text{CO})_4\text{Br}_2]_2$  was then dissolved in freshly distilled DCM (10 mL) and excess 3,5-dimethylpyrazole in dichloromethane (10 mL) was added to the yellow solution and the mixture stirred at room temperature for 4 hrs.

The brick red solution was filtered under nitrogen and the solvent removed under reduced pressure. The residue was recrystallized from dichloromethane/hexane, 1:2. Yield: 0.57 g (57%). IR ( $\text{CH}_2\text{Cl}_2$ ),  $\text{cm}^{-1}$ ,  $\nu(\text{N-H})$ ; 3435 br,  $\nu(\text{C=O})$ ; 2093 w, 2033 s, 1946 s,  $\nu(\text{C=N})$ ; 1615 w,  $\nu(\text{C=C})$ ; 1566 w.  $^1\text{H NMR}$  ( $\text{CDCl}_3$ , 200 MHz, rt):  $\delta$  9.37 (br s, 2H, N-H, pyrazole) 5.94 (s, 2H, CH- pyrazole), 2.37(s, 6H,  $\text{CH}_3$ -C-5, methyl), 2.25(s, 6H,  $\text{CH}_3$ -C-3, methyl).  $^{13}\text{C NMR}$   $\delta$  ( $\text{CDCl}_3$ , 200MHz, rt):  $\delta$  201.00, 196.76 (C=O), 145.30 (C-5, pyrazole), 140.28 (C-3, pyrazole), 106.49 (C-4, pyrazole), 15.97( $\text{CH}_3$ - C-5, methyl), 9.86 ( $\text{CH}_3$ - C-3, methyl).

### 2.5.4 *dibromo-bis(substituted-3,5-dimethylpyrazole)tetracarbonyl tungsten(II),*



The procedure used to prepare compound **C5** above was followed.  $\text{W}(\text{CO})_6$  (0.5 g, 1.42 mmol) was used to prepare the  $[\text{W}(\text{CO})_4\text{Br}_2]_2$ . The dark orange solid was dissolved in DCM (10 mL) and excess 3,5-dimethylpyrazole in DCM (10 mL) was added to the orange solution and the mixture stirred at room temperature for 4 h.

A greenish-brown solution was obtained after filtration under nitrogen and the solvent removed under vacuum. The residue was recrystallized from DCM/hexane mixture and vacuum dried. Yield: 0.63 g (72%). IR (CH<sub>2</sub>Cl<sub>2</sub>), cm<sup>-1</sup>,  $\nu$ (N-H); 3428 br,  $\nu$ (C=O); 2089 s, 2013 s, 1928 s,  $\nu$ (C=N); 1616 w,  $\nu$ (C=C); 1569 w. <sup>1</sup>H NMR (CDCl<sub>3</sub>, 200 MHz, rt):  $\delta$  9.49 (br s, 2H, N-H, pyrazole) 5.85 (s, 2H, CH- pyrazole), 2.25 (s, 6H, CH<sub>3</sub>-C<sup>5</sup>, methyl), 2.01 (s, 6H, CH<sub>3</sub>-C<sup>3</sup>, methyl). <sup>13</sup>C NMR  $\delta$  (CDCl<sub>3</sub>, 200MHz, rt):  $\delta$  204.23, 197.41 (C=O), 145.12 (C-5, pyrazole), 141.32 (C-3, pyrazole), 106.74 (C-4, pyrazole), 15.78 (CH<sub>3</sub>- C-5, methyl), 11.19 (CH<sub>3</sub>- C-3, methyl).

## 2.6 Synthesis of 1-(bromomethyl)-4-methylenebenzyl cyclopentadienylcarbonyl complexes

### 2.6.1 1-(bromomethyl)-4-methylenebenzyl cyclopentadienyl tricarbonyl molybdenum (II), [Cp Mo(CO)<sub>3</sub>CH<sub>2</sub>C<sub>6</sub>H<sub>4</sub>CH<sub>2</sub>Br]- (C7)

The Na (0.047 g, 2.05 mmols) was slowly reacted with mercury (6 mL) in a Schlenk tube fitted with a tap at the bottom under nitrogen. The Na/Hg amalgam was allowed to cool to room temperature and freshly distilled THF (10 mL) was added followed by cyclopentadienyl molybdenum (II) tricarbonyl dimer, [Cp(CO)<sub>3</sub>Mo]<sub>2</sub>, (0.506 g, 1.03 mmol). The mixture was stirred at a room temperature for 30 min. The formation of [Cp(CO)<sub>3</sub>Mo]<sup>-</sup> anions was established when the colour of the solution mixture turned from brick-red to pale green [13]. Meanwhile another Schlenk tube was equipped with a stirrer bar and 1,4-dibromomethylbenzene (0.545 g, 2.06 mmol) was accurately weighed and freshly distilled THF (5 mL) added to dissolved. The solution was cooled in a dry ice/acetone bath to temperature between -25 °C - -30 °C for 15 min.

The solution of  $[\text{Cp}(\text{CO})_3\text{Mo}]^-$  anions was added drop wise through the tap and the mixture stirred for 4 hrs. The colour of the solution changed from pale green to orange and finally to brown. The mixture was then filtered under nitrogen to remove NaBr salt. A yellow filtrate was obtained and the solvent was removed under vacuum to obtain a yellow residue. The residue was recrystallized in a DCM/hexane mixture, 1:2, washed with hexane (15 mL) and dried under vacuum. Yield: 0.47 g (47%). IR ( $\text{CH}_2\text{Cl}_2$ ),  $\text{cm}^{-1}$ ,  $\nu(\text{C}=\text{O})$ ; 1996 s, 1899 vs.  $^1\text{H}$  NMR ( $\text{CDCl}_3$ , 200 MHz, rt):  $\delta$  7.14 (s, 2H, Bz), 7.05 (d, 2H,  $J_{\text{HH}} = 2$  Hz, Bz), 5.07 (d, 6H,  $J_{\text{HH}} = 6$  Hz, Cp), 4.36 (s, 2H,  $\text{CH}_2\text{Br}$ ), 2.75 (s, 2H,  $\alpha$ - $\text{CH}_2$ ).  $^{13}\text{C}$  NMR  $\delta$  ( $\text{CDCl}_3$ , 200MHz, rt):  $\delta$  137.92, 129.39, 127.12 (Bz), 93.94 (Cp), 32.78 ( $\text{CH}_2\text{Br}$ ), 1.07 ( $\alpha$ - $\text{CH}_2$ ).

#### 2.6.2 1-(bromomethyl)-4-methylenebenzyl cyclopentadienyl tricarbonyl tungsten (II), $[\text{CpW}(\text{CO})_3\text{CH}_2\text{C}_6\text{H}_4\text{CH}_2\text{Br}]^-$ (C8)

The procedure used to synthesize C6 was followed. Cyclopentadienyl tungsten (II) tricarbonyl dimer,  $[\text{Cp}(\text{CO})_3\text{W}]_2$  (0.507 g, 0.877 mmol) and 1, 4-dibromomethyl benzene (0.46 g, 1.75 mmol) were used. A yellow solid was obtained. Yield: 0.94 g (53%). IR ( $\text{CH}_2\text{Cl}_2$ ),  $\text{cm}^{-1}$ ,  $\nu(\text{C}=\text{O})$ ; 2006 s, 1885 vs.  $^1\text{H}$  NMR ( $\text{CDCl}_3$ , 200 MHz, rt):  $\delta$  7.15 (s, 2H, Bz), 7.01 (s, 2H, Bz), 5.18 (s, 6H,  $J_{\text{HH}} = 6$  Hz Cp), 4.36 (s, 2H,  $\text{CH}_2\text{Br}$ ), 2.83 (s, 2H,  $J_{\text{HH}} = 6$  Hz  $\alpha$ - $\text{CH}_2$ ).  $^{13}\text{C}$  NMR  $\delta$  ( $\text{CDCl}_3$ , 200 MHz, rt):  $\delta$  137.94, 129.41, 128.63, 127.51, (Bz), 92.50 (Cp), 34.37 ( $\text{CH}_2\text{Br}$ ), 32.72 ( $\alpha$ - $\text{CH}_2$ ).

## 2.7 Synthesis of 3-(1-methylpyrrolidin-2-yl)pyridine cyclopentadienyl chlorotricarbonyl complexes

### 2.7.1 3-(1-methylpyrrolidin-2-yl) pyridine cyclopentadienyl chlorotricarbonyl molybdenum (II), [CpMo(CO)<sub>3</sub>Cl(C<sub>10</sub>H<sub>14</sub>N<sub>2</sub>)]- (C9)

The compound **C9** was prepared by first preparing [CpMo(CO)<sub>3</sub>Cl] using a modified procedure by Amor *et. al.* [14]. Cyclopentadienyl molybdenum (II) tricarbonyl dimer, [Cp(CO)<sub>3</sub>Mo]<sub>2</sub>, (0.506 g, 1.03 mmol) was dissolved in THF (10 mL) and the solution added to Na/Hg amalgam. The mixture was stirred until the brick red solution of, [Cp(CO)<sub>3</sub>Mo]<sub>2</sub> turned pale green to confirm the formation of [Cp(CO)<sub>3</sub>Mo]<sup>-</sup> anions [13]. The pale green solution was filtered under nitrogen to another Schlenk tube and excess CCl<sub>4</sub> was added. The solution quickly turned yellow which indicated the formation of [CpMo(CO)<sub>3</sub>Cl]. The yellowish solution of [CpMo(CO)<sub>3</sub>Cl] was then added drop wise to a solution of 3-(1-methylpyrrolidin-2-yl) pyridine (0.33 mL, 2.06 mmol) in THF (5 mL) put in acetone/dry ice bath at a temperature between -25 °C - -30 °C) for 15 min.

The mixture was stirred at a room temperature for 12 hrs after which the solvent was removed under reduced pressure to obtain reddish brown residue. The residue was recrystallized in DCM/hexane ratio 1:2 and dried under vacuum. Yield: 0.55 g (61%). IR (CH<sub>2</sub>Cl<sub>2</sub>), cm<sup>-1</sup>, ν(C=O); 2046 s, 1976 vs, 1939 sh. <sup>1</sup>H NMR (CDCl<sub>3</sub>, 200MHz, rt): δ 8.53, 8.51 (d, 1H, N=CH, 1H, N-CH), 7.89 (d, 1H, CH α-pyrrolidine), 7.30 (t, 1H, CH-β-pyrrolidine), 5.78 (s, Cp), 3.30 (m, 1H, CH-α-Pyrrolidine), 2.53-1.86 (m, 6H, Pyrrolidine ring), 2.24 (s, 3H, CH<sub>3</sub>-pyrrolidine). <sup>13</sup>C NMR δ (CDCl<sub>3</sub>, 200MHz, rt): δ 149.57, 149.21 (N=CH, N-CH), 135.30 (CH α-pyrrolidine), 123.86 (CH-β-pyrrolidine), 95.67 (Cp), 69.18 (CH-Pyrrolidine), 56.63 (N-CH<sub>2</sub>, pyrrolidine), 39.75 CH<sub>3</sub>-pyrrolidine), 34.29 (CH<sub>2</sub> α-Pyridine), 22.23 (CH<sub>2</sub> β-pyridine).

### 2.7.2 3-(1-methylpyrrolidin-2-yl) pyridine cyclopentadienyl tricarbonyl tungsten (II),

#### [CpW(CO)<sub>2</sub>Cl(C<sub>10</sub>H<sub>14</sub>N<sub>2</sub>)]- (C10)

The procedure used to prepare C9 was followed. Cyclopentadienyl tungsten (II) tricarbonyl dimer, [Cp (CO)<sub>3</sub>W]<sub>2</sub>, (0.5 g, 0.865 mmol) and 3-(1-methylpyrrolidin-2-yl) pyridine (0.277 mL, 1.73 mmol) were used as starting materials. An orange residue was obtained. Yield: 0.42 g (51%). IR (CH<sub>2</sub>Cl<sub>2</sub>), cm<sup>-1</sup>, ν(C=O); 2042 s, 1953 s, 1773 w. <sup>1</sup>H NMR (CDCl<sub>3</sub>, 200MHz, rt): δ 8.50, 8.46 (d, 1H, J<sub>HH</sub> = 2 Hz, N=CH, 1H, J<sub>HH</sub> = 2 Hz N-CH), 7.72 (d, 1H, J<sub>HH</sub> = 12 Hz CH α-pyrrolidine), 7.27 (t, 1H, J<sub>HH</sub> = 34 Hz CH-β-pyrrolidine), 5.75 (s, Cp), 3.24 (m, 1H, J<sub>HH</sub> = 34Hz, CH-α-Pyrrolidine), 2.37-1.65 (m, 6H, Pyrrolidine ring), 2.15 (s, 3H, CH<sub>3</sub>-pyrrolidine). <sup>13</sup>C NMR δ (CDCl<sub>3</sub>, 200MHz, rt): δ (C=O), 149.54, 48.67 (N=CH, N-CH), 138.48 (C-pyridine), 134.90 (CH α-pyrrolidine), 123.60 (CH-β-pyrrolidine), 93.91 (Cp), 68.90 (CH-Pyrrolidine), 56.97 (N-CH<sub>2</sub>, pyrrolidine), 40.30 CH<sub>3</sub>-pyrrolidine), 35.08 (CH<sub>2</sub> α-Pyridine), 22.55 (CH<sub>2</sub> β-pyridine).



UNIVERSITY of the  
WESTERN CAPE

## 2.8 References

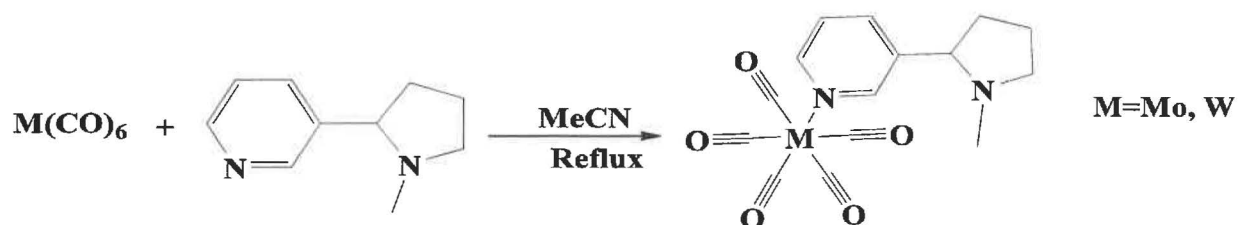
1. R. Keese, R. K. Muller, T. P. Tuobe, *Fundamentals of preparative organic chem.*, J. Wiley-Ellis, Horwood, NY. 1988
2. A.V. Malkov, I. R. Baxendale, D. Dvorack, D. J. Mansfield, P. Kocovsky, *J. Organomet. Chem.*, 1999, **64**, 2737-2750
3. (a) L. J. Barbour, *J. Supramol. Chem.*, 2001, **1**, 189-191. (b). J. L. Atwood. L. J. Barbour, *Crystal. Growth Des.*, 2003, **3**, 3
4. <http://www.povray.org>
5. M. Bregeault, *J. Chem. Soc., Dalton trans.*, 2003, 3289
6. A.A Abdel Aziz, *J. Mol. Struct.*, 2010, **979**, 77-85
7. M. Masteri-Farahani, F. Farzaneh, M. Ghandi, *J. Mol. Catal. A: Chem.*, 2003, **192**, 103-111
8. M. Abrantes, P. Neves, M. M. Antunes, S. Gago, F. A. Almeida Paz, A. E. Rodrigues, M. Pillinger, I. S. Goncalves, C. M. Silva, A. A. Valente, *J. Mol. Catal. A: Chem.*, 2010, **320**, 19-26
9. M. Bagherzadeh, L. Tahsini, R. Latifi, L. K. Woo, *Inorg. Chim. Acta.*, 2009, **362**, 3698-3702
10. J. Zhao, A. M. Santos, E. Herdtweck, F. E. Kuhn, *J. Mol. Catal. A: Chem.*, 2004, **222**, 265-271
11. J. Zhao, E. Herdtweck, F. E. Kuhn, *J. Organomet. Chem.*, 2006, **691**, 2199-2206
12. D. P. Tate, R. Knipple, J. M. Augul, *Inorg. Chem.*, 1962, **1**, 433-434
13. H.B. Friedrich, M.O. Onani, O. Q. Munro, *J. Organomet. Chem.*, 2001, **633**, 39-50
14. F. Amor, P. Royo, T. P. Spaniol, J. Okuda, *J. Organomet. Chem.*, 2000, **604**, 126-131



## CHAPTER 3

### 3.0 Results and Discussion

#### 3.1 3-(1-methylpyrrolidin-2-yl) pyridine pentacarbonyl complexes (C1=Mo, C2= W)



**Scheme 3.1:** Synthesis of pentacarbonyl complexes C1 and C2

Compounds C1 and C2 were prepared as illustrated by Scheme 3.1 above. The coordination of 3-(1-methylpyrrolidin-2-yl) pyridine onto the metal centres occurred after decarbonylation of the metal hexacarbonyls. The complexes could not be prepared by direct reaction of the metal hexacarbonyls with the ligand because the metal hexacarbonyls exhibit strong metal-carbonyl, M-CO bonds as seen from the literature.

The process of coordination of 3-(1-methylpyrrolidin-2-yl) pyridine is proposed to be initiated when one of the terminal carbonyl ligands is first substituted by the weakly coordinating acetonitrile solvent molecule. The coordinated acetonitrile ligand is then easily replaced by the 3-(1-methylpyrrolidin-2-yl) pyridine because of the weak  $\pi$ - $d\pi$  bonds that exist between it and the metals [1]. The remaining terminal carbonyl ligands act to stabilize the complexes against oxidation and thermal decomposition by accepting the extra charge of the metal centre into their  $\pi^*$ -orbitals [2].

### 3.1.1 IR spectroscopic analysis of C1 and C2

Figure 3.1 shows the IR spectrum for compound C2. The spectrum obtained for C1 is given in Fig A3.1 (See appendix).

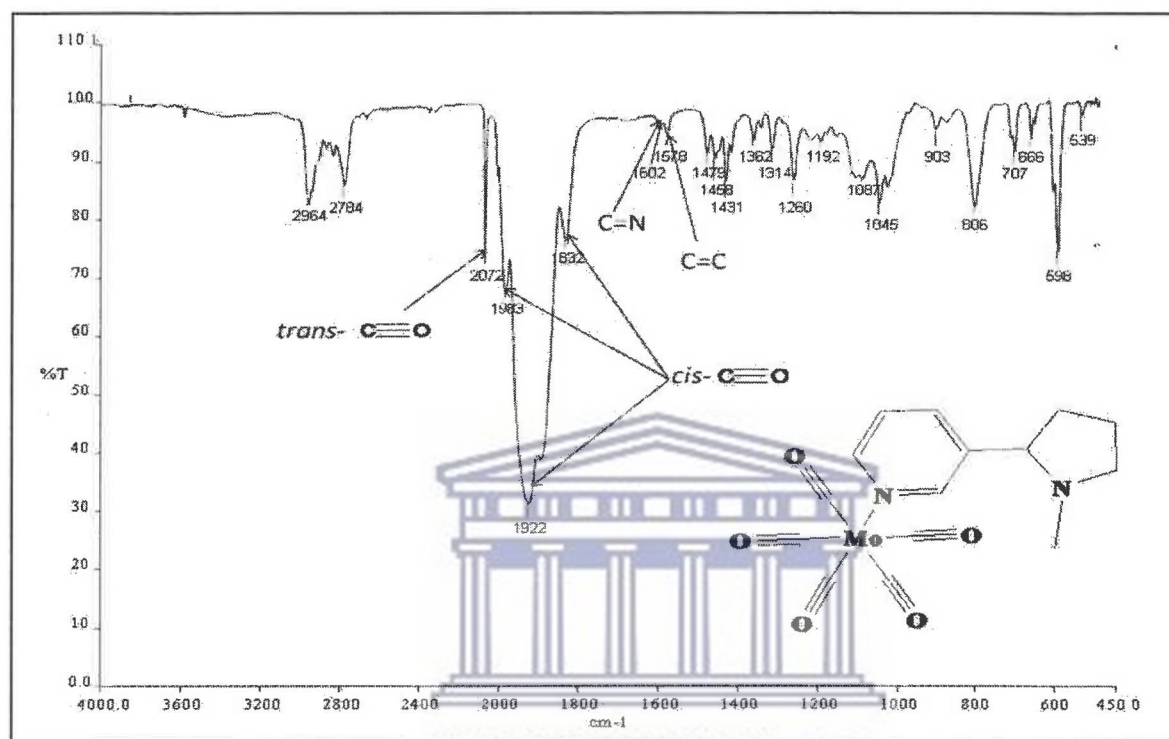


**Fig 3.1:** IR spectrum for 3-(1-methylpyrrolidin-2-yl) pyridine pentacarbonyl molybdenum (0)- (C1)

The stretching frequencies of the selected functional groups for compounds C1 and C2 are compared with the corresponding frequencies of uncoordinated ligand. While the 3-(1-methylpyrrolidin-2-yl) pyridine spectrum has no peaks in the region between 1700 cm<sup>-1</sup> and 2100 cm<sup>-1</sup>, the spectra of compounds C1 and C2 showed four peaks between 1826 cm<sup>-1</sup> and 2075 cm<sup>-1</sup>. These peaks are attributed to the IR stretching frequencies of the terminal carbonyl ligands. The presence of the band with the highest stretching frequency at 2072 cm<sup>-1</sup> and 2075 cm<sup>-1</sup> for compounds C1 and C2 respectively is suggesting that these compounds are metal pentacarbonyls. This band which is weak is characteristically common for the

pentacarbonyl compounds for example those prepared by Stolz *et al.* and Kraihanzel *et al* [3]. Kraihanzel *et. al* reported this peak in the region between 2071  $\text{cm}^{-1}$  and 2079  $\text{cm}^{-1}$  for amine substituted molybdenum and tungsten pentacarbonyl compounds. Fowles and Jenkins reported the values between 2080  $\text{cm}^{-1}$  and 2069  $\text{cm}^{-1}$  wavenumbers for the N-coordinated molybdenum and tungsten pentacarbonyl compounds. The band having the highest frequency is most intense and characteristically broad. It is usually observed at the region between 1900  $\text{cm}^{-1}$  and 1950  $\text{cm}^{-1}$  as previously reported [3-6]. These substituted metal pentacarbonyl compounds are characterized with the square pyramidal arrangements of the terminal carbonyl ligands which gives rise to 3-4 absorption bands [3,5,6]. The carbonyl stretching frequency values recorded for these compounds, C1 and C2 are consistent with those observed by Wen-Li *et al.* and Zingales *et al.* for the pentacarbonyl complexes such as pyridine, ferrocenylpyrazole and 4-picoline pentacarbonyl molybdenum complexes. Tang *et al.* reported 5-6 terminal carbonyl bands, the lowest at 1825  $\text{cm}^{-1}$  and the highest at 2075  $\text{cm}^{-1}$  [6,7].

Significant shifts from 1590  $\text{cm}^{-1}$  to 1599  $\text{cm}^{-1}$  (C1) and 1604  $\text{cm}^{-1}$  (C2) of the pyridine ring C=N bond IR stretching frequencies are observed indicating the coordination of the 3-(1-methylpyrrolidin-2-yl) pyridine ligands. The increase in C=N bond stretching frequency can be attributed to the effect of bond polarization because the  $\sigma$  donation from the N-atom of the 3-(1-methylpyrrolidin-2-yl) pyridine reducing the electron density on it. The electron back donated to  $\pi^*$ -orbitals is delocalized over the N=C bond. This implies that the N atom becomes positively charged while the C atom is negatively charged. The bond polarization therefore increases the stretching frequency of the C=N bond as observed [8]. The shifts observed on the IR stretching frequencies of the C=N bonds is proposed to be influenced by the electronegativity of the transition metals. The more electronegative the metal is the greater the shift because the  $\sigma$ -donation is expected to be least. This effect was observed

when the IR stretching frequencies of the C≡N bond were compared for divalent complexes of Ni, Pd and Pt which are all in group 10. The results show that the C≡N bond stretching frequencies were 2128 cm<sup>-1</sup>, 2143 cm<sup>-1</sup> and 2150 cm<sup>-1</sup> for Ni, Pd and Pt respectively; the order of their increasing electronegativity [9]. The spectrum of compound **C2** showed the highest value for the C=N stretching frequency compared to **C1** which is consistent with the higher electronegativity exhibited by W when compared to Mo [10].

The IR stretching frequencies values 1314 cm<sup>-1</sup> (**C1**) and 1315 cm<sup>-1</sup> (**C2**) were attributed to the C-N bond of the pyrrolidine ring. They showed no significant shift from the value recorded for the uncoordinated 3-(1-methylpyrrolidin-2-yl) pyridine (1314 cm<sup>-1</sup>). This observation and those discussed above indicate that the pyrrolidine ring nitrogen atom did not coordinate to the metal centre. A summary of the IR stretching frequencies for the important functional groups is given in Table 3.1.

**Table 3.1:** A summary of IR data for 3-(1-methylpyrrolidin-2-yl) pyridine, **C1** and **C2**

Compound	Stretching frequencies, cm <sup>-1</sup>			
	CO	C≡N	C=C	C-N
Ligand	-	1590	1576	1314
<b>C1</b>	2072, 1983, 1922, 1832	1602	1578	1314
<b>C2</b>	2075, 1997, 1904, 1826	1604	1581	1315

### 3.1.1. $^1\text{H}$ NMR spectroscopic analysis of C1 and C2

Figure 3.2 shows the  $^1\text{H}$  NMR spectrum obtained for the compound **C1**. A section of the spectrum and the spectrum obtained for **C2** are given in Fig A3.2 (See Appendix).

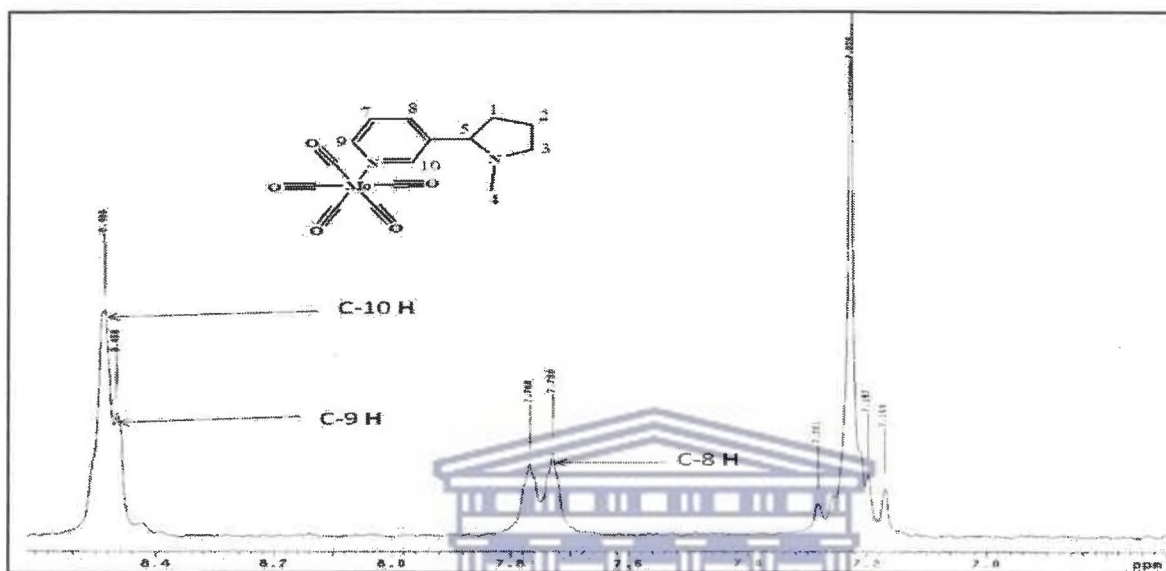


**Fig 3.2:**  $^1\text{H}$  NMR spectrum for 3-(1-methylpyrrolidin-2-yl) pyridine pentacarbonyl molybdenum (0)-(C1)

The  $^1\text{H}$  NMR spectra for compounds **C1** and **C2** indicated that there are noticeable chemical shifts on the protons of the pyridine ring of the coordinated 3-(1-methylpyrrolidin-2-yl) pyridine ligand compared to the uncoordinated ligand. The proton,  $\text{H}-\text{C}=\text{N}$  chemical shift values is recorded at 0.03 ppm up field and 0.16 ppm down field for **C1** and **C2** respectively compared to that of the uncoordinated ligand. Similarly, noticeable shifts were observed in the protons coordinated to the carbon atoms, C-9 and C-8. The chemical shifts, **C2** for the protons  $\text{HC}-9$  and  $\text{HC}-10$  are shifted more down field compared those of **C1**. This may be as a result of unequal deshielding of the electron density on the carbon atoms surrounding the pyridine nitrogen by the different metal centres. The electron density reduction on C-10 and C-9 cause the down field proton chemical shift.

The reduction in electron density is observed to be relatively greater in the tungsten complex compared to the molybdenum. Table 3.2 summarises the chemical shifts of important functional groups in the ligand, 3-(1-methylpyrrolidin-2-yl) pyridine and the compounds **C1** and **C2**.

**Table 3.2:** A summary of  $^1\text{H}$  NMR data for 3-(1-methylpyrrolidin-2-yl) pyridine, **C1** and **C2**

Compound	C-10 <i>H</i>	C-9 <i>H</i>	C-5 <i>H</i>	C-4 <i>3H</i>
Ligand	8.52	8.49	3.17	2.17
<b>C1</b>	8.49	8.46	3.18	2.15
<b>C2</b>	8.68	8.50	3.11	2.18

Significant shifts are observed on the protons at position 9 and 10 on the pyridine ring which indicated the coordination of the 3-(1-methylpyrrolidin-2-yl) pyridine via the (N=CH) in the pyridine ring. The protons attached to the carbon atoms C-9 and C-10 are close to the imine nitrogen which is involved in the coordination. The changes in the chemical shifts observed for the C-9 and C-10 are due to the change in electron density on the imine moiety (C=N) after coordination. Other chemical shifts associated with the potential atoms liable for coordination did not show any observable change and this led to the conclusion made.

The electron donated to the empty *p*-orbitals of the metal is transferred to the  $\pi$ -orbitals of the carbon atom of the *trans*-carbonyl ligand, since it is a good  $\pi$ - acceptor compared to the nitrogen atom [11]. Through induction the amine nitrogen becomes partially positively charged resulting to the down field shift observed.

### 3.1.2 $^{13}\text{C}$ NMR spectroscopic analysis of C1 and C2

Figure 3.3 shows a  $^{13}\text{C}$  NMR spectrum of C1. The  $^{13}\text{C}$  NMR spectrum obtained for C2 is given in Fig A3.3 (See Appendix).

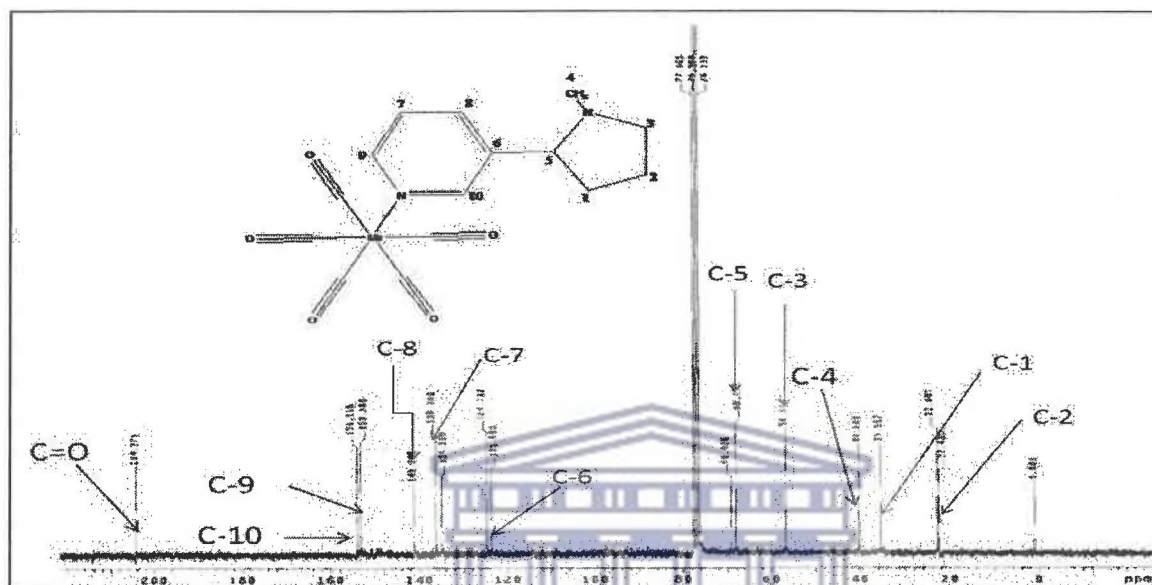


**Fig 3.3:**  $^{13}\text{C}$  NMR spectrum for 3-(1-methylpyrrolidin-2-yl)pyridine pentacarbonylmolybdenum (0)-(C1)

The characteristic chemical shifts, 154.11 ppm and 155.32 ppm (C1) and 153.38 ppm and 154.59 ppm (C2) for the pyridine ring C=N and -C-N= carbon respectively show significant downfield shifts compared to those of the uncoordinated ligand, 149.45 ppm and 148.51 ppm. These two carbon atoms are deshielded by the coordination of the 3-(1-methylpyrrolidin-2-yl)pyridine resulting to the down field chemical shifts observed. The shifts are generally greater in the compound C2 than C1 which can be explained by the difference in the electronic properties of the two metal centres. The shifts observed at 204.37 ppm (C1) and 191.10, 198.92 ppm (C2) are associated with the carbon atoms of the terminal carbonyl ligands.

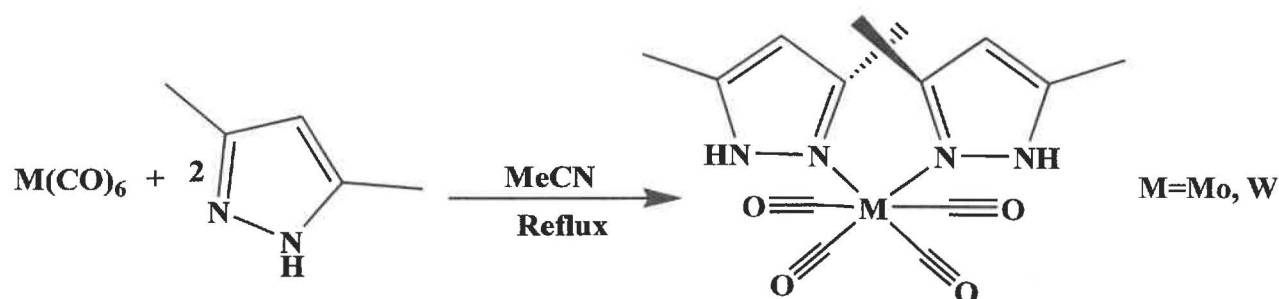
The  $^{13}\text{C}$  NMR spectrum of **C2** shows that the terminal carbonyls are inequivalent sites. The chemical shift that appears further down field, 198.92 ppm, is attributed to the *cis*-carbonyl while the *trans*-carbonyl, 191.91 ppm because it is shielded by the  $\pi^*$ -back donation of electrons from the metal centre [12]. A summary of the chemical shifts recorded for selected carbon atoms are given in Table 3.2.

**Table 3.3:** A summary of  $^{13}\text{C}$  NMR for 3-(1-methylpyrrolidin-2-yl) pyridine, **C1** and **C2**

Compound	C=O	C-10	C-9	C-5	C-4
Ligand	-	149.45	148.51	68.83	40.32
<b>C1</b>	204.37	154.11	153.38	68.03	40.24
<b>C2</b>	198.92, 191.10	155.32	154.59	69.12	40.24

### 3.2 *Bis*-3, 5-dimethylpyrazole tetracarbonyl complexes

Compounds **C3** and **C4** were prepared by following the procedure used to prepare and isolate **C1**, (section 2.4.1). The procedure is illustrated by the Scheme 3.2. Compound **C3** and **C4** were isolated as light yellow and yellow air stable solids respectively.



**Scheme 3.2:** Synthesis of 3, 5-dimethylpyrazole tetracarbonyl metal complexes **C3** and **C4**



### 3.2.1 IR spectroscopic analysis of C3 and C4

Figure 3.4 shows the IR spectrum for compound C4. The IR spectrum obtained for C3 is given in Fig A3.4 (See appendix).

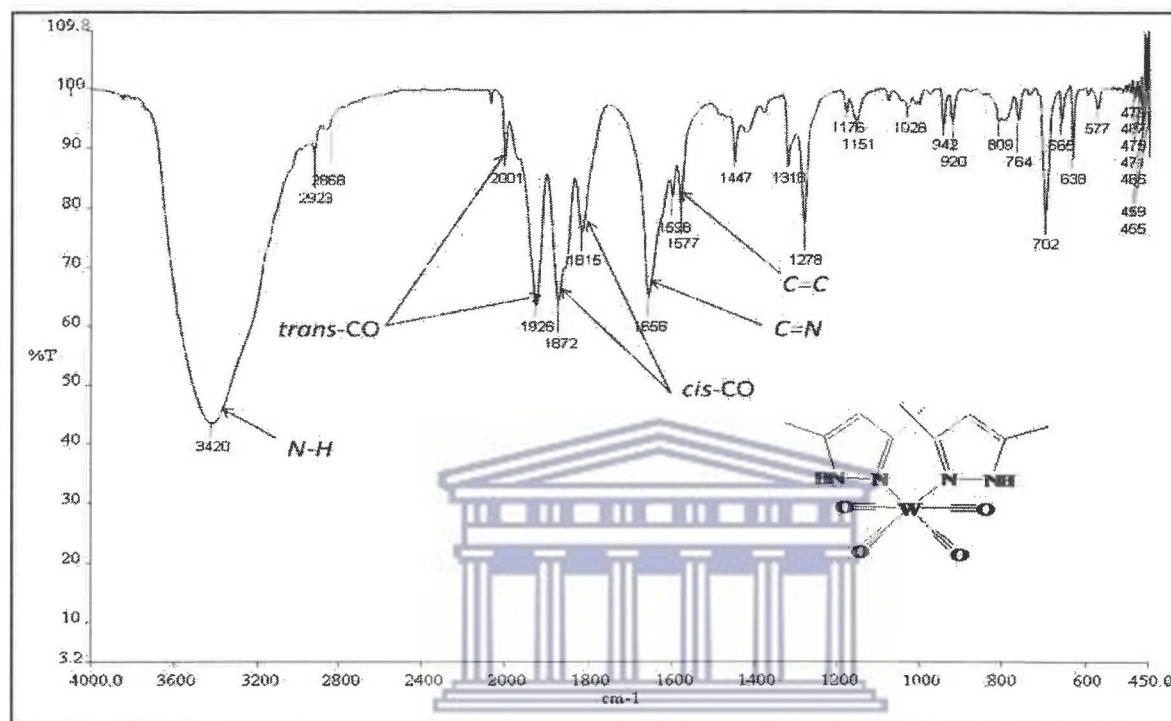


Fig 3.4: IR spectrum for 3, 5-dimethylpyrazole tetracarbonyl tungsten (0) - (C4)

The IR spectra show four absorption peaks between 1799 cm<sup>-1</sup> and 2011 cm<sup>-1</sup> and N-H absorption peaks at 3382 cm<sup>-1</sup> (C3) and 3420 cm<sup>-1</sup> (C4). The four absorption bands are as a result of all the four non-degenerate terminal C≡O bond stretching modes. The peaks display a familiar pattern associated with *bis*-coordinated tetracarbonyl Mo and W complexes and the two middle terminal C≡O absorption bands are of almost the same intensity but stronger than the two at a higher and lower frequencies as previously observed by Kraihanzel and Cotton [Error! Bookmark not defined.]. These peaks are also in the same stretching frequency region (2015 cm<sup>-1</sup> -1831 cm<sup>-1</sup>) observed by Ardon *et al.* for similar complexes [13,14].

The IR bands for N-H bond shifted to lower stretching frequencies compared to  $3450\text{ cm}^{-1}$  recorded for the uncoordinated 3, 5-dimethylpyrazole ligand. They were in the same range as  $3446\text{ cm}^{-1}$ , and  $3384\text{ cm}^{-1}$  by Tang *et al.* [15]. The shifts on the stretching frequency observed for the N-H bond can be attributed to the intramolecular interaction due to the  $\text{N-H}\cdots\text{O}\equiv\text{C}$  hydrogen bonding [15,16]. The  $\pi^*$ -back donation cause the mesomeric,  $\text{O}=\text{C}=\text{M}^+$ , form of the *trans*-carbonyl ligands resulting to the interaction between the acidic N-H and the basic oxygen  $\text{O}=\text{C}=\text{M}^+$ . The hydrogen bonding interaction weakens the N-H bond hence the observed shift on the IR stretching frequencies to the lower wave numbers. The hydrogen bonding also causes the broadening of the N-H absorption peak as observed in the IR spectra of **C3** and **C4** [19,17,18].

The absorption peaks initially not observed in the uncoordinated 3,5-dimethylpyrazole ligand were observed at  $1650\text{ cm}^{-1}$  and  $1656\text{ cm}^{-1}$  for the **C3** and **C4** respectively and are attributed to the C=N bond stretching frequency. The C=C bond stretching frequencies are observed to shift to the lower frequencies by  $\sim 10\text{ cm}^{-1}$  in both compounds. This is proposed to be indication the electronic effect on the pyrazole ring after coordination onto the metal centre. The reduction of the electron density on the ring due to the  $\sigma$  bonding improved the electron donation from the methyl group attached to C-5 this in turn causes the electron repulsion between the C=C  $\pi$ -electrons and the electron from the methyl group. The C=C bond is weakened as a result hence the observed reduction in stretching frequencies.

It is also observed that the intensity of the C=C absorption band has greatly reduce after coordination. A summary of the stretching frequencies for the main functional groups for the **C3** and **C4** are given in Table 3.4.

**Table 3.4:** A summary of IR data for 3, 5-dimethylpyrazole, C3 and C4

Compound	Melting Point (°C)	Stretching frequencies, cm <sup>-1</sup>			
		CO	C=N	C=C	N-H
Ligand		-	-	1586	3450
C3	143-146	2011, 1886, 1860, 1799	1650	1575	3382
C4	128-132	2001, 1926, 1872, 1815	1656	1577	3420

### 3.2.2 <sup>1</sup>H NMR spectroscopic analysis of C3 and C4

Figure 3.5 shows the <sup>1</sup>H NMR spectrum obtained for the compound C3. The spectrum obtained for C4 is given in Fig A3.5 (See appendix). The <sup>1</sup>H NMR spectra of the compounds C3 and C4 suggests that the two coordinated pyrazole ligands are chemically equivalent.

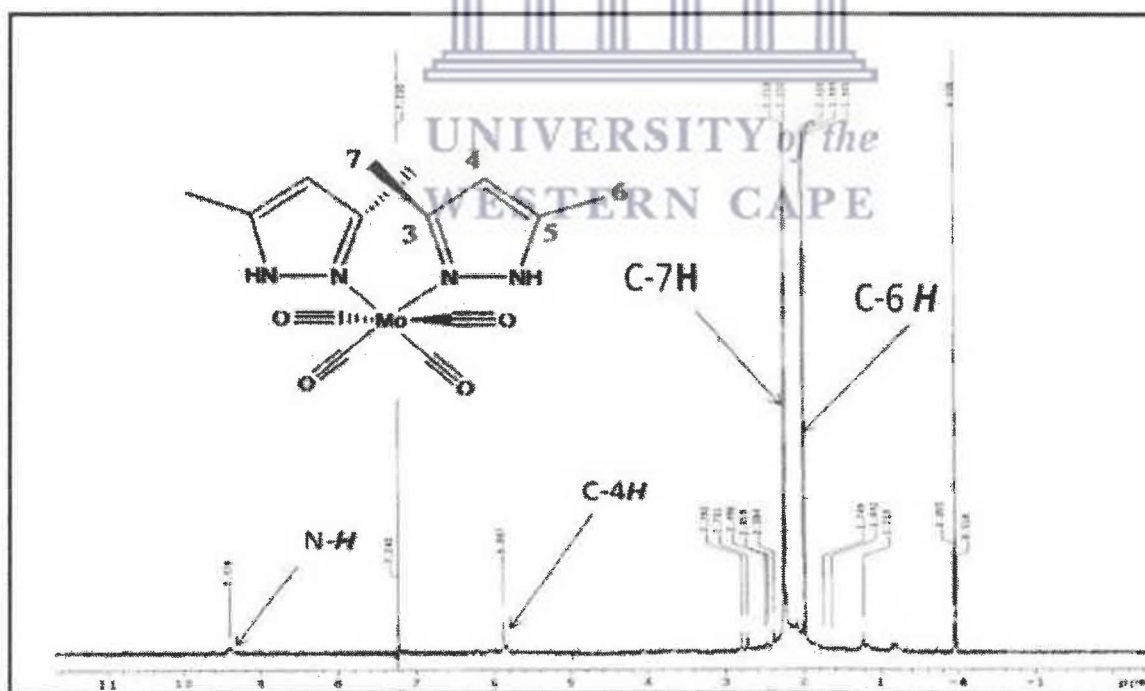


**Fig 3.5:** <sup>1</sup>H NMR spectrum for 3, 5-dimethylpyrazole tetracarbonyl molybdenum (0)-(C3)

The signals for the pyrazole protons had a general downfield shift compared to those of the uncoordinated ligand. The C-7 methyl proton chemical shifts for the **C3** and **C4** are observed to differ by 0.22 ppm. This observation may be as a result of the difference in the properties of the two metal centres. The shift that is greater for W compound compared to the Mo compound may be as a result of the difference in the extent of deshielding of the carbon atoms directly bonded to the coordinated N-atoms as a result of  $\sigma$ -bonding onto the metal centre. The C=N may have been greatly deshielded by the W metal centre compared to the Mo.

The N-H chemical shift appeared as a small hump at 9.47 ppm for **C3** and was not observed on compound **C4**. The N-H chemical shifts have been reported in the range between 9.34-9.58 ppm for most of the pyrazole and pyrazole derivative metal complexes [15,19,20]. It is always observed as a small broad hump because of intramolecular or intermolecular hydrogen bonding between the N-H and the terminal carbonyl moiety  $M^+ = C=O^-$ ,  $N-H \cdots O=C-M$  and the possible exchange of the amine proton, N-H with deuterium atom, D, from  $CDCl_3$ . The intramolecular and intermolecular hydrogen bondings are responsible for the downfield chemical shifts that are observed in the  $^1H$  NMR spectra of **C3** and **C4** while the proton exchange causes the broadening and the disappearance of the amine proton chemical shift. The amine protons (**C3**) showed down field shifts of approximately 0.2ppm compared to that of the free ligand [19,21,22].

The chemical shifts for the protons C-4 H appear at 5.88 (**C3**) and 6.08 ppm (**C4**). This is comparable to 5.87 ppm and 6.08 ppm for  $[Mo(CO)_4(Hdmpz)_2]$  and 3-methylferrocenylpyrazole pentacarbonyl tungsten complexes reported by Paredes *et al.* and Tang *et. al* [15, 19]. The high values for C-4H chemical shift observed for the **C4** compared to the **C3** can be attributed the difference in the electronic effects caused by these two metals. Table 3.5 summarizes the proton chemical shifts for the compounds **C3** and **C4**

**Table 3.5:** A summary of  $^1\text{H}$  NMR for 3, 5-dimethylpyrazole, **C3** and **C4**

Compound	N-H	C- 4 <i>1H</i>	C- 6 <i>3H</i>	C- 7 <i>3H</i>
Ligand (Pz)	9.22	5.81	2.16	2.26
<b>C3</b>	9.47	5.88	1.95	2.25
<b>C4</b>	-	6.08	2.01	2.47

### 3.2.3 $^{13}\text{C}$ NMR spectroscopic analysis of **C3** and **C4**

**Table 3.6:** A summary of  $^{13}\text{C}$  NMR for compounds **C3** and **C4**

Compound	C=O	C-5	C-3	C-4	C-6	C-7
<b>C3</b>	211.88, 204.03	145.30	140.15	106.49	10.85	15.46
<b>C4</b>	219.28, 190.71	144.45	137.59	104.72	11.92	14.71

Table 3.6 gives a summary of the  $^{13}\text{C}$  NMR chemical shifts observed for the compounds **C3** and **C4**. From the  $^{13}\text{C}$  NMR spectra values obtained for the compounds **C3** and **C4**. The two chemical shifts for each compound in the region above 190 ppm observed were attributed to the terminal carbonyl groups. The chemical shifts further downfield 211.88 ppm (**C3**) and 219 ppm (**C4**) are assigned to the *cis*- carbonyl ligands while those observed at 204 ppm (**C3**) and 190 ppm (**C4**) were both attributed to the *trans*-carbonyl.

### 3.2.4 X-ray crystallographic analysis

The molecular structure obtained was a bimolecular and crystallized in Triclinic P1 space system. The molecular structure is shown in Fig. 3.6 and the selected bond lengths and bond angles of the crystal are listed in Table 3.7.

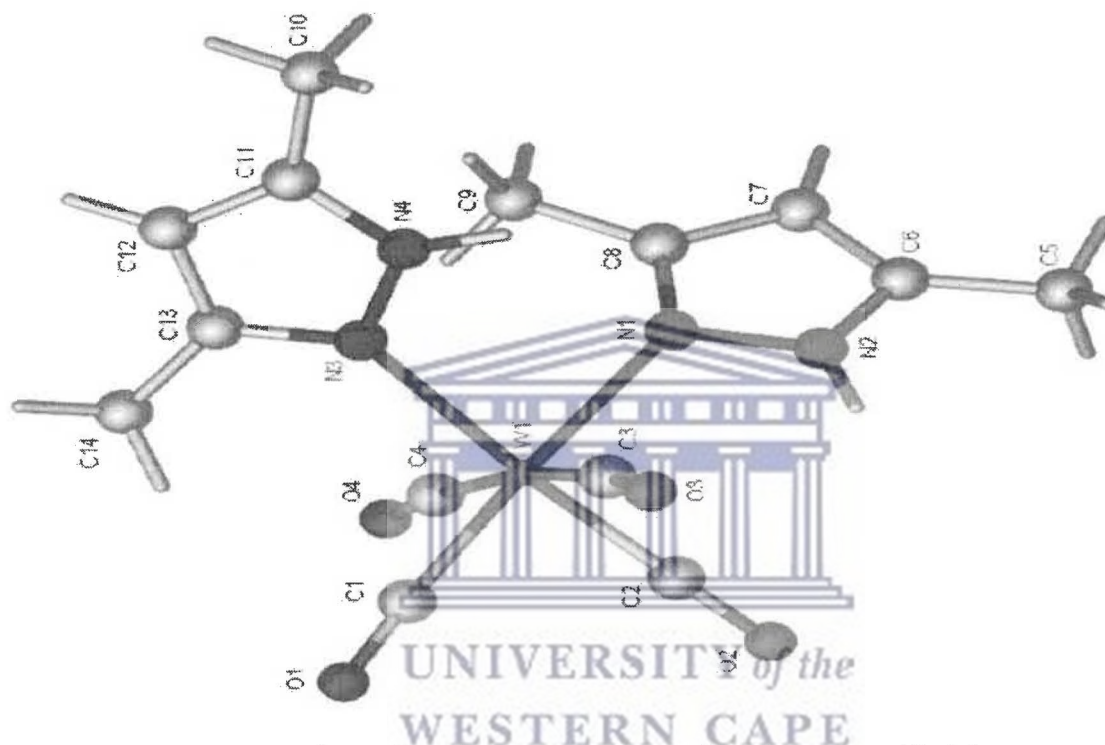


**Fig 3.6:** Crystal structure of 3, 5-dimethylpyrazole tetracarbonyl tungsten (0)-C4

The hydrogen atoms H2 and H4 of the N-H groups were located in the electron difference maps and refined with simple bond length constraints [ $d(\text{N-H}) = 0.97(2) \text{ \AA}$ ]. All other hydrogen atoms were placed at geometrically calculated positions with  $d(\text{C-H}) = 0.95 \text{ \AA}$  for the aromatic hydrogen and  $d(\text{C-H}) = 0.98 \text{ \AA}$  for the methyl hydrogen and refined as riding on their parent atoms with  $U_{\text{iso}}(\text{H}) = 1.2$  or  $1.5 U_{\text{eq}}(\text{C})$ .

**Table 3.7:** Selected bond angles (°) and bond lengths (Å) for compound **C4**

Bond	Angles (°)	Bond	Length (Å)
N(3)-W(1)-N(1)	85.48(6)	W(1)- C(2)	1.941(2)
C(2)-W(1)-N(1)	90.34(8)	W(1)- C(1)	1.951(2)
C(3)-W(1)-N(1)	94.39(8)	W(1)- C(4)	2.029(2)
C(1)-W(1)-N(3)	98.25(8)	W(1)- C(3)	2.037(2)
C(4)-W(1)-N(3)	93.67(8)	W(1)- N(3)	2.2523(18)
C(1)-W(1)-C(2)	85.95(8)	W(1)- N(1)	2.2842(18)

The data obtained confirms the structure of **C4** as a *bis*-coordinated 3,5- dimethylpyrazole tetracarbonyl tungsten (0) complex with similar properties as compound **C3** previously characterized by X-ray crystallography [19]. The structure shows that the pyrazole ligands are *cis*-coordinated to the W metal centre. The bond angles around the W metal atom, N(3)-W(1)-N(1) (85.48(6)°), C(3)-W(1)-N(1) (94.39(8)°) and C(2)-W(1)-N(1) (90.34(8)°) show deviations from the octahedral angles of 90° therefore the coordination geometry about the metal centre is distorted octahedral. The corresponding bond angles N(3)-W(1)-N(1) 85.48(6)° and C(1)-W(1)-C(2) 85.95(8)° are slightly different and the W(1)- C(1) and W(1)-C(2) bond lengths are notably slightly longer than W(1)- C(3) and W(1)- C(4) as a result of the *trans* effect from the *cis*-substituted pyrazole ligands.

The W-N bonds lengths reported here for the compound **C4** are slightly different from 2.276 Å and 2.304 Å reported for the [Mo(CO)<sub>4</sub>(Hdmpz)<sub>2</sub>], (Hdmpz= 3,5-dimethylpyrazole). The metal-*trans* carbonyl, M-C<sub>trans</sub>, W(1)-C(1) and W(1)-C(2) bonds are relatively shorter compared to the M-C<sub>cis</sub>, W(1)- C(3) and W(1)- C(4) bonds because of the stronger M-C bond as a result of electron back-donation into the π\*-orbitals the corresponding C atoms [23].

The average bond length between the metal, W, and the surrounding carbonyl carbons, 1.945 Å (W-C(1),W-C(2)) and 2.033 Å (W-C (3),W-C(4)) compare with 2.04 Å and 1.96 Å reported for carbonyl complexes [24, 25]. The W-N bond lengths are also closely comparable the value 2.27 Å obtained for W-N bond of 3-(1-methylpyrrolidin-2-yl) pyridine pentacarbonyl tungsten complex and the average of Mo-N(1) and Mo-N(3) [Mo(CO)<sub>4</sub>(Hdmpz)<sub>2</sub>], (Hdmpz= 3,5-dimethylpyrazole) [19,26]. The parameters for crystal data collection are contained in Table 3.8.



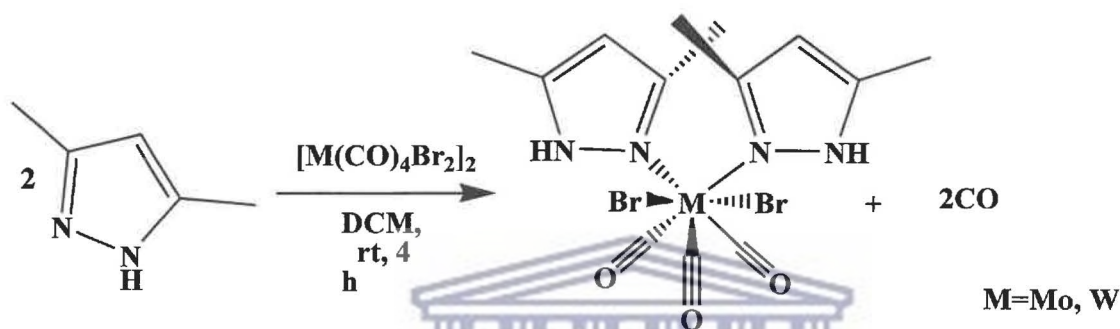


**Table 3.8:** Crystallographic data and structure refinement for compound **C4**

Empirical formula	C <sub>14</sub> H <sub>16</sub> N <sub>4</sub> O <sub>4</sub> W
Formula weight	488.16
Temperature	173(2) K
Wavelength	0.71073 Å
Crystal system, space group	Triclinic, P $\bar{1}$
Unit cell dimensions	a = 7.7986(4) Å    alpha = 93.0840(10) <sup>o</sup> b = 8.8284(5) Å    beta = 90.2660(10) <sup>o</sup> c = 12.9654(7) Å    gamma = 111.7790(10) <sup>o</sup>
Volume	827.45(8) Å <sup>3</sup>
Z, Calculated density	2, 1.959 Mg/m <sup>3</sup>
Absorption coefficient	7.005 mm <sup>-1</sup>
F(000)	468
Crystal size	0.16 x 0.10 x 0.04 mm
Theta range for data collection	1.57 to 28.42 deg.
Limiting indices	-10 < h < 10, -11 < k < 11, -17 < l < 17
Reflections collected / unique	23910 / 4154 [R(int) = 0.0271]
Completeness to theta = 28.42 <sup>o</sup>	99.5 %
Absorption correction	Semi-empirical from equivalents
Max. and min. transmission	0.7670 and 0.4003
Refinement method	Full-matrix least-squares on F <sup>2</sup>
Data / restraints / parameters	4154 / 2 / 220
Goodness-of-fit on F <sup>2</sup>	1.070
Final R indices [I > 2sigma(I)]	R1 = 0.0147, wR2 = 0.0341
R indices (all data)	R1 = 0.0164, wR2 = 0.0347
Largest diff. peak and hole	0.906 and -0.641 e. Å <sup>-3</sup>

### 3.3 Dibromo-bis-3, 5-dimethylpyrazole complexes tetra carbonyl complexes, (C5=Mo, C6=W)

Compounds **C5** and **C6** were then prepared and isolated as described in the experimental section 2.5.3 and illustrated by Scheme 3.3. Freshly prepared dibromotetracarbonyl metal dimers,  $[M(CO)_4Br_2]_2$ , ( $M=Mo, W$ ), with 3,5-dimethylpyrazole were reacted in DCM at room temperature.



**Scheme 3.3:** Synthesis of dibromo-bis-3, 5-dimethylpyrazole tricarbonyl metal complexes **C5** and **C6**

#### 3.3.1 IR spectroscopic analysis for **C5** and **C6**

Figure 3.7 shows the IR spectrum obtained for compound **C6**. The spectrum obtained for compound **C5** is given in Fig A3.7 (See appendix). The IR spectra of the compounds **C5** and **C6** indicate the presence of the 3, 5-dimethylpyrazole ligands and the three terminal carbonyl ligands. The presence of the 3,5-dimethylpyrazole ligands is indicated by the observed relatively intense peaks at  $1615\text{ cm}^{-1}$  (**C5**) and  $1616\text{ cm}^{-1}$  (**C6**) attributed to the C=N bonds and the broad strong peak observed at  $3435\text{ cm}^{-1}$  and  $3420\text{ cm}^{-1}$  for compounds **C5** and **C6** respectively. The latter sets of stretching frequencies are attributed to the N-H bonds. These values are lower than the value,  $3450\text{ cm}^{-1}$ , recorded for the uncoordinated ligand. The shifts are proposed to be due to the effect intermolecular/intermolecular hydrogen bonding between the  $N-H\cdots O=C=M$  of the terminal carbonyl ligand.

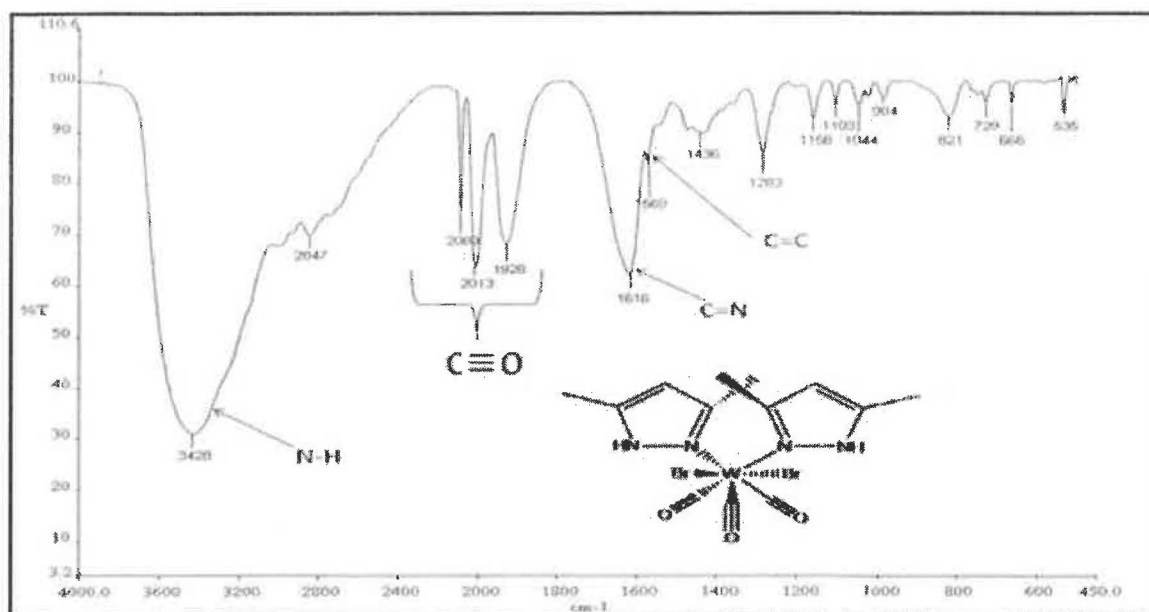


**Fig 3.7:** IR spectrum for dibromo-bis-3, 5-dimethylpyrazole tricarbonyl tungsten (II)- (C6)

The hydrogen bonding weakens the N-H bond hence the recorded decrease in the IR stretching frequencies and causes the observed peak broadening compared to the uncoordinated ligand [17, 27,28].

The terminal carbonyl ligands' stretching frequencies were observed at the range between 1928 cm<sup>-1</sup> and 2093 cm<sup>-1</sup> and the values reported were within the close range with those reported previously between 2080 cm<sup>-1</sup> and 1948 cm<sup>-1</sup> previously reported for the *heptacoordinated* diiodo tricarbonyl complexes [29] They depict that all the three terminal carbonyl ligands are not stereochemically equivalent. The absorption bands at 1566 cm<sup>-1</sup> and 1569 cm<sup>-1</sup> display 20 cm<sup>-1</sup> and 17 cm<sup>-1</sup> shift to the lower frequencies compared to the uncoordinated ligand and were attributed to C=C bond. This was of ~10 cm<sup>-1</sup> more than the observed shift for the zero valent compounds C3 and C4.

The same electronic effect proposed to have caused this observation in compounds C3 and C4 is suspected here aswell; however the extent of the shift is enhanced by the presence of

the electron withdrawing groups, Br<sup>-</sup> ions which increased the strength  $\sigma$  donation by the ligands. Table 3.9 summarises the IR data for the compounds C5 and C6

**Table 3.9:** A summary of IR data for 3, 5-dimethylpyrazole, C5 and C6

Compound	Melting Point (°C)	Stretching frequencies, cm <sup>-1</sup>			
		CO	C=N	C=C	N-H
Ligand		-	-	1586	3450
C5	126-129	2093,2033,1946	1615	1566	3435
C6	>220	2089,2013,1928	1616	1569	3428

The IR spectra show three absorption bands in the region between 2093 cm<sup>-1</sup> and 1928 cm<sup>-1</sup>. The values of the terminal carbonyl stretching frequencies recorded for the molybdenum compound C5 are relatively higher than those recorded for the tungsten compound C6. Similarly, it was noted that they are equally higher than those recorded for the corresponding tetracarbonyl compounds C3 and C4. This can be attributed to the effect of the electron withdrawing bromine groups attached to the metal centre which have reduced the *trans* effect of the coordination on the terminal carbonyl ligands.

### 3.3.2 $^1\text{H}$ NMR spectroscopic analysis for C5 and C6

Figure 3.8 shows  $^1\text{H}$  NMR spectrum obtained for C6. The spectrum obtained for C5 is given in Fig A3.8 (See appendix).

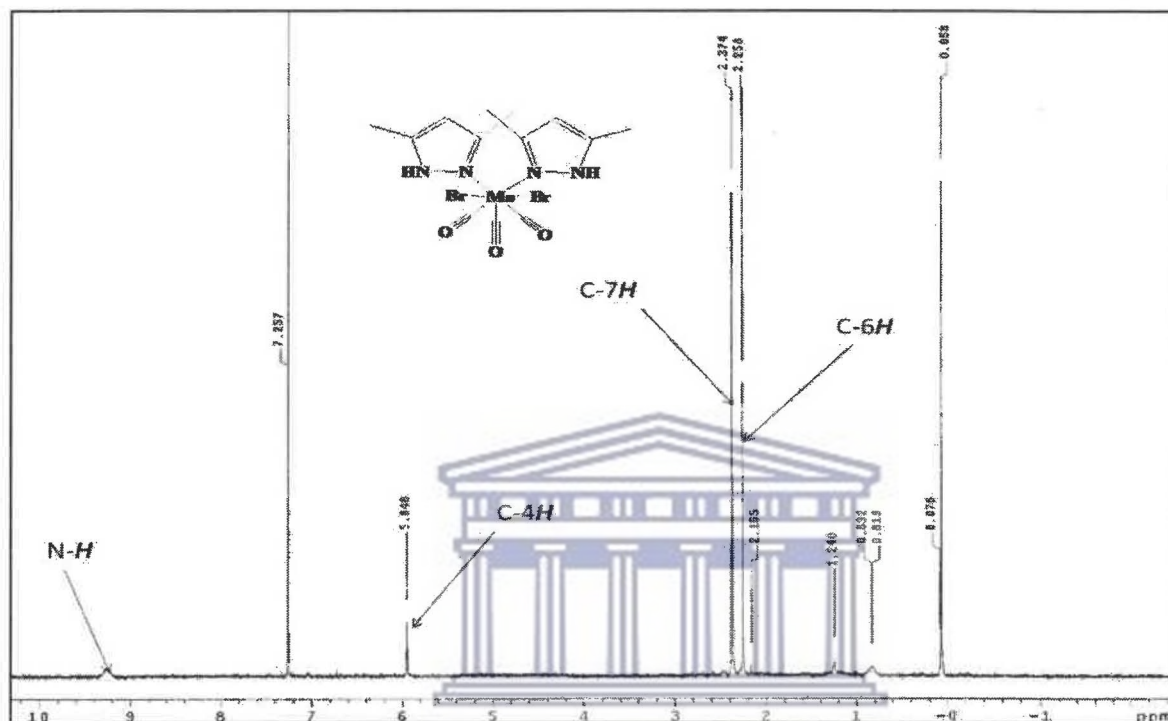


**Fig 3.8:**  $^1\text{H}$  NMR spectrum for dibromo-bis-3,5-dimethylpyrazole tricarbonyl molybdenum (II)-(C5)

The spectrum above show the chemical shifts of the coordinated 3,5-dimethylpyrazole. The amine protons appear as a small hump at about 9.40 ppm. This was a notable down field shift compared to the uncoordinated ligand because of the proposed effect of either intramolecular or intramolecular hydrogen bonding,  $\text{N-H}\cdots\text{O}=\text{C}=\text{M}^+$  between the N-H and the terminal carbonyl moiety  $\text{M}^+=\text{C}=\text{O}$  or  $\text{N-H}\cdots\text{Br}$ . The possible exchange of the amine proton, N-H with deuterium atom, D, from  $\text{CDCl}_3$  may be the responsible cause of the amine peak broadening or disappearance as previously reported [18,30,31]. The difference noted in the

chemical shifts of the N-H proton (9.37 ppm vs 9.49) is as a result of the difference in the strength of the hydrogen bonding resulting from the different metal centres.

The C-4H proton show shifts from the value recorded for the uncoordinated ligand and this may be due to the electronic pyrazole ring induction arising from the effect of coordination. It has been previously observed by Lopez *et al.* that coordination of piperidine to the metal resulted to the chemical shifts on the protons not directly bonded to the coordinated atom be proposed that the effect of coordination resulted to the down field chemical shifts on the proton attached to the non-coordinated atoms [32]. The value recorded for the N-H chemical shift (C6) compared to (C5) suggest that the N- atom is relatively more acidic, it can therefore be expected that the carbon atom, C-5 is relatively basic because of the presence of the electron donating methyl group hence the C-4H becomes more shielded compared to that of compound (C5). Table 3.10 give the summary of the proton chemical shifts. The methyl protons attached to C-6 and C-7 are both deshielded hence the observed downfield shifts. The shift is greater for the C-7 3H protons because they are closer to the coordinated N-atom compared to the C-6 3H protons.

UNIVERSITY of the  
WESTERN CAPE

**Table 3.10:** A summary of <sup>1</sup>H NMR for 3, 5-dimethylpyrazole, compounds C5 and C6

Compound	N-H	C- 4H	C-6 3H	C-7 3H
Ligand	9.22	5.81	2.16	2.26
C5	9.37	5.94	2.25	2.37
C6	9.49	5.85	2.	2.25

### 3.3.3 $^{13}\text{C}$ NMR spectroscopic analysis for C5 and C6

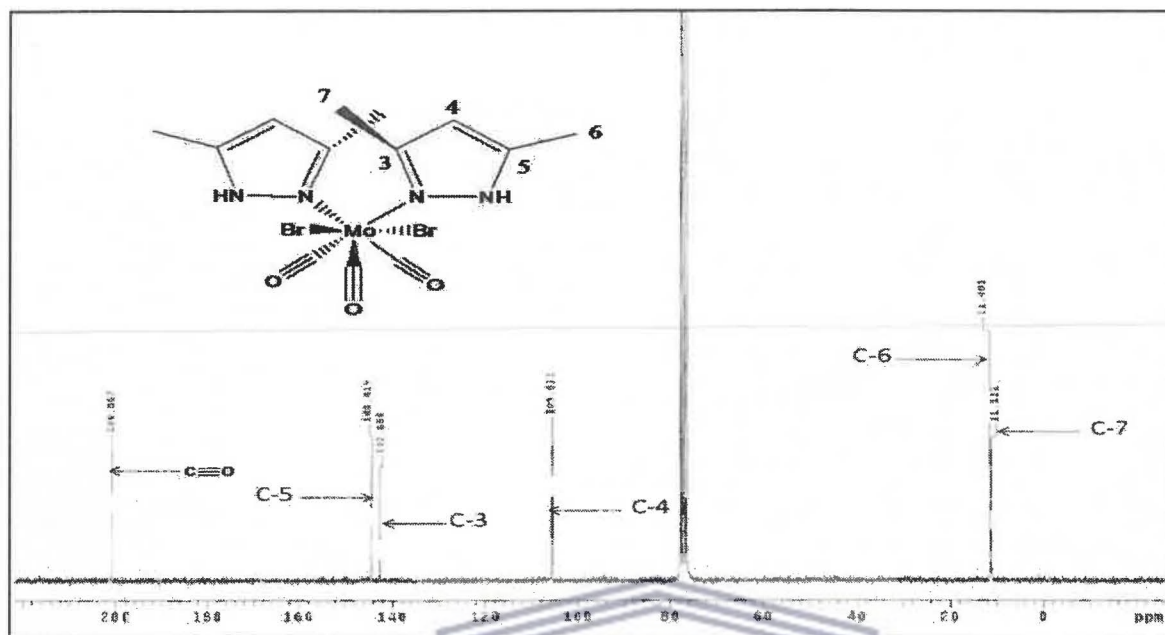


**Fig 3.9:**  $^{13}\text{C}$  NMR spectrum for dibromo-bis-3, 5-dimethylpyrazole tricarbononyl tungsten (II)-  
(C5)

Figure 3.9 is a  $^{13}\text{C}$  NMR spectrum obtained for compound C5. The  $^{13}\text{C}$  NMR chemical shifts observed in the region beyond 200 ppm were attributed to the terminal carbonyl carbons. This showed that the three carbonyl ligands have the same chemical and electronic properties and are expected to have a single chemical shift as previously reported for tetrahydroquinoline tricarbononyl complexes of Cr, Mo and W [32]. The chemical shifts for the methyl carbons, C-6 and C-7 appear up field at 11.11 ppm and 11.40 ppm and 11.19 ppm and 15.78 ppm for C5 and C6 respectively. The difference in the C-7 chemical shifts, 11.40 ppm and 15.78 ppm for C5 and C6 respectively is attributed to the difference in the difference in the properties of the two metal centres. The relatively high electronegativity of the W, (Mo (C5) (2.16 Pauling scale) and W (C6) (2.36 Pauling scale), causes the deshielding of the C-7 metals hence the observed difference in the chemical shifts between [10].

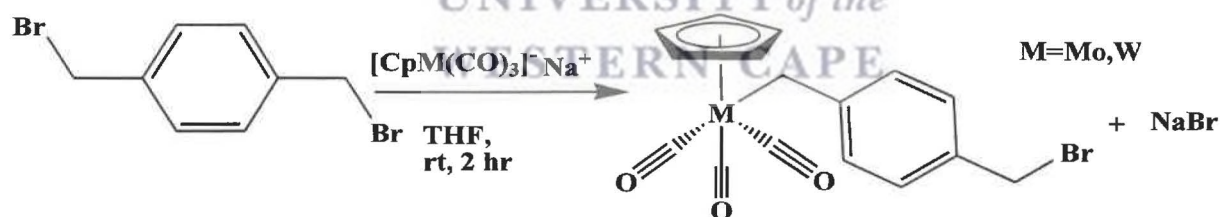
The same effect is not great on the C-6 because it far from the N-atom coordinated to the metal centre. The  $^{13}\text{C}$  NMR spectra data for the C5 and C6 is summarized in Table 3.11.

**Table 3.11:** A Summary of  $^{13}\text{C}$  NMR for compounds C5 and C6

Compound	CO	C-5	C-3	C-4	C-6	C-7
C5	200.86	144.41	142.68	105.61	11.11	11.40
C6	197.41	145.12	141.32	106.74	11.19	15.78

### 3.4 1-(bromomethyl)-4-methylenebenzyl cyclopentadienyl tricarbonyl complexes, (C7=Mo, C8=W)

Compounds C7 and C8 were prepared as discussed in experimental Section 2.6.1 and illustrated by Scheme 3.4.



**Scheme 3.4:** Synthesis of 1-(bromomethyl)-4-methylenebenzyl cyclopentadienyl metal complexes, C7 and C8



### 3.4.1 IR spectroscopic analysis of compounds C7 and C8

Figure 3.10 shows the IR spectrum for compound C7. The IR spectrum obtained for C8 is given in Fig A3.10 (See appendix).

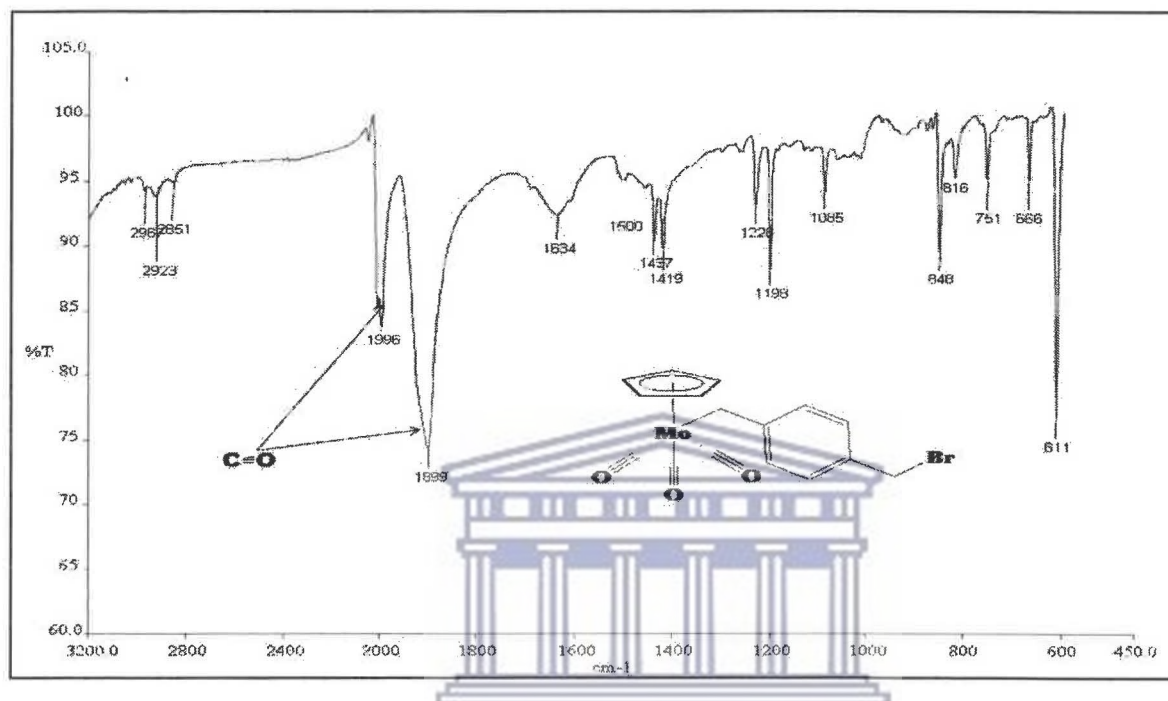


**Fig 3.10:** IR spectrum for 1-(bromomethyl)-4-methylenebenzyl cyclopentadienyl tricarbonyl molybdenum (II) - (C7)

The IR spectra of these compounds C7 and C8 have absorption bands observed at 1899 s and 1996 vs (C7) and 1885 s and 2006 vs (C8) which are as a result of the terminal carbonyl ligands stretching frequencies.

The spectra only show two bands which suggests that two of the carbonyl ligands have the same stretching frequency possibly due to their geometrical similarity with respect to the other ligands. The third carbonyl ligand differ from the other two hence the observed two stretching bands. The band of the higher stretching frequency is weaker and may be attributed to the carbonyl ligand/s *cis* to the cyclopentadienyl ligand. A broad weak peak is appearing at  $1634\text{ cm}^{-1}$  in both spectra is assignable to C=C bond stretching.

A summary of stretching frequencies for carbonyl and C=C bonds are given in Table 3.12.

**Table 3.12:** A Summary of IR data for compounds **C7** and **C8**

Compound	Melting Point (°C)	Stretching frequencies, $\text{cm}^{-1}$		C=C
		CO	CO	
<b>C5</b>	141-143	1996	1899	1634
<b>C6</b>	143	2006	1885	1634

UNIVERSITY of the  
WESTERN CAPE

### 3.4.2 $^1\text{H}$ NMR spectroscopic analysis of compounds C7 and C8

Figure 3.11 is a  $^1\text{H}$  NMR for compound C7. The spectrum obtained for C8 is given in Fig A3.11 (See appendix).

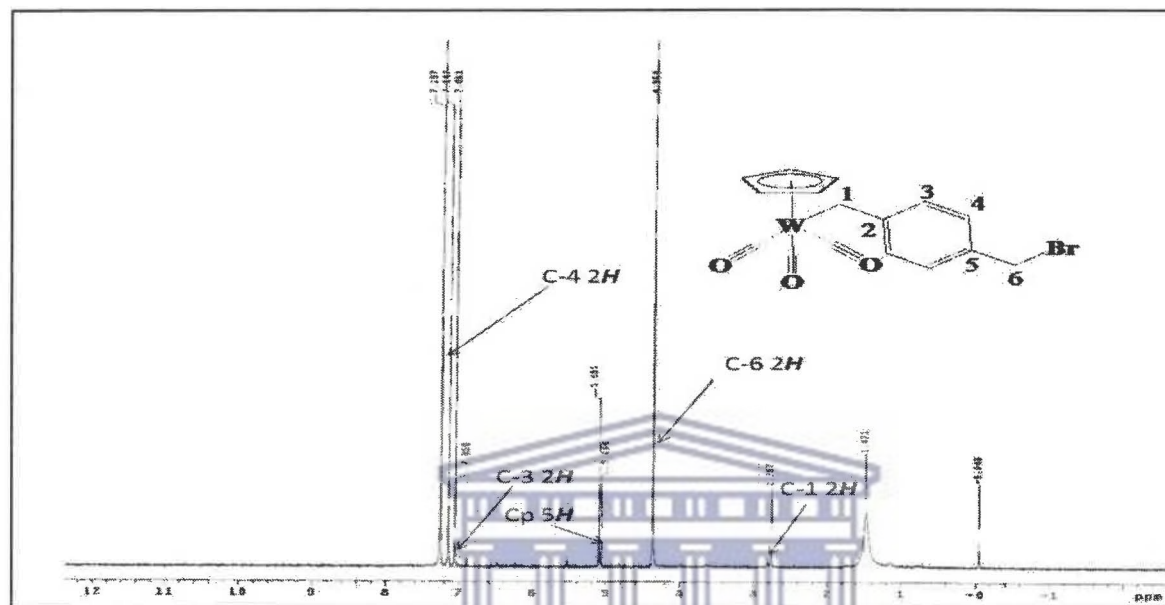


**Fig 3.11:**  $^1\text{H}$  NMR spectrum for 1-(bromomethyl)-4-methylenebenzyl cyclopentadienyl tricarbonyl molybdenum (II)-(C8)

The similarity observed in the spectra of compounds C7 and C8 suggest the similarity of the structures of the two compounds. The chemical shifts for the protons attached to C-1 and C-6 appeared as singlets depicting the mononuclear structure of the compounds formed. Since the complex is mononuclear the protons attached to C-3 and C-4 are not chemically equivalent and therefore had their chemical shifts appearing at about 7.05 ppm and 7.15 ppm respectively. They both appear as doublets due to the relative coupling between them. This observation suggests that the compound formed was a mononuclear complex. If the compound was symmetrical, *i.e.* binuclear then there would be an expectation of a single chemical shift instead of two. The Cp ring proton chemical shifts were observed at 5.07 ppm and 5.18 ppm for compounds C7 and C8 respectively.

The observed chemical shift of 5.07 ppm and 5.18 ppm are very close to the reported values of 5.10 ppm and 5.12 ppm for the *ansa* bridge cyclopentadienyl tricarbonyl complexes prepared by Zhao and Neves *et al.* [33, 34]. The observed difference in the chemical shift assigned to C-1 may be attributed to the difference in the reactivity between the W and Mo. W is less reactive than Mo and since C-1 is directly attached to the metal centre the difference is pronounced. Similarly it may be as a result of the effect of the high electron density associated with W compared to Mo. The <sup>1</sup>H NMR data for compound **C7** and **C8** are summarized in the Table 3.13.

**Table 3.13:** A summary of <sup>1</sup>H NMR for compounds **C7** and **C8**

Compound	C-1 2H	C-3 2H	C-4 2H	C-6 2H	Cp-5H
<b>C7</b>	2.75	7.05	7.14	4.36	5.07
<b>C8</b>	2.83	7.01	7.15	4.36	5.18

### 3.4.3 <sup>13</sup>C NMR spectroscopic analysis of compounds **C7** and **C8**

The <sup>13</sup>C NMR spectrum, Figure 3.12 shows a spectrum for compound **C8**. Seven carbon chemical shifts observed confirm the proposed structure, Fig. 3.12. The <sup>13</sup>C NMR spectrum for compound **C7** is given in Appendix 1 (Fig A3.12). The C-2 and C-5 have different chemical shifts assigned as 129.39 ppm and 137.92 ppm respectively.

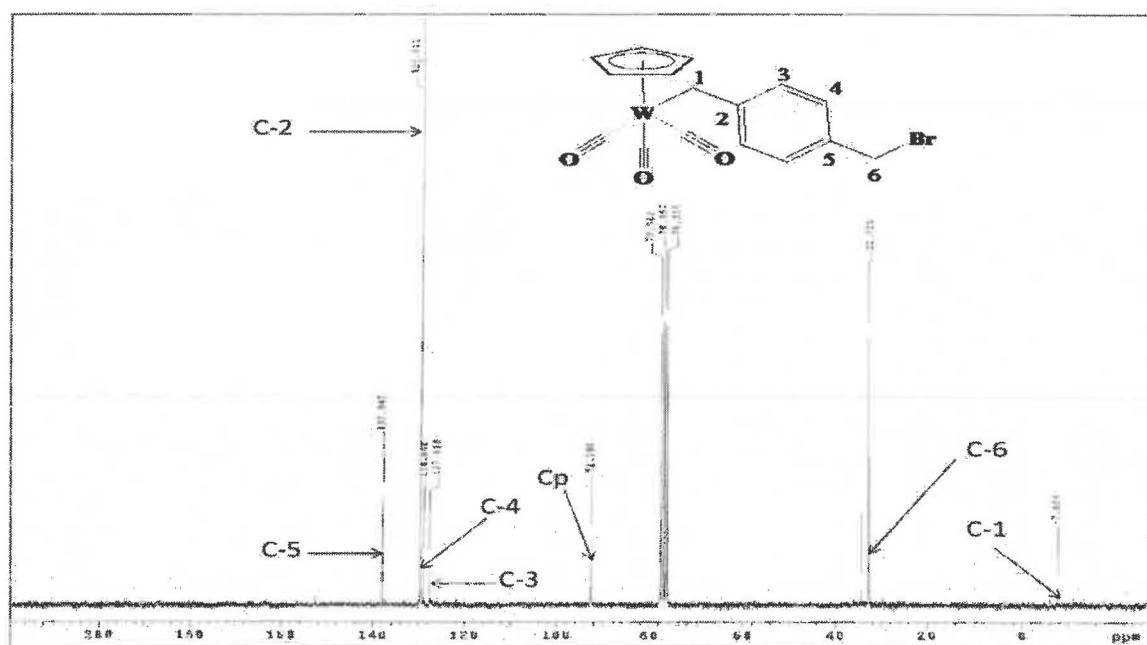


**Fig 3.12:**  $^{13}\text{C}$  NMR spectrum for 1-(bromomethyl)-4-methylenebenzyl cyclopentadienyl tricarbonyl tungsten (II) - (C7)

The chemical shift for C-5 appears down field because of the effect of the bromomethyl,  $\text{BrCH}_2-$ , group attached to it. On the other hand, the chemical shift for C-2 appears relatively up field as a result of the increased electron density of the metal centre. This indicates the mononuclear structure of the complexes as proposed. Table 3.14 gives the summary of the  $^{13}\text{C}$  NMR data.

**Table 3.14:** A Summary of  $^{13}\text{C}$  NMR data for compounds C7 and C8

Compound	C-1	C-2	C-3	C-4	C-5	C-6	Cp
C7	1.07	129.39	127.66	128.68	137.92	32.78	93.94
C8	-7.82	129.41	127.51	128.64	137.99	32.72	92.54

The chemical shifts for the carbonyl ligands were not observed in the spectrum. The chemical shift for the C-1 for the two compounds do not fall in the same region, 1.07 ppm

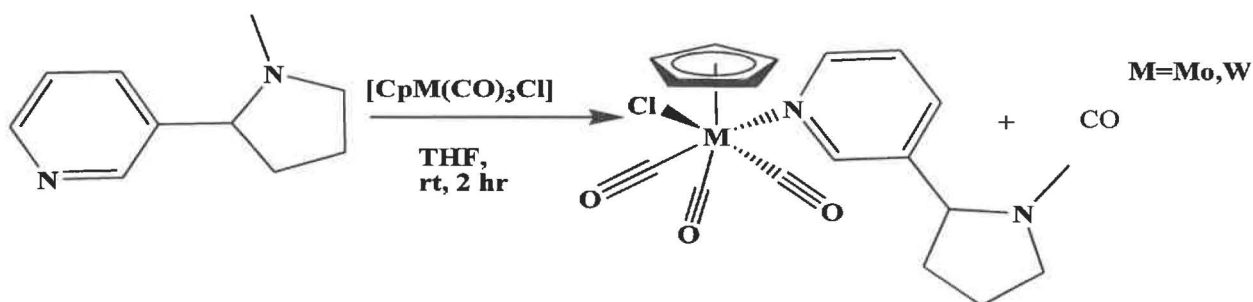
(C7) and -7.82 ppm (C8). The chemical shift for the C-1 for compound C8 is observed further up field compared to compound C7 Zhao *et al.* reported the chemical shift for a similar  $\alpha$ -carbon at -7.3 ppm [33]. The same chemical shift for  $\alpha$ -carbon has been reported in the range of -12.1 ppm and -9.9 ppm [35]. The difference observed in the chemical shift for the  $\alpha$ -carbon between the Mo compound (C7) and W compound (C8) can be attributed to the difference in electronegativity of the two metals. Tungsten being more electronegative accumulate more charge from the carbonyl ligand causing the shielding of the  $\alpha$ -carbon and the Cp ring carbons hence the observed comparable up field shifts observed.



### 3.5 3-(1-methylpyrrolidin-2-yl) pyridine cyclopentadienyl tricarbonyl complexes

(C9=Mo, C10=W)

Compounds C9 and C10 were prepared by following the procedure described in the experimental section 2.7.1 and illustrated the Scheme 3.5.



**Scheme 3.5:** Synthesis of 3-(1-methylpyrrolidin-2-yl) pyridine cyclopentadienyl tricarbonyl metal compounds C9 and C10

#### 3.5.1 IR spectroscopic analysis for compounds C7 and C8

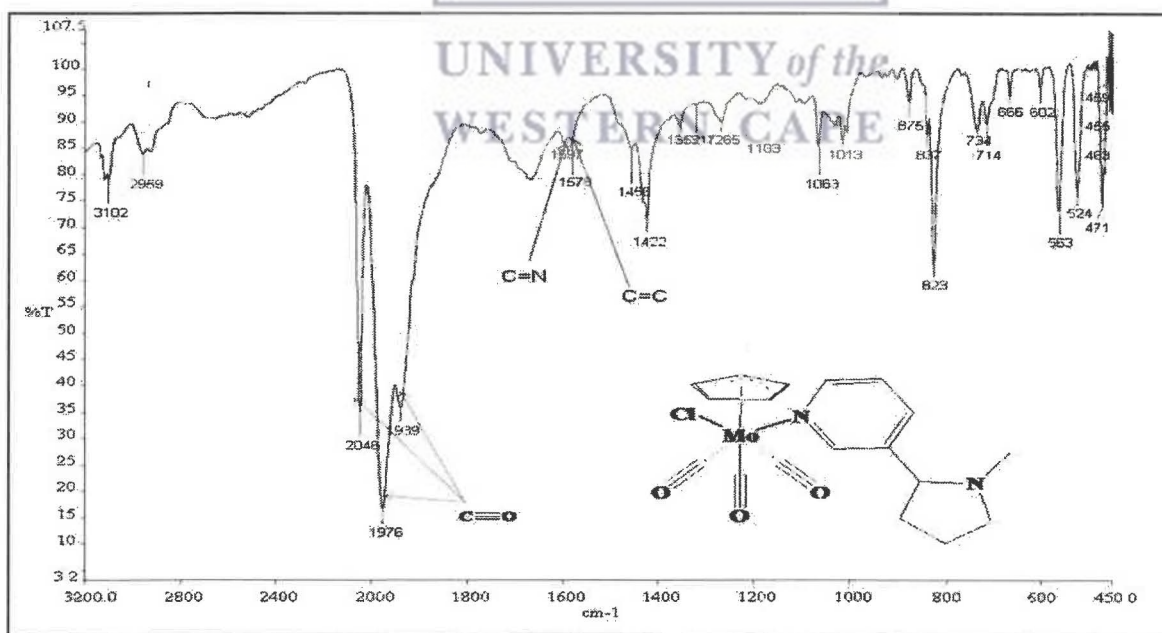


Figure 3.13 shows the IR spectrum for compound **C9**. The spectrum obtained for compound **C10** is given in Fig A3.13 (See appendix). The IR spectra were used to identify the compounds formed. Three absorption peaks, two of almost the same intensity and a weak one are observed in both the spectra, 1939 sh, 1976 vs and 2046 s for compound **C9** and 1773 w, 1953 s and 2042 s for compound **C10**. These peaks are assignable to the three terminal carbonyl ligands. A shift of 5  $\text{cm}^{-1}$  and 2  $\text{cm}^{-1}$  to a higher stretching frequencies compared to the uncoordinated 3-(1-methylpyrrolidin-2-yl) pyridine ligand is observed for the C=N bond stretching. These shifts are attributed to the increase of the C=N bond strength. N- ligands are weaker  $\pi$ -acceptor Lewis base ligand compared to the carbonyl ligands. The difference in the electronegativity between molybdenum and tungsten causes the observed difference in the C=N bond stretching frequencies [36].

A summary of the IR data for the relevant bond stretching frequencies of compounds **C9** and **C10** is given in Table 3.15.

**Table 3.15:** A summary of IR data for 3-(1-methylpyrrolidin-2-yl) pyridine, **C9** and **C10**

Compound	Stretching frequencies, $\text{cm}^{-1}$			
	CO	C=N	C=C	C-N
Ligand	-	1590	1576	1314
<b>C1</b>	2046,1976, 1939	1597	1578	1317
<b>C2</b>	2042,1953, 1773	1592	1578	1316



### 3.5.2 $^1\text{H}$ NMR spectroscopic analysis for compounds C9 and C10

Figure 3.14 shows a  $^1\text{H}$  NMR spectrum obtained for compound C10. A section of the spectrum and the spectrum obtained for C9 is given in Fig A3.14 (See appendix).

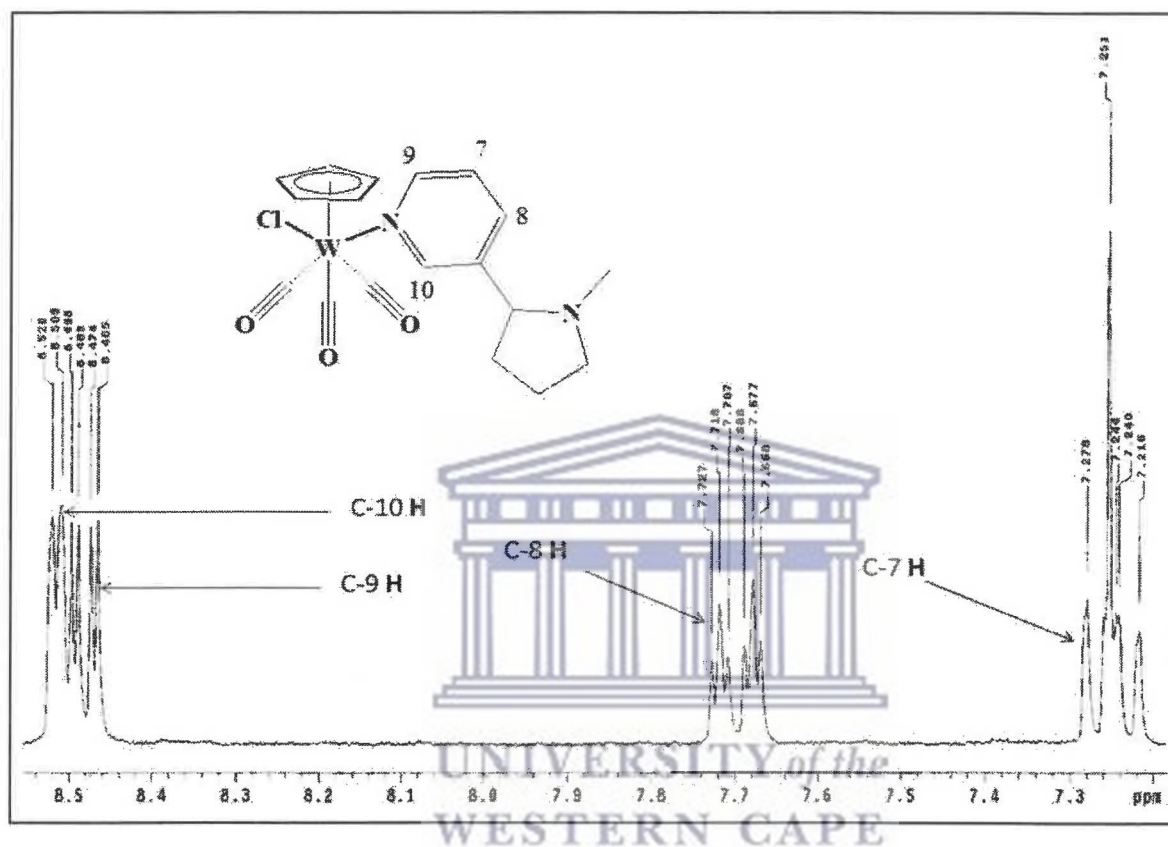


**Fig 3.14:**  $^1\text{H}$  NMR spectrum for 3-(1-methylpyrrolidin-2-yl) pyridine cyclopentadienyl tricarbonyl tungsten (II) - (C10)

The  $^1\text{H}$  NMR spectra shows that the two compounds are structurally similar. Even though no significant difference are observed on the chemical shifts for the compounds C9 and C10 compared to that of the uncoordinated 3-(1-methylpyrrolidin-2-yl) pyridine ligand. The spectra indicate the presence of both 3-(1-methylpyrrolidin-2-yl) pyridine and cyclopentadienyl ligands in both compounds. The chemical shift for the Cp ligand appears as a singlet at 5.78 ppm and 5.75 ppm for compounds C9 and C10 respectively. The  $^1\text{H}$  NMR spectra data is summarized in the Table 3.16.

**Table 3.16:** A summary of  $^1\text{H}$  NMR for 3-(1-methylpyrrolidin-2-yl) pyridine, **C9** and **C10**

Compound	C-10 <i>H</i>	C-9 <i>H</i>	C-8 <i>H</i>	C-5 <i>H</i>	C-4 <i>3H</i>	Cp- <i>5H</i>
Ligand	8.52	8.49	7.71	3.17	2.17	-
<b>C9</b>	8.53	8.51	7.89	3.30	2.24	5.78
<b>C10</b>	8.50	8.46	7.72	3.24	2.15	5.75

### 3.5.3 $^{13}\text{C}$ NMR spectroscopic analysis for compounds **C9** and **C10**

Figure 3.15 is a  $^{13}\text{C}$  NMR spectrum for compound **C10**. The spectrum obtained for **C9** is given in Fig. A3.15 (see Appendix)

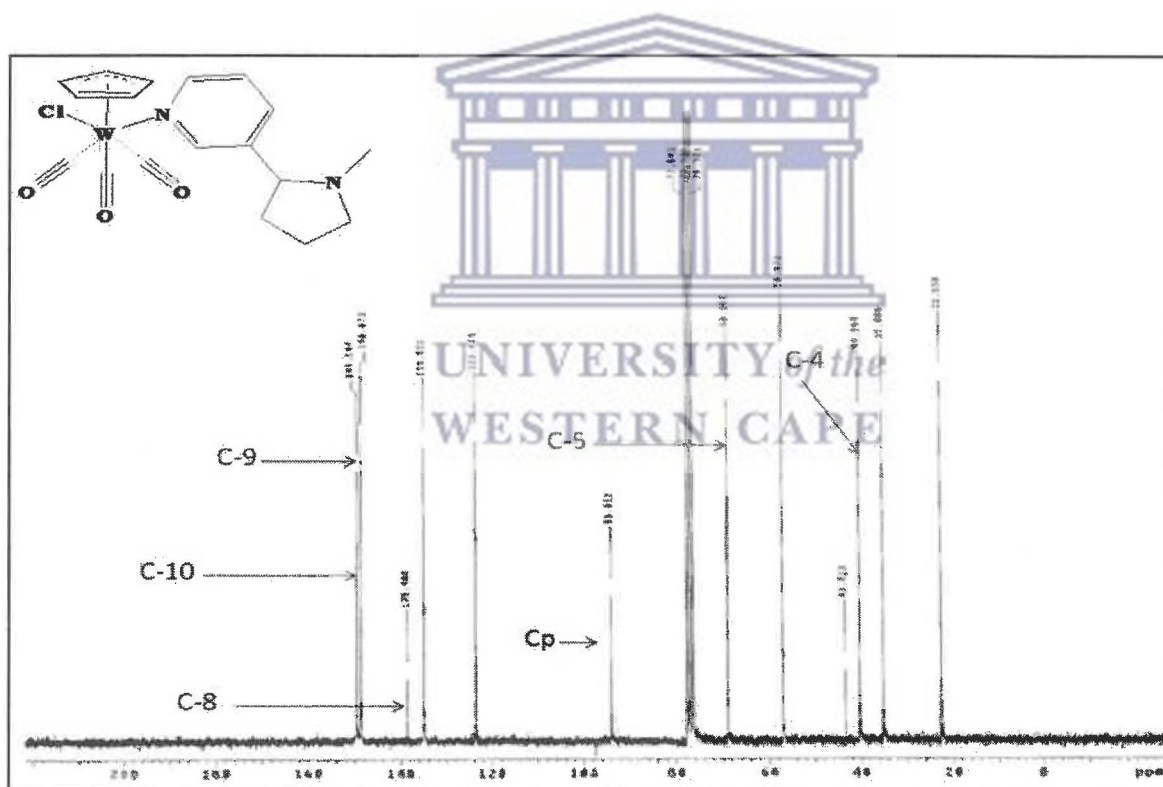


**Fig 3.15:**  $^{13}\text{C}$  NMR spectrum for 3-(1-methylpyrrolidin-2-yl) pyridine cyclopentadienyl tricarbonyl tungsten (II) - (**C10**)

The spectra show the chemical shifts due to the carbons atoms of the 3-(1-methylpyrrolidin-2-yl) pyridine and cyclopentadienyl ligand. The chemical shifts due to the carbonyl ligands expected in the region above 190 ppm were not observed in the spectra because the chemical shifts of non-hydrogen bonded carbons are always less intense. The intensity of the carbon atom chemical shift increases with increase in decoupling of the attached protons. Since there are no attached protons on these carbonyl ligands' the intensities of their signals are highly suppressed [37]. The cyclopentadienyl, Cp, ligand carbon chemical shifts of 95.67 ppm and 93.91 ppm are close to the values between 91.02 ppm and 92.98 ppm reported by Friedrich *et al.* [38]. The difference observed is attributed to the shielding effect of the benzene Table 3.16 gives a summary of the  $^{13}\text{C}$  NMR spectra data for the compounds C9 and C10. A summary of the  $^{13}\text{C}$  NMR data is given in Table 3.17

**Table 3.17:** A summary of  $^{13}\text{C}$  NMR for 3-(1-methylpyrrolidin-2-yl) pyridine, C9 and C10

Compound	CO	C-10	C-9	C-8	C-5	C-4	Cp
Ligand	-	149.45	148.51	138.80	68.83	40.32	-
C9	-	149.57	149.21	-	69.18	39.75	95.67
C10	-	149.54	148.67	138.48	68.90	40.30	93.91

### 3.6 Electronic transition measurements

Generally, three absorption peaks were observed in the electronic spectra of the complexes both in DCM and MeOH solutions. The absorption spectrum of 3, 5-dimethylpyrazole measures in DCM displayed two bands at 226 nm and 256 nm assigned to  $\pi \rightarrow \pi^*$ ,  $n \rightarrow \pi^*$  transitions respectively. In the corresponding M (0) and M (II), (M=Mo, W) complexes, slight shifts on the absorption wavelengths and new absorptions were observed in the spectra of the complexes. Compounds **C3** and **C4** showed a general red shift particularly on the  $n \rightarrow \pi^*$  transition observed at 254 nm and 252 nm for the measurement in DCM and 252 nm and 252 nm for the measurements taken in MeOH. These observed red shifts illustrates the effect of the imine nitrogen coordination on the  $n \rightarrow \pi^*$  transitions. The lone pair electron have been utilized in coordination hence higher energy is required to cause the  $n \rightarrow \pi^*$  transition. Weak absorptions were observed in the spectra of most of the compounds in the region between 383-478 nm, which were attributed to spin-allowed metal ligand transfer, MLCT, field transitions [39,40]. It is observed that these transitions occur at a lower energy in Mo compared to the corresponding W compounds. Absorptions of the higher energy observed 288 nm- 338 nm are believed to be due to the  $M \rightarrow \pi^*$  CO charge transfer transitions [41,42]. The high energy absorption bands < 254 nm are supposedly due to spin-allowed intra-ligand transitions for example  $\pi \rightarrow \pi^*$ ,  $n \rightarrow \pi^*$  transitions [43, 44]. The proposal is supported by the observation made on the intensities and the effect of the solvent on these absorption bands, Table 3.18.

**Table 3.18:** Electronic Spectral data for compounds **C1- C10** in DCM and MeOH

Entry	$\lambda_{\text{max}}$ , nm	Solvent
1	244, 310, 388	CH <sub>2</sub> Cl <sub>2</sub>
	242, 311, 388	MeOH
2	230, 290	CH <sub>2</sub> Cl <sub>2</sub>
	229, 288	MeOH
3	226, 254, 386	CH <sub>2</sub> Cl <sub>2</sub>
	223, 252, 383	MeOH
4	226, 252, 400	CH <sub>2</sub> Cl <sub>2</sub>
	<i>a</i> , 252, 394	MeOH
5	212, 230, 290	CH <sub>2</sub> Cl <sub>2</sub>
	<i>a</i> , 231, 288	MeOH
6	210, 252, 336	CH <sub>2</sub> Cl <sub>2</sub>
	215, 250, 338	MeOH
7	214, 246, 318	CH <sub>2</sub> Cl <sub>2</sub>
	<i>a</i> , 242, 311	MeOH
8	202, 246, 310	CH <sub>2</sub> Cl <sub>2</sub>
	206, 244, 304	MeOH
9	208, 228, 478	CH <sub>2</sub> Cl <sub>2</sub>
	200, 226, 469	MeOH
10	206, 234, 464	CH <sub>2</sub> Cl <sub>2</sub>
	200, 230, 448	MeOH

<sup>a</sup> All complexes exhibited an intense absorption near 200 nm

### 3.7 Evaluation of compounds C1-C10 as catalysts for epoxidation

In this section the results obtained from the catalytic evaluation of the compounds C1-C10 towards the epoxidation of the selected alkenes are discussed. The compounds showed low to high conversions with varied selectivities towards the epoxide products. Typical GC chromatograms obtained for *cis*-cyclooctene, 1, 2-epoxycyclooctane and styrene, styrene epoxide standard samples are attached, Fig. A3.17 and A3.18 (see Appendix) and a summary of the retention times extracted from them are given in Table 3.19. These chromatograms were obtained specifically for the calculation of the retention factors for the alkene substrates and the corresponding products.

The solution mixtures were prepared by accurately weighing 1, 2-epoxycyclooctane and pipetting 10  $\mu$ L of each of the liquid components (*cis*-cyclooctene, styrene epoxide) and topping up with DCM to 1.4 mL. The substrate conversions and yields obtained from the catalytic reactions were calculated based on the initial substrate concentrations. The maximum conversions reached were observed to be dependent on the type of substrate, oxidation state of the catalyst, reaction time and the type of the metal.

**Table 3.19:** A summary of the retention times for the standard samples (Cy<sub>8</sub>, Cy<sub>8</sub> epoxide, Sty, Sty epoxide and Isooctane)

Compound	Retention time (min)	Compound	Retention time (min)
1 Isooctane	1.826	Isooctane	0.965
2 <i>cis</i> -cyclooctene	3.651	Styrene	2.294
3 1,2-epoxycyclooctane	6.024	Styrene epoxide	4.031

Pentacarbonyl complexes, compound **C1** and **C2** showed a moderate activity towards the conversion of the alkenes. Conversions of the cyclic alkenes were higher compared to the conversions of the straight chain alkenes and styrene. Their activity was comparable to those of the tetracarbonyl metal compounds **C3** and **C4**. However, 87% conversion was reached by compound **C3** for the *cis*-cyclooctene within the same time period. The stability and performance of Compound **C4** was tested by extending the reaction time beyond the average 24 h to 48 h. The compound showed increase conversion with time; the conversion of *cis*-cyclooctene increased from 49 to 69%, 1-octene from 18 to 30%, cyclohexene from 35 to 56% and styrene from 24 to 44%.

The divalent compounds, **C5** and **C6** showed a relatively high activity out of ten the compounds evaluated. Compound **C5** displayed the highest conversion of *cis*-cyclooctene and styrene observed for the 24 h reaction. Despite of the high conversion recorded for the compound **C5**, low selectivity towards the desired epoxides was observed. The two compounds also showed catalytic activity even after 24 h depicted by the increased conversions.

Compound **C7** equally displayed high catalytic activity compared to other compound. Conversion of 94% was reached for *cis*-cyclooctene which improved to 96% when the reaction time was extended to 48 h. Relative high conversions were also achieved for the other substrate with that of the styrene which generally showed poor conversion being 58% after 24 h. However, the analogous tungsten compound, **C8** did not perform as molybdenum compound **C7**. With **C8**, only 37% conversion was obtained as opposed to the 94% obtained with compound **C7**.

Compounds **C9** and **C10** though expected to be more active than **C1-C4** showed a low activity. 53% conversion was achieved for the *cis*-cyclooctene after 48 h reaction. Similarly, the selectivities of the complexes towards the intended products were equally poor.

The substrate conversions by the catalysts were observed to initially increase rapidly and thereafter reduce with time. This observation is associated with the increasing formation of a by-product, *tert*-butanol and the decrease in the concentration of the substrate with time. The *tert*-butanol competes with TBHP for the coordination sites of the catalysts [45]. Generally, conversions of between 25%- 55% were reached in the first 4 h of the epoxidation of  $Cy_8$  and  $Cy_6$  as shown in Fig. 3.16.

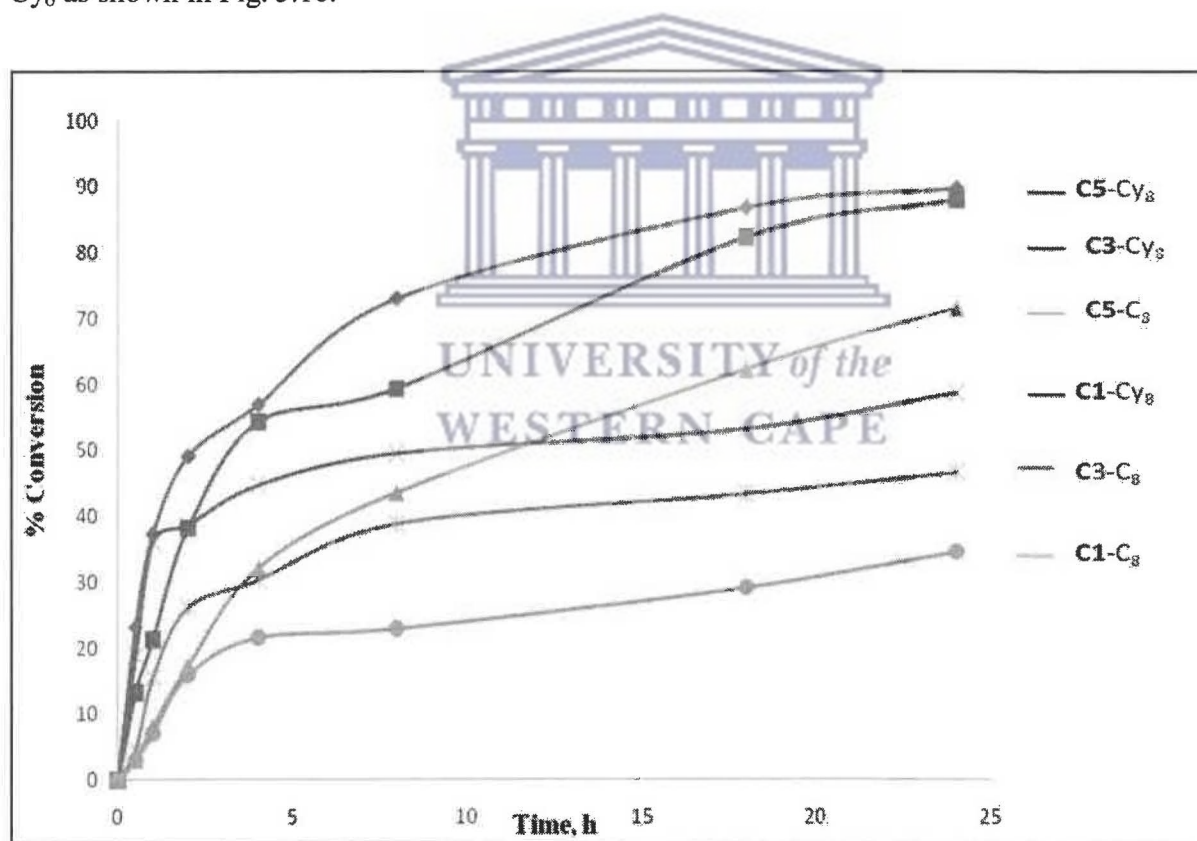


**Fig. 3.16:** Conversions of  $Cy_8$  and  $C_8$  using TBHP as oxygen donor.



Straight chain alkenes C<sub>8</sub>, C<sub>6</sub> and Sty generally showed comparable low reactivity. The conversion between 94%-40% was reached for *cis*-Cyclooctene by the Mo (II) complexes. These conversions fall above 64% to the higher side but slightly lower than 45% reported by Saraiva *et al.* [46]. The results show that high conversions are obtained for cyclic alkenes compared to the corresponding straight chain alkenes. This is because of increases electronic effect exhibited by these cyclic alkenes as compared to their corresponding chain alkenes [47]. The table below shows typical results obtained for the epoxidation reactions using C1-C10

**Table 3.20:** Epoxidation results for the compound C4

Entry	Alkene	Conversion (%)	Selectivity	TOF <sup>h</sup>
1	Cy <sub>8</sub>	69.19	22.30	2.88
2	C <sub>8</sub>	30.48	24.15	1.27
3	Cy <sub>6</sub>	56.96	17.65	2.37
4 <sup>a</sup>	C <sub>6</sub>	38.28	25.44	1.60
5	Sty	44.30	16.52	1.84

<sup>a</sup> Results obtained after 24 h period.

The following sections discussed the effects of substrate types, the oxidation state of the metal, time and the metal centre in the catalytic activities of these compounds towards alkene epoxidation.

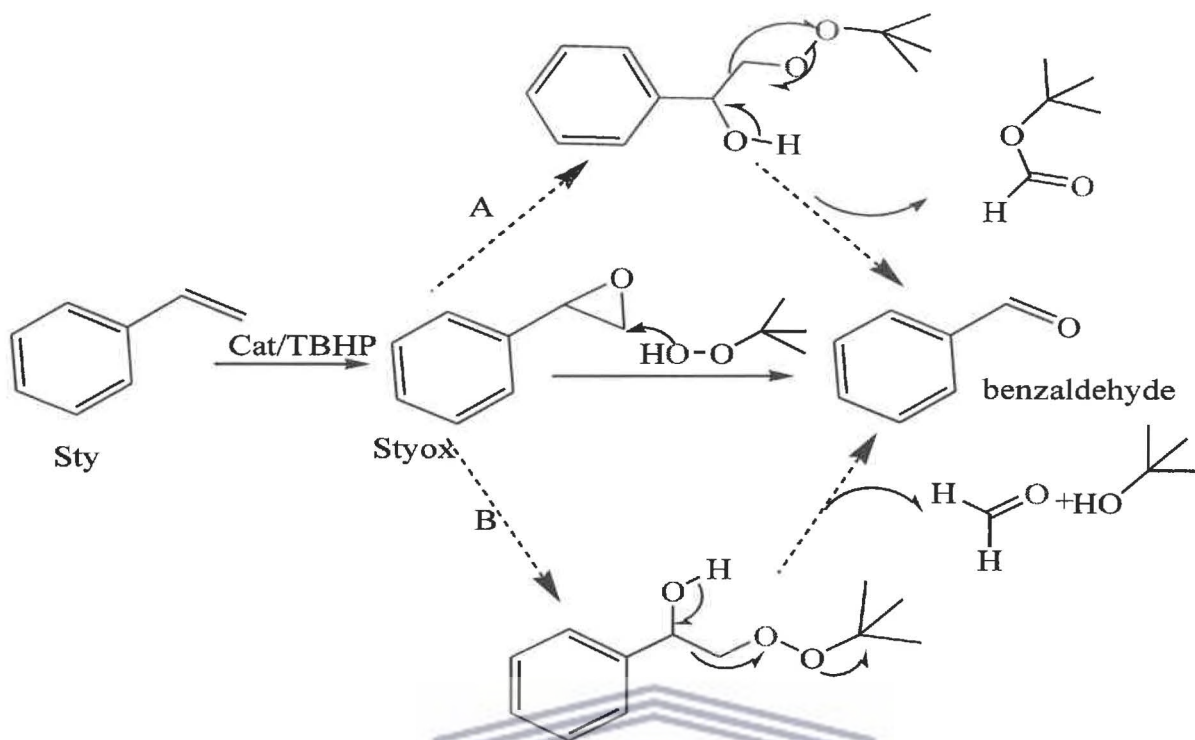
### 3.7.2.1 Cyclic vs Straight chain alkenes

Comparison of the catalytic activities of the C1-C10 towards different type of alkenes was one of the key objectives of this study. Three type of alkene was used in this study, cyclic (*cis*-cyclooctene, cyclohexene), straight chain alkenes (1-octene, 1-hexene) and styrene which has both multi-unsaturated bonds on the ring and a vinyl arm. From the results, Table 3.19, it

is observed that the conversions were higher for the cyclic alkenes compared to the corresponding straight chain alkenes. This was in agreement with the observation made by Bagherzade and Esfahani [45]. Most of the experiments showed relatively high conversions with comparable yields and selectivity. As earlier reported the structure of the olefins and the catalyst influences the catalyst activity.

The conversions were generally higher for *cis*-cyclooctene and cyclohexene compared to their corresponding straight chain alkenes, 1-octene and 1-hexene respectively. The *cis*-cyclooctene is more reactive compared to the cyclohexene due to the presence of relatively more electron donating CH<sub>2</sub>. It has also been reported that the cyclohexene has a tendency to form diols that may have affected the yields [48]. On the other hand 1-hexene reached higher conversions compared to 1-octene and this has been attributed to the steric factor, large *hexyl* group versus relatively small *butyl* group on the 1-hexene [49]. It was observed that percentage conversions reached for styrene were relatively high but this did not correspond to the yields recorded; this observation was attributed to the reported tendency of the styrene to forming epoxides prone to ring-opening reactions to form diols, benzaldehydes and benzoic acid [50].

The mechanism here show how the oxidant attack the oxirane ring leading to ring opening followed by subsequent bond shifts to produce benzaldehyde and 3,3-dimethylformate (Path A), benzaldehyde, formaldehyde and butanol (Path B)



**Scheme 3.6:** Ring opening reaction of 2-phenyloxirane to form benzaldehyde and other by-products

### 3.7.2.2 Zero vs divalent catalysts

UNIVERSITY of the  
WESTERN CAPE

From the catalytic results, it was noted that the divalent complexes gave rise to higher conversions compared to the zero valent complexes. This observation was associated with the high electrophilic properties associated with the divalent complexes, Table 3.20 compare the catalytic activities of compound C1 Mo (0)-complex) and compound C5, Mo (II) -complex.

**Table 3.21:** A summary of conversion, yield and selectivity for **C1** and **C5** for the substrate after 24 h epoxidation reactions

Substrate	C1			C5		
	Conversion (%)	Selectivity (%)	TOF <sup>-h</sup>	Conversion (%)	Selectivity (%)	TOF <sup>-h</sup>
<b>Cis-Cyclooctene</b>	58.80	24.26	2.45	90.08	32.69	3.75
<b>1-Octene</b>	34.95	6.29	1.45	71.19	54.63	2.97
<b>Cyclohexene</b>	42.32	38.73	2.37	45.56	84.14	1.89
<b>1-hexene</b>	46.29	11.59	1.76	71.37	17.71	2.97
<b>Styrene</b>	42.53	36.43	1.77	41.04	36.17	1.71

The table indicate that there is an increased conversion with the increase of the Lewis acidity of the metal centre, i.e. from oxidation state 0 to +2. The Lewis acidic property associated with divalent metal complexes is responsible for both the high conversions observed for each of the substrates tested. The influence of the oxidation state of the metal centre is very much depicted by the results obtained by Wong *et al.* [51]. This observation can be explained by the fact that the halides are good electron withdrawing group, they therefore reduce the electron density on the metal centre which enhances the substrate binding.

This proposal is supported by the observations made by Pearson *et al.* [52]. Contrary to the high conversions achieved with the divalent complexes, the yields and the selectivities are comparably low, except for the cyclohexene substrate. This observation is associated with the high concentration of the by-product, *tert*-butanol resulting from high conversions which is responsible for the ring-opening reactions with the preformed epoxides, resulting to low yield recorded; refer to Scheme 3.8 [34].

### 3.7.2.3 Time

**Table 3.22:** A summary of conversion, yield and selectivity of the substrates by of C4 after 24 h and 48 h reactions

Substrate	24 h			48 h		
	Conversion (%)	Selectivity (%)	TOF <sup>-h</sup>	Conversion (%)	Selectivity (%)	TOF <sup>-h</sup>
Cis-Cyclooctene	48.57	25.57	2.02	69.19	22.30	2.88
1-Octene	18.31	29.05	0.76	30.48	24.15	1.27
cyclohexene	35.08	27.68	1.46	56.96	17.65	2.37
Styrene	23.91	16.52	0.99	44.30	16.52	1.84

The conversions were observed to progress very fast between the times 0-2.5 h and thereafter slow with time indicating that there is a formation of an active compound. Table 3.21, indicates that an increase in length of reaction time from 24 h to 48 h led to an increase in conversion as well as yield. This observation has been supported by the reported data of studies previously done [53]. However, the by-product, *tert*-butanol, produced at the initial reaction stages competes both with the oxidant and the substrate for the coordination sites there by resulting in the reduced activity of the catalyst with increase in time slowing the rate of conversion [54,55].

### 3.7.2.4 Molybdenum vs tungsten compounds

A general low activity of the tungsten complexes compared to their corresponding molybdenum analogues was observed, Table 3.22. This is attributed to the difference in the reactivity of these two metals and a true reflection of the previously reported results. The oxidant, TBHP is more suitable for use with Mo catalyst as opposed to W catalysts [5454]. The difference in the catalytic performance of these two elements is reinforced by the results obtained for the catalytic epoxidation done by analogous complexes of the two metals.

The results indicate that Mo generally performs better than W in most of the catalytic reactions based on the substrate conversions obtained for their similar compounds in these literature and many others [51,56]. The activity of the W complexes towards epoxidation reactions has been reported to be temperature dependent *i.e.* the activity increases with increase in temperature indicated by the results they obtained. It can be proposed that the increase in temperature increases the reactivity of the W hence the increase in the catalytic activity [33,57]

**Table: 3.23** A summary of conversion, yield and selectivity of the substrate by C7 and C8 after 48 h reaction

Substrate	C7 (Mo)			C8 (W)		
	Conversion (%)	Selectivity (%)	TOF <sup>-h</sup>	Conversion (%)	Selectivity (%)	TOF <sup>-h</sup>
Cis-Cyclooctene	95.57	99.22	1.99	41.39	84.92	0.86
1-Octene	59.25	7.81	1.23	12.12	27.50	0.25
Cyclohexene	73.17	4.24	1.52	37.34	20.97	0.78
1-hexene <sup>a</sup>	42.39	36.64	0.88	21.07	43.69	0.44
Styrene <sup>a</sup>	58.04	7.27	1.20	45.78	-	0.95

<sup>a</sup> The results were obtained after 24h reaction

### 3.8 References

1. R. B. King, A. Fronzaglia *Inorg. Chem.*, 1966,**5**,1837-1846
2. U. Radius, F. M. Bickerlhaupt, A. W. Ehlers, N. Goldberg, R. Hoffman, *Inorg. Chem.*, 1998,**37**,1080-1090
3. I. W. Stolz, G. R. Dobson, R. K. Sheline, *Inorg. Chem.*, 1963,**2**,323-352
4. C. S. Kraihanzel, F. A. Cotton, *Inorg. Chem.*, 1963, **2**, 533-540
5. G. W.A. Fowles, D. K. Jenkins, *Inorg. Chem.*, 1964, **3**, 257-259
6. F. Zingales, F. Fraone, P. Uguagliati, U. Belluco, *Inorg. Chem.*, 1967,**7**,1653-1655
7. L. Tang, W. Jia, Z. Wang, J. Chai, J. Wang, *Transit Metal Chem.*, 2001, **26**, 400-403
8. R. H. Crabtree, *The organometallic Chemistry of transition metals*, John Wiley and Sons, Inc., Hoboken, New Jersey, 6<sup>th</sup> Ed., 2005, 110-111
9. K. Nakamoto, *Infrared and Raman Spectra of Inorganic and Coordination Compounds*, John Wiley and Sons, Inc., Hoboken, New Jersey, 6<sup>th</sup> Ed., 2009, 110-111
10. M. K. Ahn, H. S. Kwon, H. M. Lee, *Corros. Sci.*, 1998, **40** , 307-322
11. C. D. Montgomery, *J. Chem. Educ.*, 2007, **84**, 102-105
12. E. Peris, J. A. Mata, V. Moliner, *J. Chem. Soc., Dalton Trans.*, 1999, 3893-3898
13. M. Ardon, G. Hogarth, D. T. W. Oscroft, *J. Organomet. Chem.*, 2004, **689**, 2429-2435
14. A. Mentos, *Transit. Metal. Chem.*, 1999, **24**, 77-80
15. L. Tang, W. Jia, Z. Wang, J. Chai, J. Wang, *J. Organomet. Chem.*, 2001, **637-639**, 209-215
16. L. Tang, *Transit. Metal. Chem.*, 2004,**29**, 31-34
17. J. Coates, *Encyclopaedia of Analytical Chemistry*, John Wiley & Sons Ltd, Chichester, 2000, 10815-10837

- 
18. D. Carmona, J. Ferrer, J. M. Arilla, J. Reyes, F. J. Lahoz, S. Elipe, F. J. Modrego, L. A. Oro, *Organometallics*, 2000, **19**, 798-808
19. P. Paredes, M. Arroyo, D. Muigel, F. Villafane, *J. Organomet. Chem.*, 2003, **667**, 120-125
20. D. Rottger, G. Erker, M. Grehl, R. Frohlich, *Organometallics* 1994, **13**, 3897-3902
21. <http://www.chem.ucalgary.ca/courses/351/Carey5th/Ch13/ch13-nmr-3.html>, accessed on 26/10/2010
22. <http://www.chem.wisc.edu/areas/reich/nmr/05-hmr-02-delta.htm>, accessed on 26/10/2010
23. <http://www.chem-faculty.lsu.edu/Stanley/web/pub/.../chap11-substitution-rxns.doc>, accessed on 26/10/2010
24. M. A. Reynolds, I. A. Guzei, B. C. Logsdon, L. M. Thomas, R. A. Jacobson, R. J. Angelici, *Organometallics*, 1999, **18**, 4075-4081
25. G. Sanchez, J. L. Serrano, C.M. Lopez, J. Garcia, J. Perez, G. Lopez, *Inorg. Chim. Acta.*, 2000, **306**, 168-173
26. M. O. Onani, R. A. Lalancette, A. T. Muriithi, E. A. Nyawade, B. V. Kgarebe, *Acta Crystallogr. E* **66**, 2010, M480
27. <http://www.umsl.edu/orglab/documents/IR/IR.html>, accessed on 2/11/2011
28. S. Forsen, B. Arkermark, *Acta Chem. Scand.*, 1963, **17**, 1907-1916
29. M. Al-jahdali, P. K. Baker, A. J. Lavery, M. M. Meehan, D. J. Muldoon, *J. Mol. Catal. A: Chem.*, 2000, **159**, 51-62
30. A. P. Sadimenko, S. S. Basson, *Coord. Chem. Rev.* 1996, **147**, 247-297
31. W. Liu, J. Xiong, Y. Wang, X. Zhou, R. Wang, J. Zuo, X. You, *Organometallics*, 2009, **28**, 755-762



- 
32. C. Lopez, M. A. Munoz-Hernandez, D. Morales-morales, F. del Rio, S. Hernandez-Ortega, R. A. Toscano, J. J. Garcia, *J. Organomet. Chem.*, 2003, **672**, 58-65
33. J. Zhao, K. R. Jain, E. Herdtweck, F. E. Kuhn, *Dalton Trans.*, 2007, **222**, 5567-5571
34. P. Neves, C. C. L. Pereira, f. A. Almeida Paz, S. Gago, S. Pillinger, C. M. Silva, A. A. Valente, C. C. Romao, I. S. Gonclaves, *J. Organomet. Chem.*, 2010, **695**, 2311-2319
35. E. O. Changamu, H. B. Friedrich, M. O. Onani, M. Rademeyer, *J. Organomet. Chem.*, 2006, **691**, 4615-4625
36. (a) <http://www.webelements.com/molybdenum/electronegativity.html>, (b) <http://www.webelements.com/tungsten/electronegativity.html>, accessed on 31/10/2011
37. R. J. Anderson, D. J. Bendell, P. W. Groundwater, *Organic spectroscopic analysis*, the Royal society of chemistry, Thomas graham House, Science park, Milton road, Cambridge, CBE OWF, UK, 2004, 103
38. H.B. Friedrich, M.O. Onani, O. Q. Munro, *J. Organomet. Chem.*, 2001, **633**,39-50
39. F. Lee, M. C. Chan, K. Cheung, C. Che, *J. Organomet. Chem.*, 1998, **563**, 191-200
40. G. Boxhoorn, G. C. Schoemaker, D. J. Stufkens, A. D. Akam, A. J. Rest, D. J. Darensbough, *Inorg. Chem.*, 1980,**19**, 3455-3461
41. D. J. Darensbourg, M. A. Murphy, *J. Am. Chem. Soc.* 1978, **100**, 463-468
42. S. Cai, L. Wang, C. Fan, *Molecules*, 2009, **14**, 2935-2946
43. R. Packheiser, P. Ecorchard, T. Ruffer, M. Lohan, B. Brauer, F. Justaud, C. Lapinte, H. Lang, *Organometallics* 2008, **27**, 3444-3457
44. J. N. Zhao, Y. Wu, H.M. Wen, X. Zhang, Z. Chen, *Organometallics*, 2009, **28**, 5603-5611
45. M. Bagherzade, S. Esfahani, *Transact. C: Chem. And Eng.*, 2010, **17**, 131-138

- 
46. M. S. Saraiva, C. D. Nunes, T. G. Nunes, M. J. Calhorda, *J. Mol. Catal. A: Chem.*, 2010, **321**, 92–100
47. A. A. Valente, J. D Sexias, I. S. Gonclaves, M. Abrantes, M. Pilliger, C. C. Romao, *Catal. Lett.*, 2005, **101**, 127-130
48. D. Hoegaerts, B. F. Sels, D. E. De Vos, F. Verpoort, P. A. Jacobs, *Catal. Today*, 2000, **60**,209-218
49. M. Masteri-Farahani, *J. Mol. Catal. A: Chem.*, 2010, **316**, 45-51
50. M. Abrantes, A. Sakthivel, C. C. Romao, F. E Khun, *J. Organomet. Chem.*, 2006, **691**, 3137-3145
51. Y. Wong, D. K. P. Ng, H. K. Lee, *Inorg. Chem.*, 2002, **41**, 5276-5285
52. A. J. Pearson, E. Schoffers, *Organometallics*, 1997,**16**, 5367
53. M. Bagherzadeh, L. Tahsini, R. Latifi, L. K. Woo, *Inorg. Chim. Acta.*, 2009, **362**, 3698-3702
54. J. Zhao, A. M. Santos, E. Herdtweck, F. E. Kuhn, *J. Mol. Catal. A: Chem.*, 2004, **222**, 265-271
55. J. Zhao, E. Herdtweck, F. E. Kuhn, *J. Organomet. Chem.*, 2006, **691**, 2199-2206
56. A. de Angelis, P. Pollesel, D. Molinari, W.O. Parker Jr., A. Frattini, F. Cavani, S. Martins, C. Perego, *Pure Appl. Chem.*, 2007, **79**, 1887–1894.
57. L. Feng, E. Urnezius, R.L. Luck , *J. Organomet. Chem.*, 2008, **693**, 1564–1571

## CHAPTER 4

### 4.1 Conclusions

In this study, a literature review of the chemistry of the zero and divalent carbonyl complexes of Mo and W was discussed. The application of Mo and W carbonyl complexes in olefin epoxidation is briefly highlighted and various exiting discoveries in the physical and chemical properties of the molybdenum and tungsten carbonyl complexes brought out by the review lead to the synthesis, characterization and eventual catalytic evaluation of the new carbonyl complexes of Mo and W.

**Chapter 2** outlined the synthesis procedure and spectral characterization carried out on these new molybdenum and tungsten metal carbonyl complexes. **Chapter 3** gives a detailed discussion of the synthesis, characterization and catalytic evaluation is reported. Each spectral data obtained for the compounds were interpreted, compared and discussed for the corresponding compounds. The spectral data were also compared for analogous compounds and to those of similar compounds previously reported in the literature.

The IR,  $^1\text{H}$ ,  $^{13}\text{C}$ -NMR, elemental analysis, x-ray crystallographic (C4) techniques were used to identify the compounds and the data obtained used to explain their physical and chemical properties. Similarly, the data obtained was also used to deduce the observed difference in the catalytic performance of the compounds towards the epoxidation of alkenes.

The electronic spectra data of the compounds were further used explain the chemical properties of the compounds and to establish effect of polarity in the chemical properties of these compounds.

All the compounds were evaluated towards epoxidation of *cis*-Cyclooctene, 1-octene, cyclohexene, 1-hexene and styrene. The compounds showed low to high conversions towards the tested alkenes tested. From the results obtained molybdenum complexes were better catalysts compared to their corresponding tungsten analogues. It was also observed that divalent complexes, **C5-C10** were generally having a higher activity compared to the zero valent, **C1-C4**. This observation was attributed to the improved nucleophilic nature of the metal centre caused by the presence of the electro withdrawing groups. It was found that these compounds were catalytically active beyond the average 24 h reaction period leading to higher conversions and in most of the cases high yields as well.

#### 4.2 Recommendations

In this study new molybdenum and tungsten carbonyl complexes were synthesized and characterized by various spectroscopic techniques. They were tested towards epoxidation of some selected alkenes. The results obtained indicated that they are potential catalyst for epoxidation of olefins. However, we recommend the following for future actions on this work:

1. Single X-ray crystal studies should be done on the compounds, **C5-C10** to establish their molecular structures to replace the expected elemental analyses results.
2. The effect of different reaction conditions on the catalytic performance of the complexes should be investigated. The conditions to be investigated include, temperature, solvent, catalyst concentration, substrate loading and different oxidants. This is necessary to establish the optimum condition necessary for the application of these compounds for laboratory and possible industrial epoxidation reaction.
3. Heterogenized the compounds **C3-C10** to enhance catalyst recycling, and catalyst-product separation.

4. To vary the ligand substituents, particularly for compounds **C3-C6** and study the effect of such variation in the catalytic activities of the compounds.





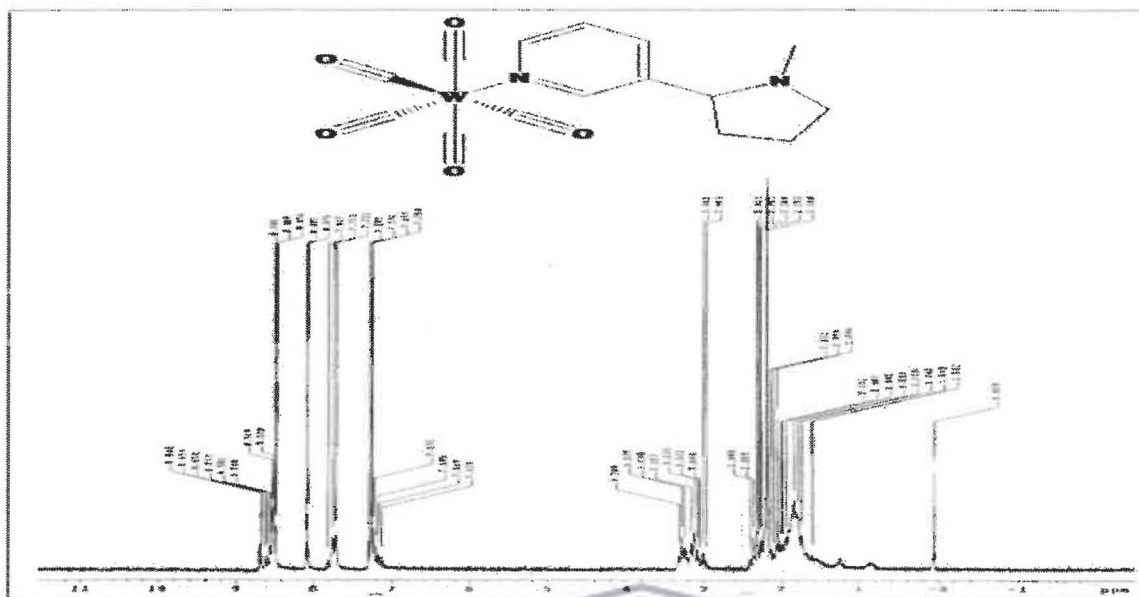


Fig A3.2: <sup>1</sup>H NMR spectrum for 3-(1-methylpyrrolidin-2-yl) pyridine pentacarbonyl tungsten (0)-(C2)

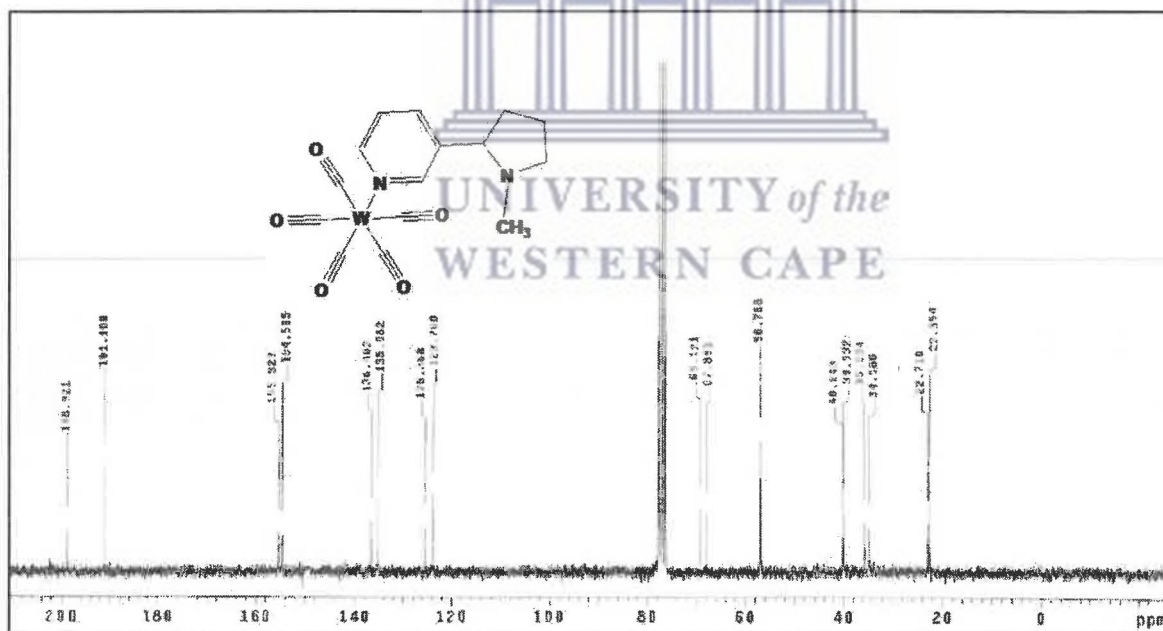


Fig A3.3: <sup>13</sup>C NMR spectrum for 3-(1-methylpyrrolidin-2-yl) pyridine pentacarbonyl tungsten (0)-(C2)

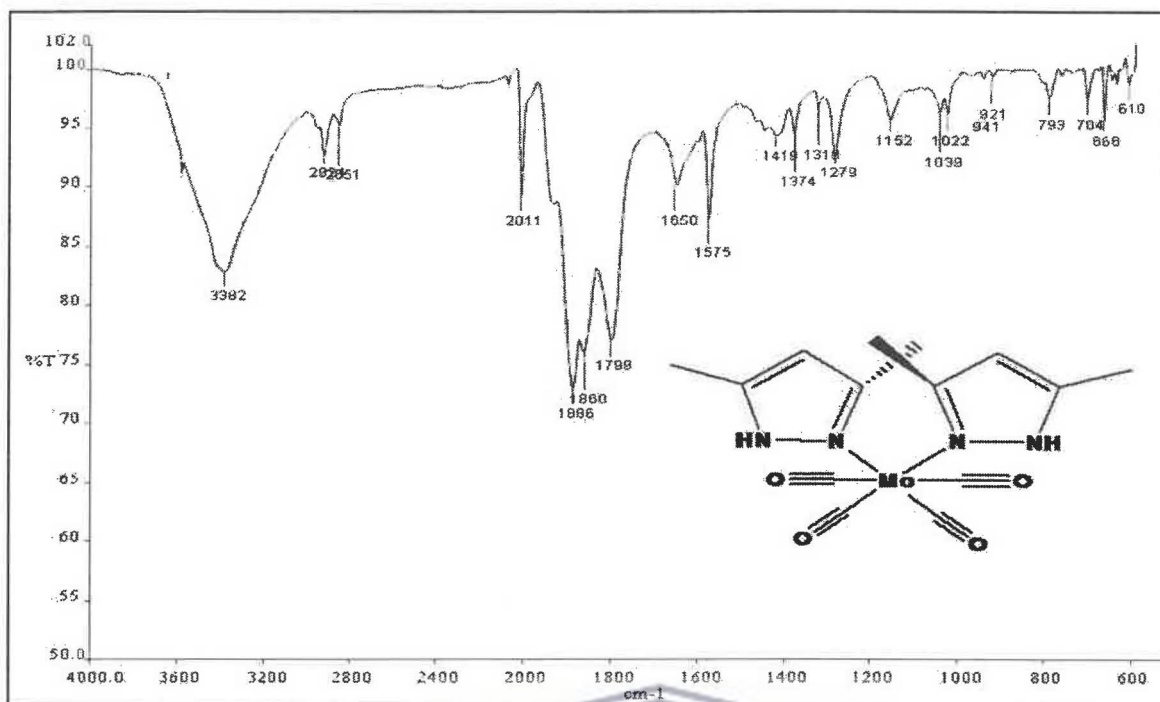


Fig A3.4: IR spectrum for 3, 5-dimethylpyrazole tetracarbonyl molybdenum (0)-(C3)

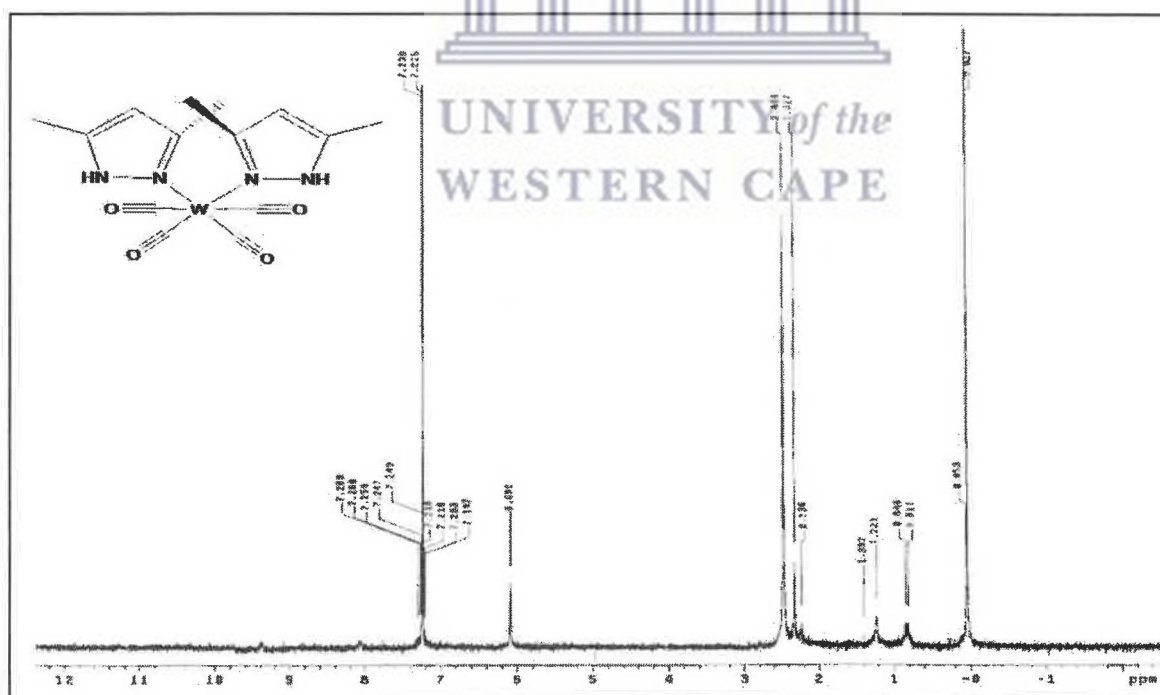


Fig A3.5: <sup>1</sup>H NMR spectrum for 3, 5-dimethylpyrazole tetracarbonyl tungsten (0)-(C4)



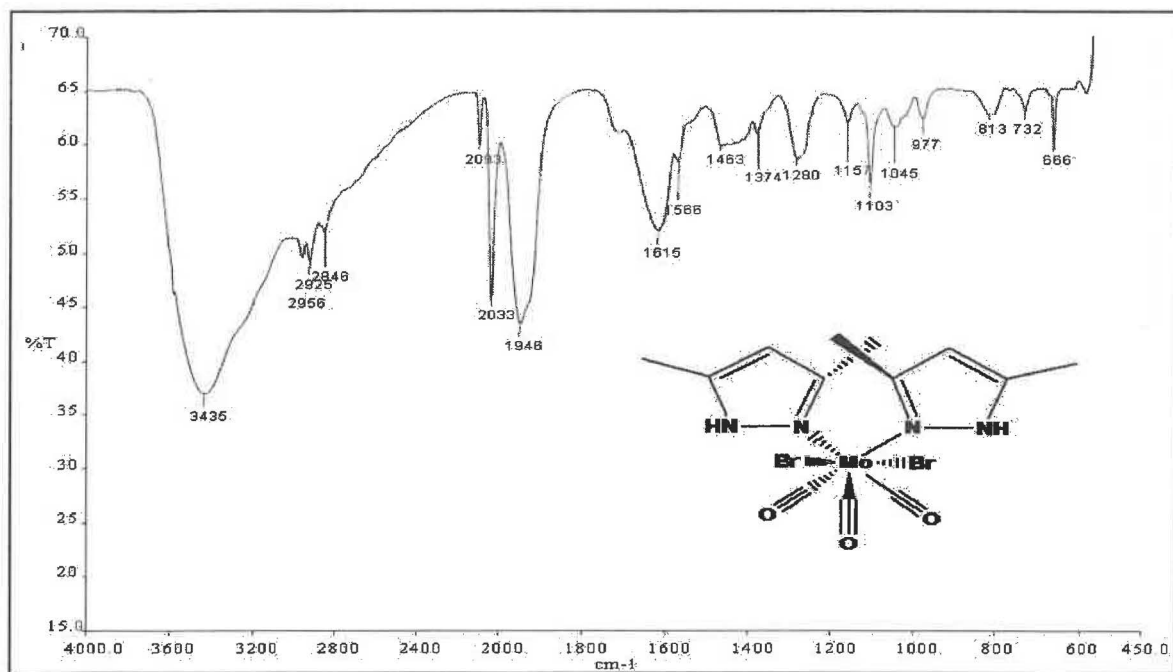


Fig A3.7: IR spectrum for dibromo-bis-3,5-dimethylpyrazole tricarbonyl molybdenum (II)-(C5)

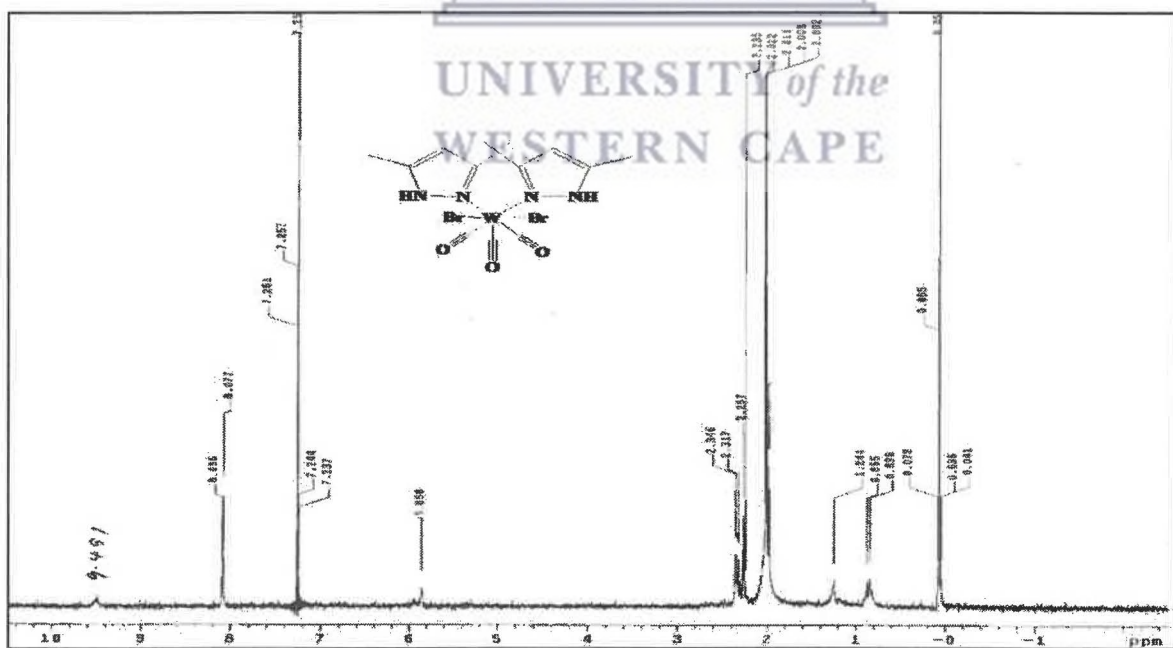


Fig A3.8: <sup>1</sup>H NMR spectrum for dibromo-bis-3,5-dimethylpyrazole tricarbonyl tungsten (II)-(C6)

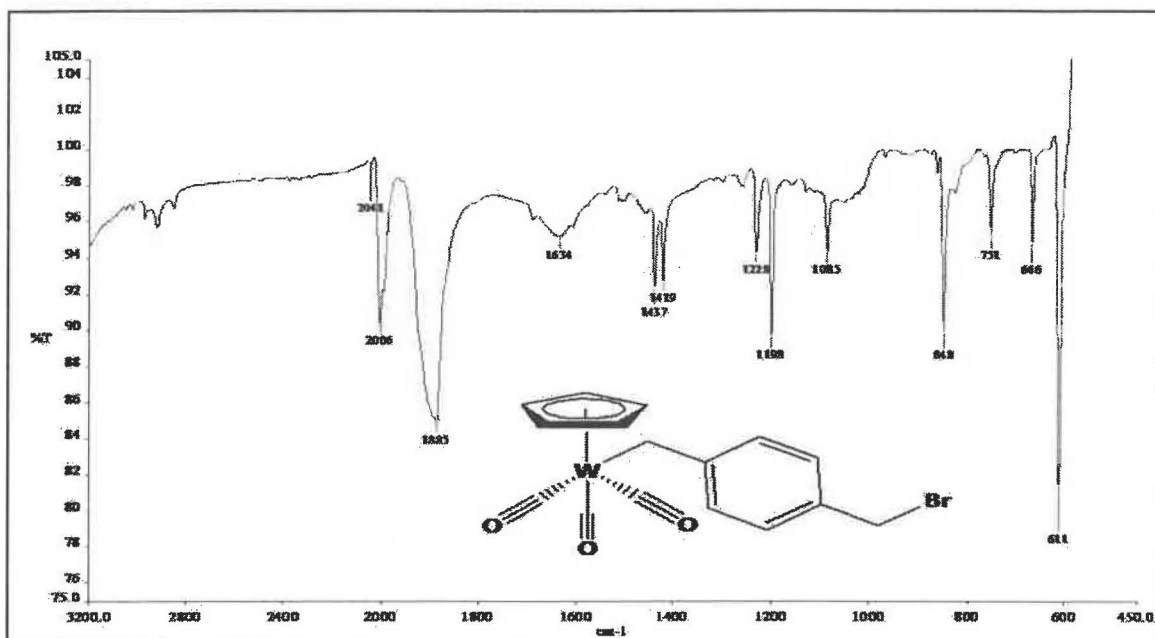


Fig A3.10: IR spectrum for 1-(bromomethyl)-4-methylenebenzyl cyclopentadienyl tricarbonyl tungsten (II)- (C7)

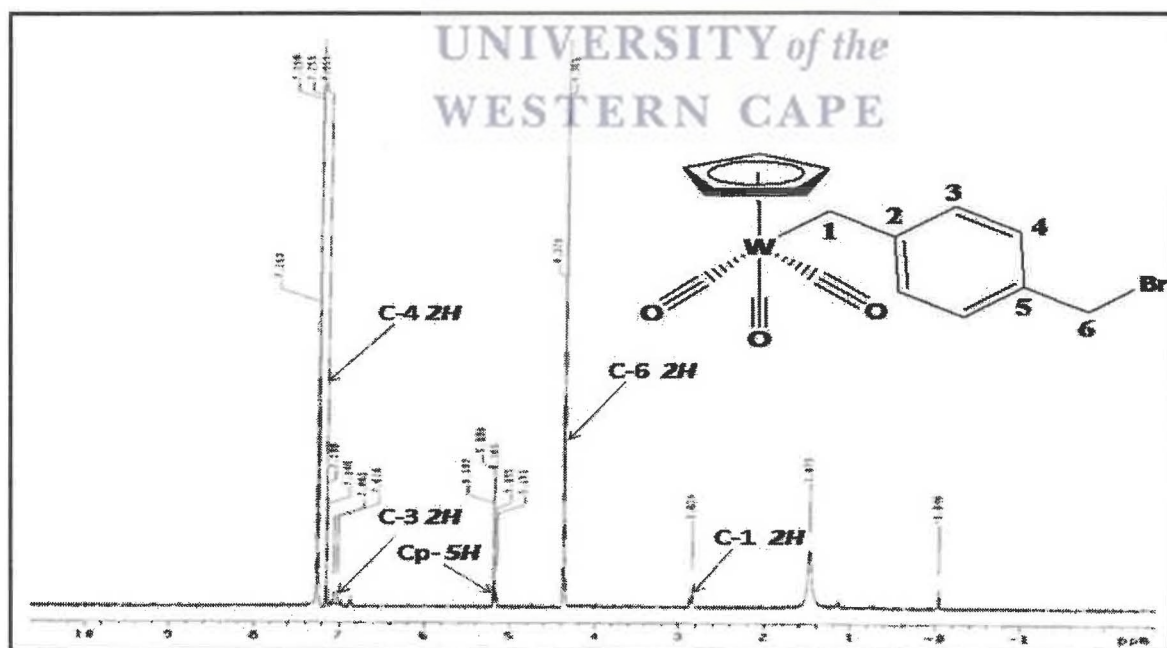
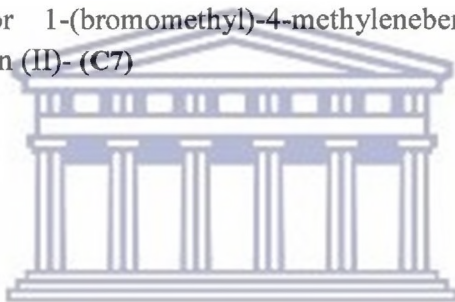


Fig A3.11:  $^1\text{H}$  NMR spectrum for 1-(bromomethyl)-4-methylenebenzyl cyclopentadienyl tricarbonyl tungsten (II)-(C7)

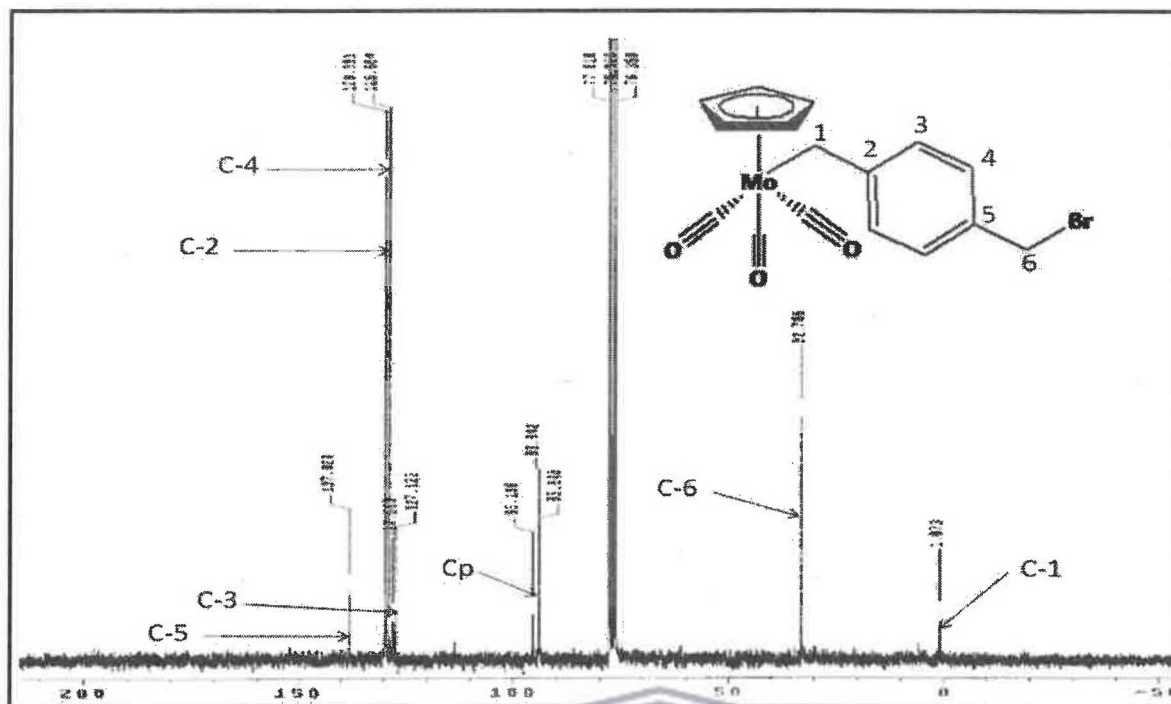


Fig A3.12:  $^{13}\text{C}$  NMR spectrum for 1-(bromomethyl)-4-methylenebenzyl cyclopentadienyl tricarbonyl molybdenum (II)-(C7)

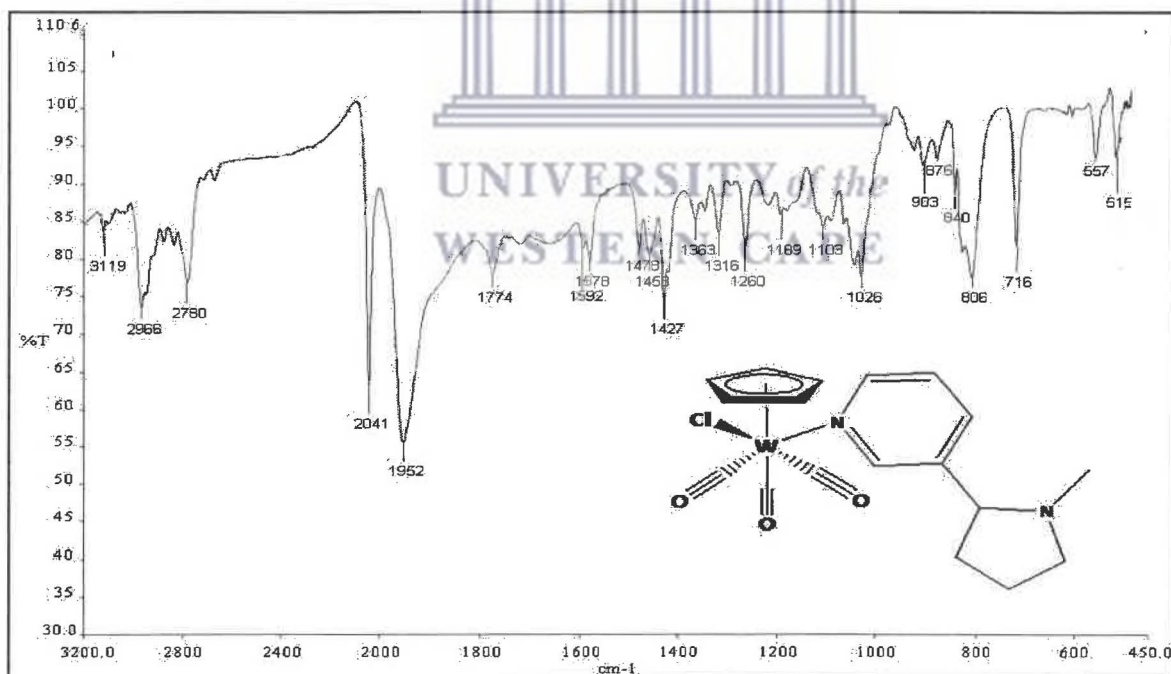
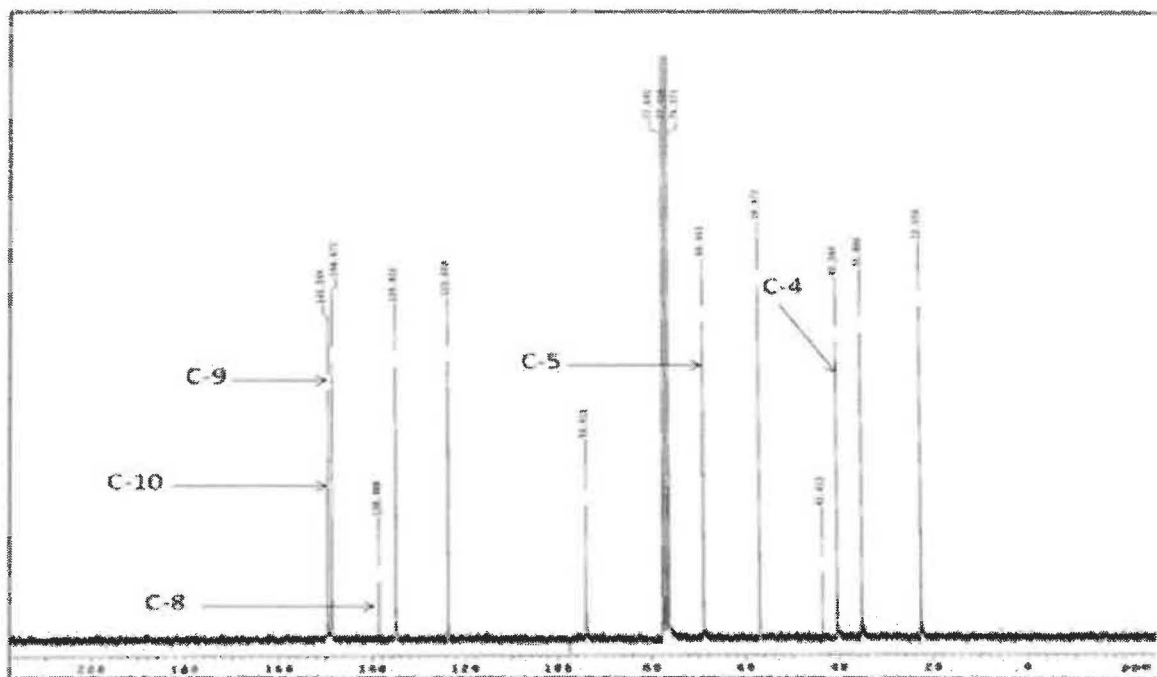


Fig A3.13: IR spectrum 3-(1-methylpyrrolidin-2-yl) pyridine chlorocyclopentadienyl tricarbonyl tungsten (II) - (C10)





**FigA3.15:**  $^{13}\text{C}$  NMR spectrum for 3-(1-methylpyrrolidin-2-yl) pyridine chlorocyclopentadienyl tricarbonyl molybdenum (II)-(C9)



**Table A3.22:** Summary of structures of C1-C10

	Proposed structure	Metal	Compound
1.		Mo	C1
2.		W	C2
		Mo	C3
3.		W	C4
		Mo	C5
3.		W	C6
4.		Mo	C7
4.		W	C8
		Mo	C9
5.		W	C10

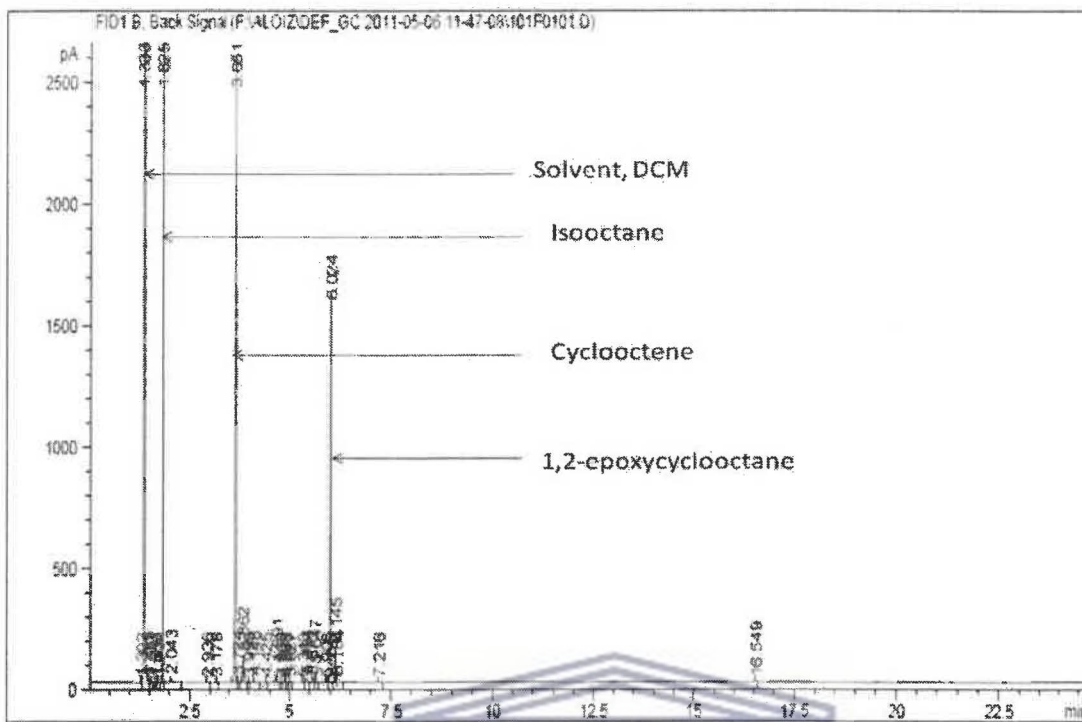


**Fig A3.17:** GC spectrum for  $Cy_8$ ,  $Cy_8$  Oxide, Isooctane standard samples

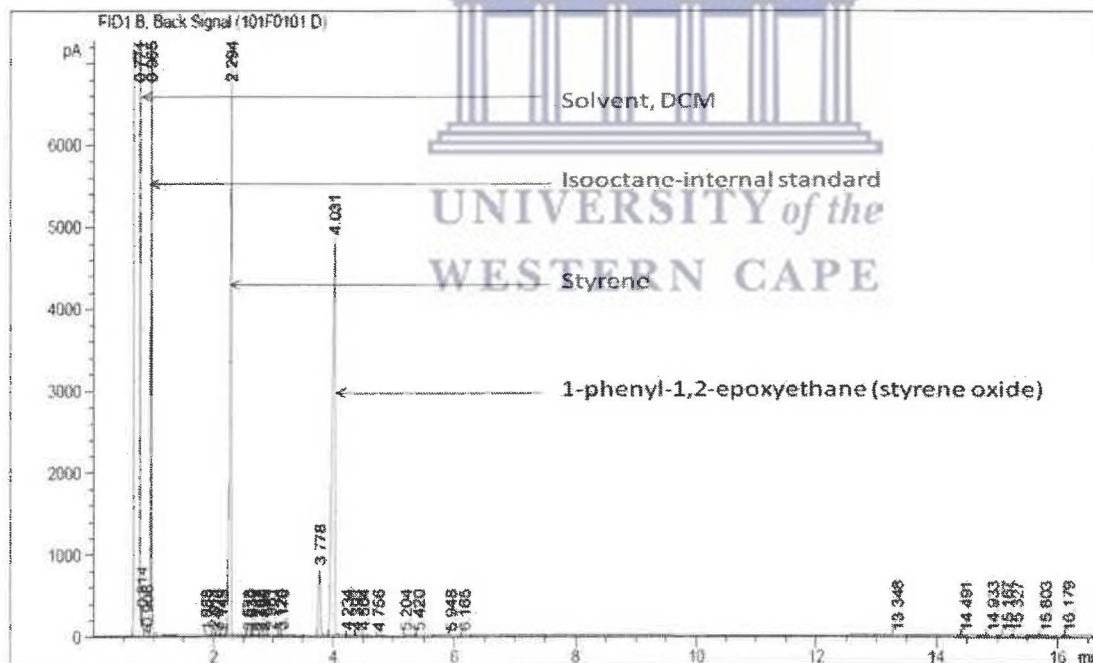


**Fig A3.18:** GC spectrum for Sty, Sty Oxide, Isooctane standard samples





**Table A3.23: Epoxidation Results**

Entry	Catalysts	Alkene	Conversion (%) <sup>a</sup>	Epoxide yield (%) <sup>b</sup>	Selectivity (%)	Time (h)
1	No Catalyst	Cis-Cyclooctene	22.32	21.58	96.71	24
		Cis-Cyclooctene	32.84	28.78	87.64	48
		1-octene	1.86	1.49	80.39	24
		1-octene	3.73	2.54	68.09	48
		cyclohexene	62.50	0.18	0.28	24
		cyclohexene	65.94	0.29	0.43	48
		Styrene	26.46	1.39	6.26	24
		Styrene	27.00	2.55	9.46	48
2	C1	Cis-Cyclooctene	58.80	14.27	24.26	24
		1-octene	34.95	2.20	6.29	24
		1-octene	42.32	16.39	38.73	48
		cyclohexene	46.29	5.37	11.59	24
		1-hexene	42.53	15.50	36.43	24
		Styrene	33.93	4.27	12.60	24
3	C2	Cis-Cyclooctene	64.11	3.35	5.23	24
		1-octene	37.45	1.23	3.28	24
		cyclohexene	46.27	13.54	29.26	24
		Styrene	51.00	0.00	0	24
4	C3	Cis-Cyclooctene	87.96	85.59	97.30	24
		1-octene	46.69	19.44	41.63	24
		cyclohexene	57.32	28.57	49.84	24
		1-hexene	40.05	3.23	8.07	24
		Styrene	33.93	4.27	12.60	24
5	C4	Cis-Cyclooctene	48.57	12.42	25.57	24
		Cis-Cyclooctene	69.19	15.42	22.30	48
		1-octene	18.31	5.32	29.05	24
		1-octene	30.48	7.36	24.15	48
		cyclohexene	35.08	9.71	27.68	24
		cyclohexene	56.96	10.05	17.65	48
		1-hexene	38.28	9.74	25.443	24
		Styrene	23.91	7.41	30.99	24
		Styrene	44.30	7.32	16.52	48

**Epoxidation Results cont....**

Entry	Catalysts	Alkene	Conversion (%) <sup>a</sup>	Epoxide yield (%) <sup>b</sup>	Selectivity (%)	Time (h)
6	C5	Cis-Cyclooctene	90.08	29.45	32.69	24
		Cis-Cyclooctene	99.75	52.01	52.14	48
		1-octene	71.19	38.89	54.63	24
		1-octene	80.72	50.30	62.32	48
		cyclohexene	45.56	38.33	84.14	24
		1-hexene	71.37	12.64	17.71	24
		Styrene	41.04	14.84	36.17	24
		Styrene	70.34	15.56	22.13	48
7	C6	Cis-Cyclooctene	48.79	12.42	25.57	24
		Cis-Cyclooctene	69.16	15.42	22.30	48
		1-octene	18.31	5.32	29.05	24
		1-octene	30.45	7.36	24.15	48
		cyclohexene	27.30	3.86	14.17	24
		1-hexene	41.71	15.94	38.22	24
		Styrene	41.77	0.32	0.83	24
		8	C7	Cis-Cyclooctene	94.09	93.35
Cis-Cyclooctene	95.57			94.83	99.22	48
1-octene	47.28			1.98	4.18	24
1-octene	59.25			4.63	7.81	48
cyclohexene	72.10			1.86	2.57	24
cyclohexene	73.18			3.11	4.24	48
1-hexene	42.39			15.53	36.64	24
Styrene	58.04			4.22	7.27	24
9	C8	Cis-Cyclooctene	37.57	22.12	58.87	24
		Cis-Cyclooctene	41.39	35.15	84.92	48
		1-octene	6.66	0.78	11.71	24
		1-octene	12.12	3.33	27.50	48
		cyclohexene	10.84	6.62	61.07	24
		cyclohexene	37.34	7.83	20.97	48
		1-hexene	21.07	9.24	43.69	24
		Styrene	74.49	2.63	3.54	24
		Styrene	45.78	0.00	-	48

**Epoxidation Results cont.....**

Entry	Catalysts	Alkene	Conversion (%) <sup>a</sup>	Epoxide yield (%) <sup>b</sup>	Selectivity (%)	Time (h)
10	C9	Cis-Cyclooctene	38.78	29.09	75.01	24
		Cis-Cyclooctene	53.33	43.63	81.81	48
		1-octene	14.45	2.60	17.88	24
		1-octene	24.24	4.36	17.98	48
		cyclohexene	11.44	5.06	44.23	24
		cyclohexene	31.32	5.96	19.04	48
		Styrene	18.67	6.06	32.46	24
		Styrene	22.28	0.00	0.00	48
11	C10	Cis-Cyclooctene	15.75	7.27	46.32	24
		Cis-Cyclooctene	26.66	10.90	40.92	48
		1-octene	4.84	1.33	27.54	24
		1-octene	8.48	4.00	47.16	48
		cyclohexene	39.15	0.44	1.13	24
		cyclohexene	45.8	1.50	3.27	48
		1-hexene	27.96	7.49	26.79	24
		Styrene	6.62	0.00	0.00	24

